SCTLD Resistance Research Consortium
Summary Report through May 2023

Florida Department of Environmental Protection
Coral Protection and Restoration Program

SCTLD Resistance Research Consortium
Summary Report through May 2023

Final Report

Prepared By:

Brian K. Walker[1], Greta S. Aeby, Andrew C. Baker[2], Samantha Buckley[1], Neha Garg[3], Aine Hawthorne[4], Julie L. Meyer[5], Karen Neely[1], Hunter Noren[1], Valerie J. Paul[6], Reagan Sharkey[1], Nikki Traylor-Knowles[2], Josh D. Voss[7], David R. Whitall[8], Gareth J. Williams[9], Cheryl M. Woodley[10], and Thierry Work[11]

[1]Nova Southeastern University, Halmos College of Arts and Sciences; [2] University of Miami, Rosenstiel School of Marine and Atmospheric Sciences; [3] Georgia Tech University; [4] U.S. Geological Survey; [5]University of Florida; [6]Smithsonian Marine Station at Fort Pierce; [7]Florida Atlantic University's Harbor Branch Oceanographic Institute; [8]NOAA NOS NCCOS; [9]Symbioseas Inc.; [10]NOAA NOS NCCOS, Coral Health and Disease Program Manager; [11]USGS National Wildlife Health Center Honolulu Field Station

June 30, 2023

Completed in Partial Fulfillment of PO C0B9A6 for

Florida Department of Environmental Protection
Coral Protection and Restoration Program
1277 N.E. 79th Street Causeway
Miami, FL 33138

This report should be cited as follows:
Walker BK, Aeby GS, Baker AC, Buckley S, Garg N, Hawthorne A, Meyer J, Neely K, Noren H, Paul VJ, Sharkey R, Traylor-Knowles N, Voss J, Whitall DR, Williams GJ, Woodley CM, and T Work. 2023. SCTLD Resistance Research Consortium Summary Report through May 2023. Florida DEP. Miami, FL, 107p.

This report was prepared for the Florida Department of Environmental Protection, Coral Protection and Restoration Program by Nova Southeastern University. Funding was provided by the Florida Department of Environmental Protection Award No. B96800. The views, statements, findings, conclusions, and recommendations expressed herein are those of the authors and do not necessarily reflect the views of the State of Florida or any of its sub-agencies.

Table of Contents

Appendix 1. Additional sample processing details.

List of Figures

List of Tables

List of Acronyms

FAU	Florida Atlantic University Harbor Branch Oceanographic Institute
DEP	Florida Department of Environmental Protection
ORCP	Office of Resilience and Coastal Protection
FWC	Florida Fish and Wildlife Conservation Commission
NSU	Nova Southeastern University
Coral ECA	Kristin Jacobs Coral Reef Ecosystem Conservation Area
FCR	Florida's Coral Reef
SCTLD	stony coral tissue loss disease
SE FL	Southeast Florida
NOAA	National Oceanic and Atmospheric Administration
NCRMP	National Coral Reef Monitoring Program
CIMAS	Cooperative Institute For Marine And Atmospheric Studies
GIS	Geographic Information System
MDS	Multidimensional Scaling
AVLP	Anisometric viral like particle

Acknowledgements

Thank you to the Florida Department of Environmental Protection's Coral Protection and Restoration Program (DEP CPR), NOAA CRCP, and US EPA for supporting these efforts. We thank the Florida Coral Disease Advisory Committee for the large number of volunteers assisting in the meeting and planning of coral disease efforts. We thank Lisa Gregg and Joanne Delaney for assisting with permitting. Thanks to the DEP CPR staff including Nick Parr and Kristi Kerrigan for contract and report-review coordination. Thank you to the many employees and graduate students involved in the collection, processing, and analyses.

Management Summary (300 words or less)

The SCTLD Resistance Research Consortium's integrated approach to understanding the underpinnings for SCTLD resistance and susceptibility among Florida *O. faveolata* populations has been a success. The synchronized core sampling across time of year, regions, and disease resistance classes of a statistically robust number of corals has given many insights into the genetic, biochemical, and physiological underpinnings in the holobiont of individuals. However, there is much work remaining to uncover the many statistical associations and pathways across the various components. The analyses of the many various components in this investigation, genomics, transcriptomics, metabolomics, proteomics, lipidomics, histopathology, microbiomes, endosymbionts, tissue regeneration, and fecundity, have elicited many future research leads to gain a wholistic understanding of the coral's condition.

Executive Summary

Coral diseases continue to cause enormous impacts to Florida's Coral Reef. Regular monitoring and treatments have reduced the loss of live tissue area and provided valuable information on the temporal and spatial variations of colonies with lesions. The resistance categories generated from these data were supported by histopathology. Disease was evident in all coral samples at varying levels. Histopathology scoring showed increased lytic necrosis and degenerative Symbiodiniaceae in the low resistance colonies, but only over certain times of year. No clear associations of Symbiodiniaceae with disease resistance were found. This prompted additional sample analyses using ITS2 to identify Symbiodiniaceae species. Once complete, the ITS2 will be used to look for associations in disease resistance and histopathology differences.

The genetics data indicated that the *Orbicella* populations were once successfully recruiting throughout the reef system. Something that happens very rarely if at all today even though over 91% of the colonies were fecund. Although differences in sampling times existed, the Lower Keys colonies were the least fecund, especially those with previous lesions.

Metabolite, lipid, and protein data all provided evidence that a coral's state is dynamic over time and varied by region. Differences in resistance were found only in specific regions at specific times of the year. In the Lower Keys, resistance classes differed by metabolite species in June and September, by lipid species in June and March, and by protein species in June. In the ECA, no significant differences were found in all metabolite, lipid, or protein species between resistance classes.

The transcriptomics data have not been fully analyzed, however preliminary results suggest that corals with previous lesions have a fingerprint of the effects in their gene expression that might contribute to recurrent infections.

Coral disease was dynamic during the study with some corals getting more disease, some for the first time, and others having less. While all corals were sampled in healthy-looking

tissue away from any disease, tracking these disease states facilitate identifying specific corals with recent disease to investigate resistance and possible disease markers. More research is needed to understand what specific aspects of these corals differed.

A key missing piece is the microbial data. Progress on this in the coming year will help elucidate the functions the microbial communities are expressing across time, regions, and resistance.

More research of the data is needed to understand the role of gametogenesis in cell functioning, histopathology, associations with disease, and associations with amoxicillin treatments.

1. BACKGROUND

Coral diseases have devastated many coral populations globally over the past few decades and are becoming more frequent and virulent. Some are associated with coral stress events like bleaching and nutrient enrichment, however others are not, which obfuscates our understanding of disease sources and pathogen identification. After decades of research using the one pathogen-one disease framework with little success, more complex paradigms investigating the members of the holobiont separately and collectively are being employed to uncover the interactions between host, agent and environment of a given coral disease.

Understanding intraspecific coral disease susceptibility is critical to disentangling causation. Comparisons in holobiont biological data (e.g. omics, symbionts, microbiomes) between highly susceptible and highly resistant conspecifics can identify reasons for the variation and possible disease markers. For example, on the Great Barrier Reef, immunity level directly relates to bleaching and disease susceptibility. Furthermore, these data could be tied to environmental conditions occurring during lesion outbreaks and cessation.

Stony Coral Tissue Loss Disease (SCTLD) has devastated the coral populations along Florida's Coral Reef over the last eight years. Its unique trait of affecting many species at varying infection and virulence rates remains perplexing. Identifying the cause of the disease and how to mitigate it is a top management priority. Populations of mountainous star coral (*Orbicella faveolata*) in Florida waters have been prioritized for intensive disease intervention efforts to stop SCTLD. These successful disease intervention treatments throughout Florida's Coral Reef have kept diseased reef-building corals alive, providing a unique opportunity to test intraspecific differences between groups of corals with differing infection patterns. Some corals get infected once, some are reinfected numerous times, and some not at all. Viewing this collection of *O. faveolata* as patients or individual cases that are grouped as at risk (no infection) or differentially affected (i.e., degrees of infection rates) by SCTLD, it is important to have a basic 'patient history' or anamnesis as a foundation to interpret and contextualize more probative or diagnostic analyses.

Between July 2021 and March 2023, DEP funded a consortium of experts (PO C0CB08), the SCTLD Resistance Research Consortium (RRC), to undertake an integrated approach

to understanding the underpinnings for SCTLD resistance and susceptibility among Florida *O. faveolata* populations. This team was assembled to target many various components in disease investigation: genomics, transcriptomics, metabolomics, proteomics, lipidomics, histopathology (tissue and subcellular structure), microbiomes, endosymbionts, tissue regeneration, and fecundity. Synchronized core samples were collected to obtain a sample for each methodology at the same location on the same coral at the same time providing the optimum chance to correlate results across the many investigated aspects and gain a wholistic understanding of the coral's condition. The RRC's goal is to understand the genetic, biochemical, and physiological underpinnings in the holobiont of individuals between infection categories to characterize risk factors that are driving differences in SCTLD infection rates and determine SCTLD resistance and susceptibility factors in corals. This report summarizes the important findings of the RRC through May 31, 2023.

2. PROJECT DESCRIPTION

Forty-five *Orbicella faveolata* colonies were selected in each region based on previous regional disease intervention monitoring data, equaling ninety total colonies. Fifteen corals with a high number of lesions and frequency of disease when visited (low resistance), fifteen corals with a single or few lesion and low frequency of disease (some resistance), and fifteen apparently healthy corals (no previous lesions) (high resistance) were sampled in each of two regions, Kristen Jacob's Southeast Florida Coral Reef Ecosystem Conservation Area (ECA) (Figure 2) and the Lower Florida Keys (Keys) (Figure 3 and Figure *4*).

Sampling was conducted for two purposes: 1) a unified sample across all colonies for each sample period (Unified Sample) and 2) collect many samples across a few colonies for each sample period to investigate within-colony variability (Colony Variability Sample). The unified sampling occurred on the 90 corals in both regions and the colony variability sampling occurred on seven colonies in the ECA. The colony variability samples are reported separately.

The unified samples were collected during three sample periods to coincide with different times of the year: late-May – mid-June (mid-gametogenesis, rainy season onset, low heat stress), mid-August – mid-September (pre spawning in ECA, post spawning in Keys, end of heat stress and rainy season), and late-February – early March (early gametogenesis, dry season, low heat stress). Tables 1 and 2 show the samples collected and dates of collections for each coral by sample period.

During each sampling period, unified core samples were collected on visually healthy-looking tissue on the horizontal upper surface of the colony (where possible) away from any present or previously diseased margins. Cores were taken as shallow as possible to limit stress on the colony. Within a 10 cm x 10 cm general sampling location, eight tissue cores were collected in sample period one, five in sample period two, and six in sample period three using various-size punch cores (Figure 5). A 10 mm cores was used to collect tissue for genotyping (Voss), microbiome analyses (Voss/Meyer); microbial metagenomes (Meyer); proteomics (Woodley); transcriptomics and symbionts (Traylor-Knowles/Baker) and an archive sample. A 14 mm core was used to collect tissue for chemical defenses

(Paul), metabolomics (Garg), and lipidomics (Paul/Garg). A 20 mm core was used to collect tissue for histology (Hawthorne). Seven colonies had a one-time 10 mm tissue core of an active disease margin and a location far away from any disease on the same colony for TEM analysis (Work). Core collections occurred at least 1 cm away from each other to allow remaining tissue to heal the wounds.

During sample period 1, the holes from the cores were left unfilled. Subsequent visits revealed varying levels of fish predation on the hole edges, therefore the sample period 1 holes and all subsequent cores were immediately filled with a Roma Plastilina #2 artist clay as recommended by NOAA to eliminate predation and facilitate tissue regeneration.

During collections all cores were placed in individually labeled WhirlPaks underwater (Figure 6). Once all cores for a single coral were collected, they were immediately transferred to the boat for processing. Once a collection of cores was received on the boat, the cores were transferred to new labeled containers and preserved. All cores were processed in less than 15 minutes from the time of initial collection.

Core samples were preserved in a variety of ways. The histology cores were transferred to a Flacon tube, preserved in Z-fix, and kept on ice. The TEM cores were placed in Tina's fixative on ice. The genotyping and microbiome cores were placed in small vials in Zymo DNA shield and placed on dry ice. The microbial metagenome, proteomics, transcriptomics/symbionts, Chemical defense/metabolomics/lipidomics, and archive samples were placed in new WhirlPaks, submerged in liquid nitrogen, and stored in a liquid nitrogen dry shipper. Once back at the lab they were transferred to a -80 freezer, where they remained until shipping. Samples were shipped to individual labs for additional processing. See Appendix 1 for additional processing details for each sample.

Each sampled area was photographed before and after the sampling using a digital camera on a sample PVC frame with a ruler for scale. Sampled areas, core sites, were revisited and photographed regularly to monitor wound healing; monthly in the ECA and every other month in the Keys. Healing was assessed in the imagery using standard scaled photographic comparison techniques (Image J, NCRI CPCe) to quantify healing rates and amounts.

At each visit, all sampled corals were photographed and visually assessed by a diver estimating the percentage of live tissue, diseased tissue, bleached tissue, recent mortality, and old mortality. If SCTLD was found, the lesion was treated with antibiotic paste. No treatments occurred before sample collections on the same day. All margins were treated with the Ocean Alchemists antibiotic ointment CoreRx B2B with amoxicillin (1:8 ratio by weight). Photographs were taken of all areas before treatment at both the 0.5 m standard distance and wider scenes. Lesion treatments were determined failures if the active disease continued progressing past the treatment line.

Data and photographs from monitoring visits were adding to the colony history database to document the number of treatments (Figure 7) and mortality (Figure 8) through time.

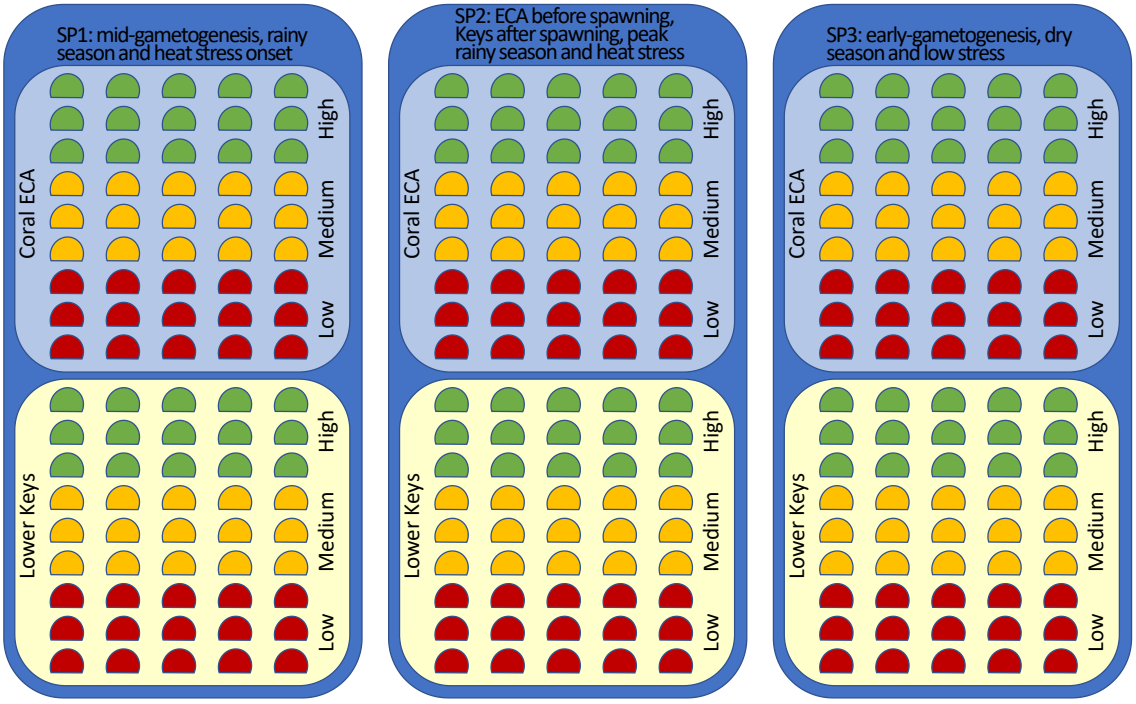

Figure 1. Illustration of sample design. Each colored semi-circle is a sampled coral colored by its disease resistance classification. Forty-five corals were sampled in each region at 3 separate times throughout the year.

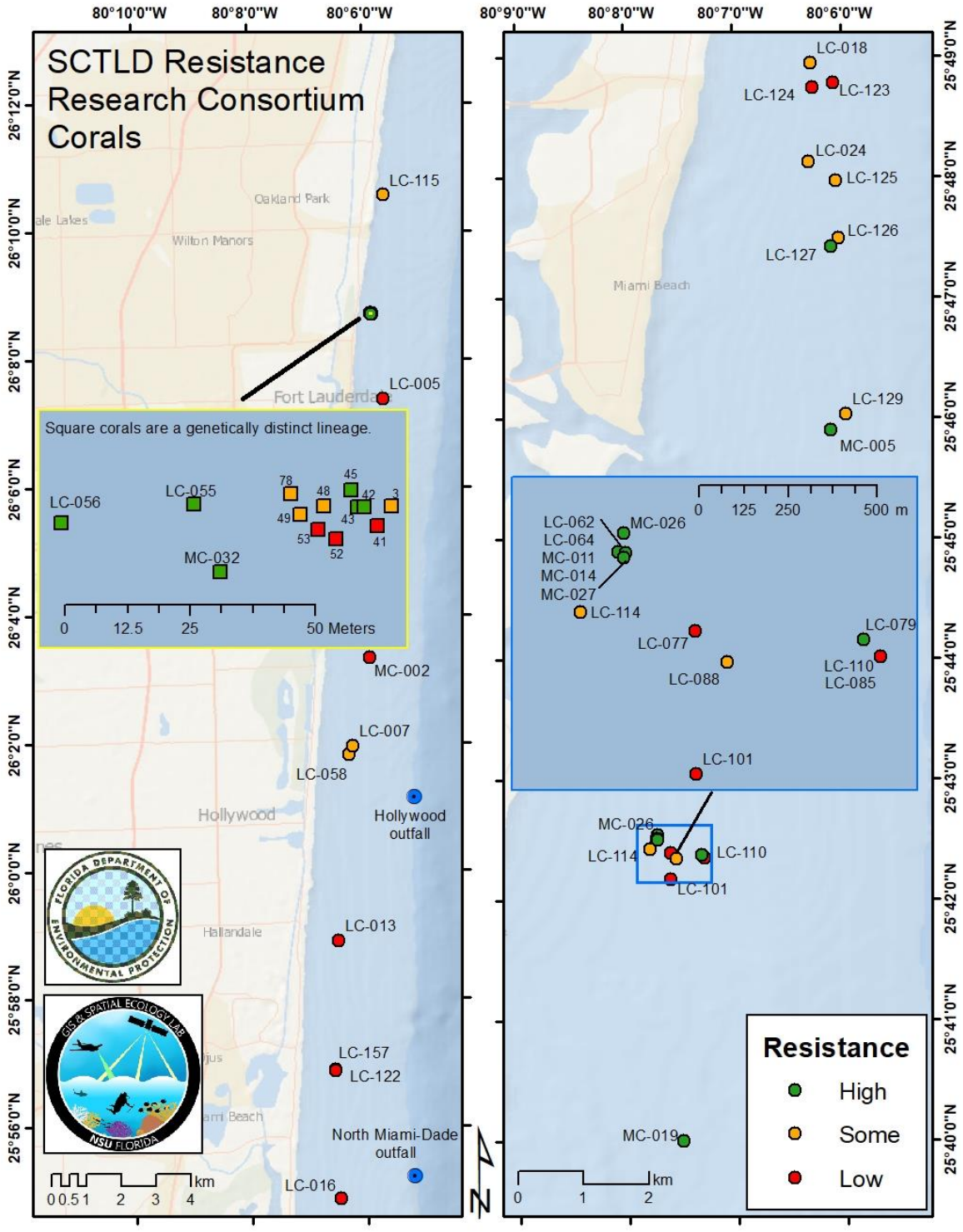

Figure 2. Map showing the location and category of the forty-five *O. faveolata* colonies sampled in the Kristen Jacob's Southeast Florida Coral Reef Ecosystem Conservation Area.

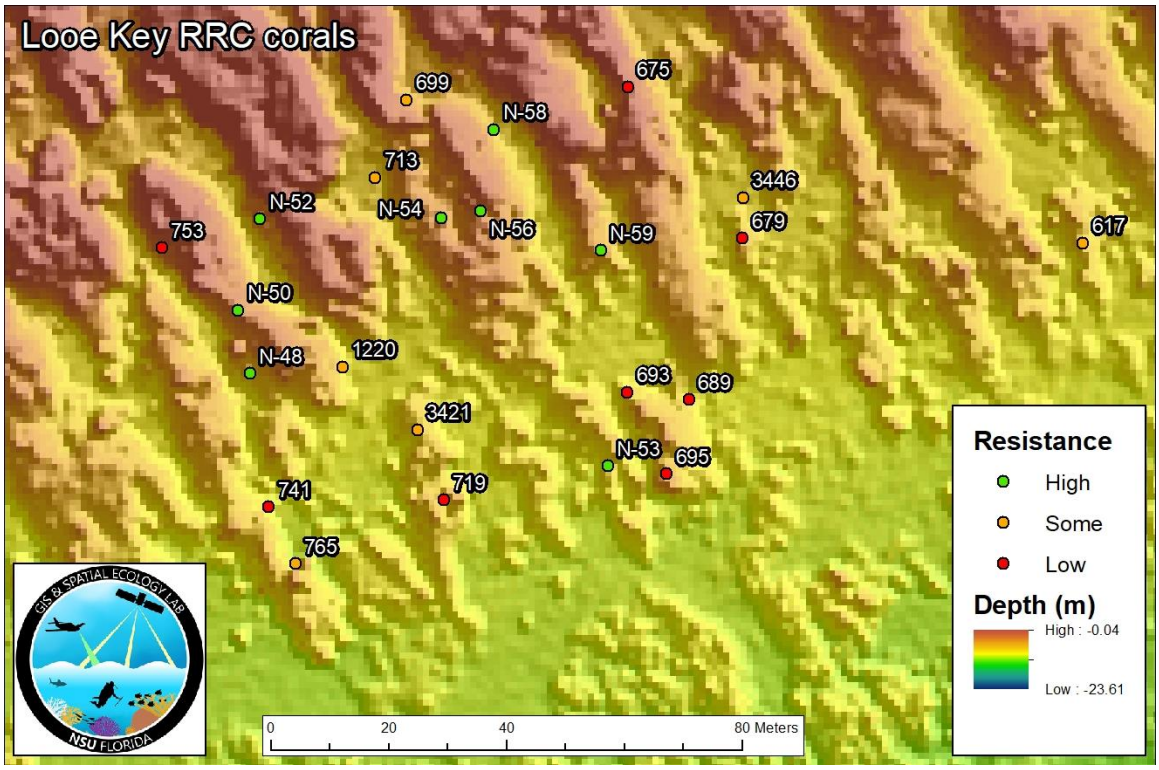

Figure 3. A map of the *O. faveolata* corals sampled at Looe Key.

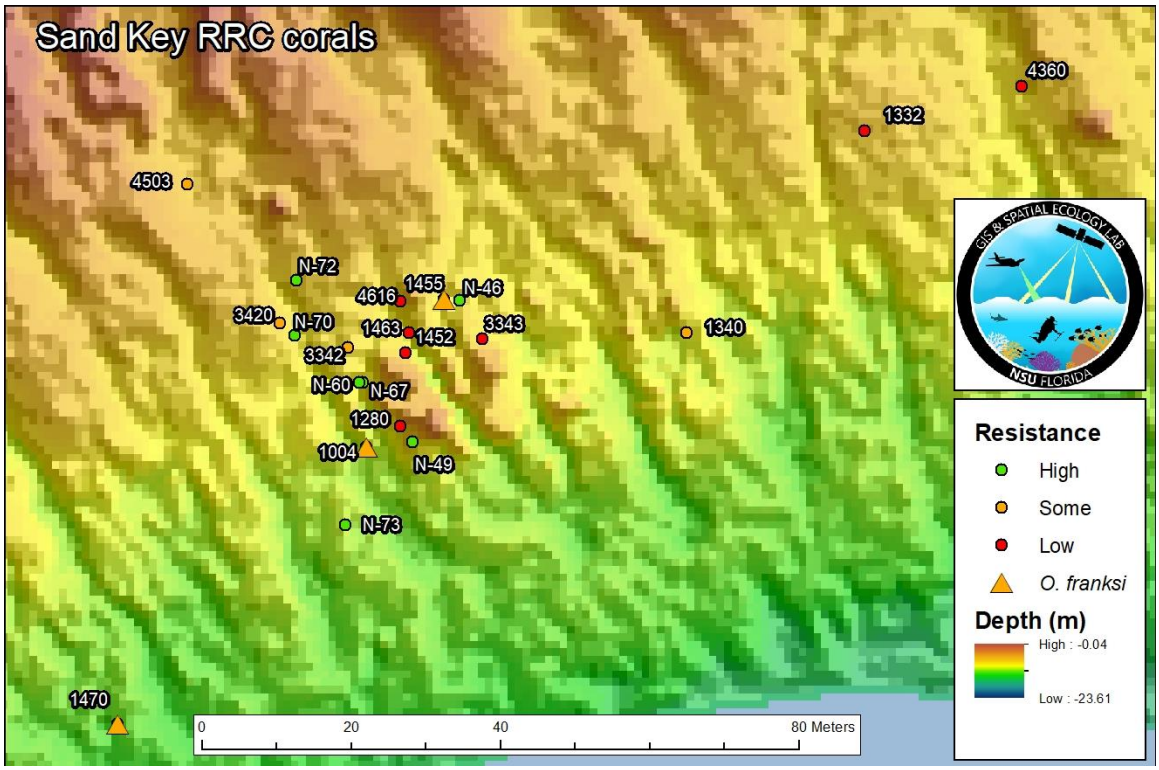

Figure 4. A map of the *O. faveolata* and inadvertently *O. franksii* corals sampled at Sand Key.

Table 1. Sample collection tables documenting the number, size, and date of each sample collected on each colony in the ECA by sample period. Colored rows indicate the SCTLD resistance categories: Green = High resistance, light coral = Medium resistance, and coral = Low resistance.

		Period:	Sample Period 1 - May/June 2021										Sample Period 2 - August 2021							Sample Period 3 - March 2022						
		Task:	Tasks 6,7,8,9,10, 11, Genotyping, Microbiome, Histo, TEM, Proteomics										Tasks 6,7,8,9,10, Microbiome, Histo							Tasks 6,7,8,9,10, Microbiome, Histo, Proteomics						
		Fixative:	Zymo & Liquid Nitrogen (10mm)		Liquid Nitrogen (4 - 10mm, 1 - 14mm)					Z fix (20mm)	Tina's fix (10mm)		Liquid Nitrogen (4 - 10mm, 1 - 14mm)				Z fix (14mm)	Tina's fix (10mm)		Liquid Nitrogen (3 - 10mm, 1 - 14mm)					Z fix (14mm)	
Coral ID	Location	Resistance Category	Genotyping (Voss)	Bacterial metagenome (Meyer)	Microbiome (Voss/Meyer)	Metabolomics (Garg/Paul)	Proteomics (Woodley)	Transcriptome, Symbionts (Baker/Traylor-Knowles)	Cryomill backup/archive	Histology (Hawthorn)	TEM (Work)	P1 Sample Date	Microbiome (Voss/Meyer)	Metabolomics (Garg/Paul)	Transcriptome, Symbionts (Baker/Traylor-Knowles)	Cryomill backup/archive	Histology (Hawthorn)	TEM (Work)	P2 Sample Date	Microbiome (Voss/Meyer)	Metabolomics (Garg/Paul)	Proteomics (Woodley)	Transcriptome, Symbionts (Baker/Traylor-Knowles)	Cryomill backup/archive	Histology (Hawthorn)	P3 Sample Date
LC-042	North	High	10	10	10	14	10	10	10	20		5/28/2021	10	14	10	10	20		8/19/2021	10	14	10	10	10	20	3/19/2022
LC-043	North	High	10	10	10	14	10	10	10	20		5/28/2021	10	14	10	10	20		8/19/2021	10	14	10	10	10	20	3/19/2022
LC-045	North	High	10	10	10	14	10	10	10	20		5/28/2021	10	14	10	10	20		8/19/2021	10	14	10	10	10	20	3/19/2022
LC-055	North	High	10	10	10	14	10	10	10	20		5/28/2021	10	14	10	10	20		8/19/2021	10	14	10	10	10	20	3/19/2022
LC-056	North	High	10	10	10	14	10	10	10	20		5/28/2021	10	14	10	10	20		8/19/2021	10	14	10	10	10	20	3/19/2022
LC-064	South	High	10	10	10	14	10	10	10	20		6/21/2021	10	14	10	10	20		8/21/2021	10	14	10	10	10	20	3/18/2022
LC-079	South	High	10	10	10	14	10	10	10	20		6/21/2021	10	14	10	10	20		8/21/2021	10	14	10	10	10	20	3/18/2022
LC-127	Middle	High	10	10	10	14	10	10	10	20		6/17/2021	10	14	10	10	20		8/20/2021	10	14	10	10	10	20	3/17/2022
MC-005	Middle	High	10	10	10	14	10	10	10	20		6/17/2021	10	14	10	10	20		8/20/2021	10	14	10	10	10	20	3/17/2022
MC-011	South	High	10	10	10	14	10	10	10	20		6/21/2021	10	14	10	10	20		8/21/2021	10	14	10	10	10	20	3/18/2022
MC-014	South	High	10	10	10	14	10	10	10	20		6/21/2021	10	14	10	10	20		8/21/2021	10	14	10	10	10	20	3/18/2022
MC-019	South	High	10	10	10	14	10	10	10	20		6/21/2021	10	14	10	10	20		8/21/2021	10	14	10	10	10	20	3/18/2022
MC-026	South	High	10	10	10	14	10	10	10	20		6/21/2021	10	14	10	10	20		8/21/2021	10	14	10	10	10	20	3/18/2022
MC-027	South	High	10	10	10	14	10	10	10	20		6/21/2021	10	14	10	10	20		8/21/2021	10	14	10	10	10	20	3/18/2022
MC-032	North	High	10	10	10	14	10	10	10	20		5/28/2021	10	14	10	10	20		8/19/2021	10	14	10	10	10	20	3/19/2022
LC-003	North	Some	10	10	10	14	10	10	10	20		5/28/2021	10	14	10	10	20		8/19/2021	10	14	10	10	10	20	3/19/2022
LC-007	Middle	Some	10	10	10	14	10	10	10	20		6/17/2021	10	14	10	10	20		8/20/2021	10	14	10	10	10	20	3/17/2022
LC-018	Middle	Some	10	10	10	14	10	10	10	20		6/17/2021	10	14	10	10	20		8/20/2021	10	14	10	10	10	20	3/17/2022
LC-024	Middle	Some	10	10	10	14	10	10	10	20		6/17/2021	10	14	10	10	20		8/20/2021	10	14	10	10	10	20	3/17/2022
LC-048	North	Some	10	10	10	14	10	10	10	20		5/28/2021	10	14	10	10	20		8/19/2021	10	14	10	10	10	20	3/19/2022
LC-049	North	Some	10	10	10	14	10	10	10	20		5/28/2021	10	14	10	10	20		8/19/2021	10	14	10	10	10	20	3/19/2022
LC-058	Middle	Some	10	10	10	14	10	10	10	20		6/17/2021	10	14	10	10	20		8/20/2021	10	14	10	10	10	20	3/17/2022
LC-062	South	Some	10	10	10	14	10	10	10	20		6/21/2021	10	14	10	10	20		8/21/2021	10	14	10	10	10	20	3/18/2022
LC-078	North	Some	10	10	10	14	10	10	10	20		5/28/2021	10	14	10	10	20		8/19/2021	10	14	10	10	10	20	3/19/2022
LC-088	South	Some	10	10	10	14	10	10	10	20		6/21/2021	10	14	10	10	20		8/21/2021	10	14	10	10	10	20	3/18/2022
LC-114	South	Some	10	10	10	14	10	10	10	20		6/21/2021	10	14	10	10	20		8/21/2021	10	14	10	10	10	20	3/18/2022
LC-115	North	Some	10	10	10	14	10	10	10	20		5/28/2021	10	14	10	10	20		8/19/2021	10	14	10	10	10	20	3/19/2022
LC-125	Middle	Some	10	10	10	14	10	10	10	20		6/17/2021	10	14	10	10	20		8/20/2021	10	14	10	10	10	20	3/17/2022
LC-126	Middle	Some	10	10	10	14	10	10	10	20		6/17/2021	10	14	10	10	20		8/20/2021	10	14	10	10	10	20	3/17/2022
LC-129	Middle	Some	10	10	10	14	10	10	10	20		6/17/2021	10	14	10	10	20		8/20/2021	10	14	10	10	10	20	3/17/2022
LC-005	North	Low	10	10	10	14	10	10	10	20		5/28/2021	10	14	10	10	20		8/19/2021	10	14	10	10	10	20	3/19/2022
LC-013	Middle	Low	10	10	10	14	10	10	10	20		6/17/2021	10	14	10	10	20		8/20/2021	10	14	10	10	10	20	3/17/2022
LC-016	Middle	Low	10	10	10	14	10	10	10	20		6/17/2021	10	14	10	10	20		8/20/2021	10	14	10	10	10	20	3/17/2022
LC-041	North	Low	10	10	10	14	10	10	10	20		5/28/2021	10	14	10	10	20		8/19/2021	10	14	10	10	10	20	3/19/2022
LC-052	North	Low	10	10	10	14	10	10	10	20		5/28/2021	10	14	10	10	20		8/19/2021	10	14	10	10	10	20	3/19/2022
LC-053	North	Low	10	10	10	14	10	10	10	20		5/28/2021	10	14	10	10	20		8/19/2021	10	14	10	10	10	20	3/19/2022
LC-077	South	Low	10	10	10	14	10	10	10	20		6/21/2021	10	14	10	10	20		8/21/2021	10	14	10	10	10	20	3/18/2022
LC-085	South	Low	10	10	10	14	10	10	10	20		6/21/2021	10	14	10	10	20		8/21/2021	10	14	10	10	10	20	3/18/2022
LC-101	South	Low	10	10	10	14	10	10	10	20		6/21/2021	10	14	10	10	20		8/21/2021	10	14	10	10	10	20	3/18/2022
LC-110	South	Low	10	10	10	14	10	10	10	20		6/21/2021	10	14	10	10	20		8/21/2021	10	14	10	10	10	20	3/18/2022
LC-122	Middle	Low	10	10	10	14	10	10	10	20		6/17/2021	10	14	10	10	20	10	8/20/2021	10	14	10	10	10	20	3/17/2022
LC-123	Middle	Low	10	10	10	14	10	10	10	20		6/17/2021	10	14	10	10	20		8/20/2021	10	14	10	10	10	20	3/17/2022
LC-124	Middle	Low	10	10	10	14	10	10	10	20		6/17/2021	10	14	10	10	20		8/20/2021	10	14	10	10	10	20	3/17/2022
LC-157	Middle	Low	10	10	10	14	10	10	10	20		6/17/2021	10	14	10	10	20	10	8/20/2021	10	14	10	10	10	20	3/17/2022
MC-002	Middle	Low	10	10	10	14	10	10	10	20		6/17/2021	10	14	10	10	20		8/20/2021	10	14	10	10	10	20	3/17/2022

Table 2. Sample collection tables documenting the number, size, and date of each sample collected on each colony in the lower Keys by sample period. Colored rows indicate the SCTLD resistance categories: Green = High resistance, light coral = Medium resistance, and coral = Low resistance.

			Sample Period 1 - June 2021										Sample Period 2 - September 2021							Sample Period 3 - February/March 2022						
Period:																										
Task:			Tasks 6,7,8,9,10, 11, Genotyping, Microbiome, Histo, TEM, Proteomics										Tasks 6,7,8,9,10, Microbiome, Histo, Proteomics							Tasks 6,7,8,9,10, Microbiome, Histo, Proteomics						
Fixative:			Zymo & Liquid Nitrogen (10mm)		Liquid Nitrogen (4 - 10mm, 1 - 14mm)					Z fix (20mm)	Tina's fix (10mm)		Liquid Nitrogen (4 - 10mm, 1 - 14mm)				Z fix (20mm)	Tina's fix (10mm)		Liquid Nitrogen (3 - 10mm, 1 - 14mm)					Z fix (14mm)	
Coral ID	Location	Resistance Catergory	Genotyping (Voss)	Bacterial metagenome (Meyer)	Microbiome (Voss/Meyer)	Metabolomics (Garg/Paul)	Proteomics (Woodley)	Transcriptome, Symbionts (Baker/Traylor-Knowles)	Cryomill backup/archive	Histology (Hawthorn)	TEM (Work)	P1 Sample Date	Microbiome (Voss/Meyer)	Metabolomics (Garg/Paul)	Transcriptome, Symbionts (Baker/Traylor-Knowles)	Cryomill backup/archive	Histology (Hawthorn)	TEM (Work)	P2 Sample Date	Microbiome (Voss/Meyer)	Metabolomics (Garg/Paul)	Proteomics (Woodley)	Transcriptome, Symbionts (Baker/Traylor-Knowles)	Cryomill backup/archive	Histology (Hawthorn)	P3 Sample Date
N-48	Looe	High	10	10	10	14	10	10	10	20		6/12/2021	10	14	10	10	20		9/15/2021	10	14	10	10	10	20	3/1/2022
N-50	Looe	High	10	10	10	14	10	10	10	20		6/12/2021	10	14	10	10	20		9/15/2021	10	14	10	10	10	20	3/1/2022
N-52	Looe	High	10	10	10	14	10	10	10	20		6/12/2021	10	14	10	10	20		9/15/2021	10	14	10	10	10	20	3/1/2022
N-53	Looe	High	10	10	10	14	10	10	10	20		6/12/2021	10	14	10	10	20		9/15/2021	10	14	10	10	10	20	3/1/2022
N-54	Looe	High	10	10	10	14	10	10	10	20		6/12/2021	10	14	10	10	20		9/15/2021	10	14	10	10	10	20	3/1/2022
N-56	Looe	High	10	10	10	14	10	10	10	20		6/12/2021	10	14	10	10	20		9/15/2021	10	14	10	10	10	20	3/1/2022
N-58	Looe	High	10	10	10	14	10	10	10	20		6/12/2021	10	14	10	10	20		9/15/2021	10	14	10	10	10	20	3/1/2022
N-59	Looe	High	10	10	10	14	10	10	10	20		6/12/2021	10	14	10	10	20		9/15/2021	10	14	10	10	10	20	3/1/2022
N-46	Sand	High	10	10	10	14	10	10	10	20		6/13/2021	10	14	10	10	20		9/14/2021	10	14	10	10	10	20	2/28/2022
N-49	Sand	High	10	10	10	14	10	10	10	20		6/13/2021	10	14	10	10	20		9/14/2021	10	14	10	10	10	20	2/28/2022
N-60	Sand	High	10	10	10	14	10	10	10	20		6/13/2021	10	14	10	10	20		9/14/2021	10	14	10	10	10	20	2/28/2022
N-67	Sand	High	10	10	10	14	10	10	10	20		6/13/2021	10	14	10	10	20		9/14/2021	10	14	10	10	10	20	2/28/2022
N-70	Sand	High	10	10	10	14	10	10	10	20		6/13/2021	10	14	10	10	20		9/14/2021	10	14	10	10	10	20	2/28/2022
N-72	Sand	High	10	10	10	14	10	10	10	20		6/13/2021	10	14	10	10	20		9/14/2021	10	14	10	10	10	20	2/28/2022
N-73	Sand	High	10	10	10	14	10	10	10	20		6/13/2021	10	14	10	10	20		9/14/2021	10	14	10	10	10	20	2/28/2022
617	Looe	Some	10	10	10	14	10	10	10	20		6/12/2021	10	14	10	10	20		9/15/2021	10	14	10	10	10	20	3/1/2022
663	Looe	Some	10	10	10	14	10	10	10	20		6/12/2021	10	14	10	10	20		9/15/2021	10	14	10	10	10	20	3/1/2022
699	Looe	Some	10	10	10	14	10	10	10	20		6/12/2021	10	14	10	10	20		9/15/2021	10	14	10	10	10	20	3/1/2022
713	Looe	Some	10	10	10	14	10	10	10	20		6/12/2021	10	14	10	10	20		9/15/2021	10	14	10	10	10	20	3/1/2022
765	Looe	Some	10	10	10	14	10	10	10	20		6/12/2021	10	14	10	10	20		9/15/2021	10	14	10	10	10	20	3/1/2022
1220	Looe	Some	10	10	10	14	10	10	10	20		6/12/2021	10	14	10	10	20		9/15/2021	10	14	10	10	10	20	3/1/2022
3421	Looe	Some	10	10	10	14	10	10	10	20	10	6/12/2021	10	14	10	10	20		9/15/2021	10	14	10	10	10	20	3/1/2022
3446	Looe	Some	10	10	10	14	10	10	10	20		6/12/2021	10	14	10	10	20		9/15/2021	10	14	10	10	10	20	3/1/2022
1004	Sand	Some	10	10	10	14	10	10	10	20		6/13/2021	10	14	10	10	20		9/14/2021	10	14	10	10	10	20	2/28/2022
1340	Sand	Some	10	10	10	14	10	10	10	20		6/13/2021	10	14	10	10	20		9/14/2021	10	14	10	10	10	20	2/28/2022
1455	Sand	Some	10	10	10	14	10	10	10	20		6/13/2021	10	14	10	10	20		9/14/2021	10	14	10	10	10	20	2/28/2022
1470	Sand	Some	10	10	10	14	10	10	10	20		6/13/2021	10	14	10	10	20		9/14/2021	10	14	10	10	10	20	2/28/2022
3342	Sand	Some	10	10	10	14	10	10	10	20		6/13/2021	10	14	10	10	20		9/14/2021	10	14	10	10	10	20	2/28/2022
3420	Sand	Some	10	10	10	14	10	10	10	20		6/13/2021	10	14	10	10	20		9/14/2021	10	14	10	10	10	20	2/28/2022
4503	Sand	Some	10	10	10	14	10	10	10	20		6/13/2021	10	14	10	10	20		9/14/2021	10	14	10	10	10	20	2/28/2022
675	Looe	Low	10	10	10	14	10	10	10	20		6/12/2021	10	14	10	10	20		9/15/2021	10	14	10	10	10	20	3/1/2022
679	Looe	Low	10	10	10	14	10	10	10	20		6/12/2021	10	14	10	10	20		9/15/2021	10	14	10	10	10	20	3/1/2022
689	Looe	Low	10	10	10	14	10	10	10	20		6/12/2021	10	14	10	10	20		9/15/2021	10	14	10	10	10	20	3/1/2022
693	Looe	Low	10	10	10	14	10	10	10	20		6/12/2021	10	14	10	10	20		9/15/2021	10	14	10	10	10	20	3/1/2022
695	Looe	Low	10	10	10	14	10	10	10	20		6/12/2021	10	14	10	10	20		9/15/2021	10	14	10	10	10	20	3/1/2022
719	Looe	Low	10	10	10	14	10	10	10	20	10	6/12/2021	10	14	10	10	20		9/15/2021	10	14	10	10	10	20	3/1/2022
741	Looe	Low	10	10	10	14	10	10	10	20	10	6/12/2021	10	14	10	10	20		9/15/2021	10	14	10	10	10	20	3/1/2022
753	Looe	Low	10	10	10	14	10	10	10	20		6/12/2021	10	14	10	10	20		9/15/2021	10	14	10	10	10	20	3/1/2022
1280	Sand	Low	10	10	10	14	10	10	10	20		6/13/2021	10	14	10	10	20		9/14/2021	10	14	10	10	10	20	2/28/2022
1332	Sand	Low	10	10	10	14	10	10	10	20		6/13/2021	10	14	10	10	20		9/14/2021	10	14	10	10	10	20	2/28/2022
1452	Sand	Low	10	10	10	14	10	10	10	20		6/13/2021	10	14	10	10	20	10	9/14/2021	10	14	10	10	10	20	2/28/2022
1463	Sand	Low	10	10	10	14	10	10	10	20		6/13/2021	10	14	10	10	20		9/14/2021	10	14	10	10	10	20	2/28/2022
3343	Sand	Low	10	10	10	14	10	10	10	20		6/13/2021	10	14	10	10	20		9/14/2021	10	14	10	10	10	20	2/28/2022
4360	Sand	Low	10	10	10	14	10	10	10	20		6/13/2021	10	14	10	10	20		9/14/2021	10	14	10	10	10	20	2/28/2022
4616	Sand	Low	10	10	10	14	10	10	10	20		6/13/2021	10	14	10	10	20	10	9/14/2021	10	14	10	10	10	20	2/28/2022

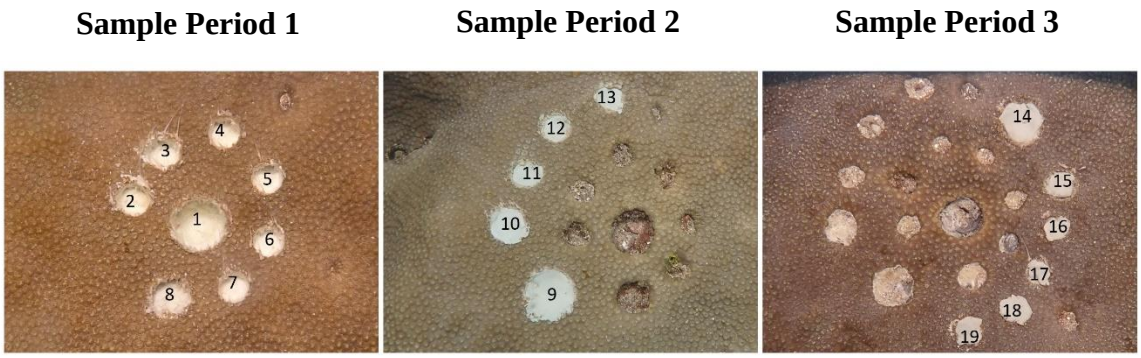

Figure 5. Example of the ideal sample core site arrangement. Core sample arrangements varied depending on colony morphology and available tissue. The example is from LC-005.

Figure 6. Photographs depicting the sample collection workflow from top left to bottom right. Photos by Karen Neely.

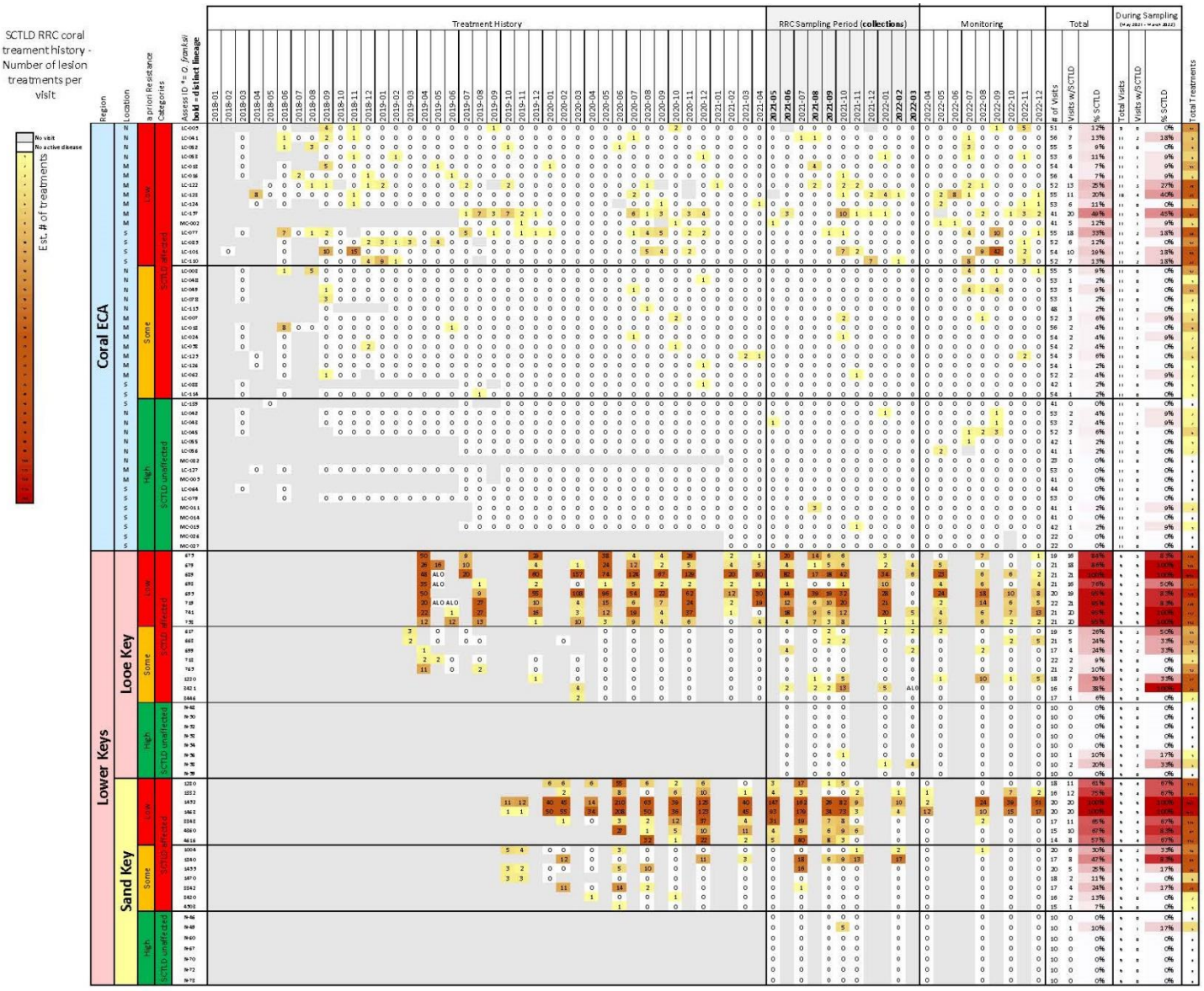

Figure 7. RRC colony disease treatment history.

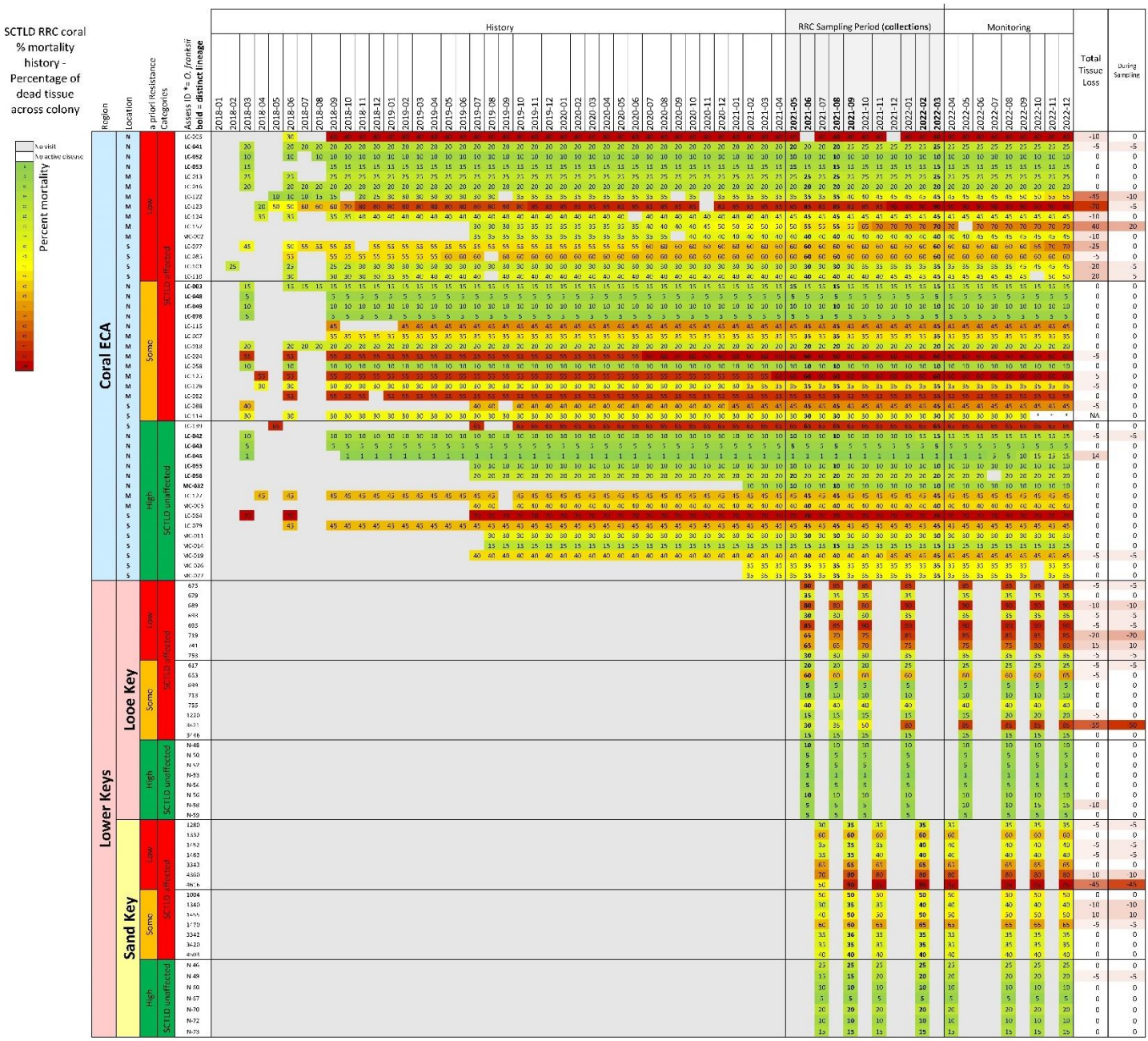

Figure 8. RRC colony percent mortality history.

3. RESULTS AND DISCUSSION

3.1. Disease History and Tissue Loss (Walker, Neely, Sharkey, and Kozachuk)

Goal: Compare the disease histories of the resistance categories by region and evaluate health trajectories of corals during and after sampling.

Significant findings: Resistance categories were significantly different within each region for total treatments and frequency of visits with disease. Frequency of diseased visits and total treatments were significantly higher in the Lower Keys than the ECA in the some and low resistance corals. Lower Keys low resistance corals had significantly more treatments as of Dec 2022 than before sampling. Some corals got relatively sicker during the project and some less. The corals with the most disease did not show relative change.

Results:
Analyses of the number of treatments and frequency of disease when visited supported the colony disease resistance classifications in both regions and elucidated differences between regions. In both regions, total treatments and frequency diseased were significantly different between resistance classes before sampling at through December 2022 (Figure 9). The Lower Keys colonies had a lot more disease than the ECA colonies. Frequency diseased was significantly higher in the lower Keys than ECA for the some and low resistance classes and total treatments were higher in the low resistance corals. In addition, Lower Keys low resistance corals had significantly more treatments as of Dec 2022 than before sampling.

MDS of the disease histories before sampling supported the resistance classes (Figure 10). Permanova testing found significance with region and resistance and between some and low resistance corals within region. The MDS of corals with at least one previous lesion showed clear separation of region and resistance. The Lower Keys some resistance and the ECA low resistance colonies were most similar with overlap on the total treatments plane but separated by the frequency of diseased visits where the Lower Keys had more. By December 2022 the separation between these groups was lessened in the plot, but significance remained when tested by permanova (Figure 11).

Combining plots graphically helped illustrate the trajectory of coral health during the project (Figure 12). The corals with the most disease did not move much before sampling and as of December 2022, however, a lot of movement occurred in the middle of the plot. Some corals like 101, 110, 123, and 3421 moved far on the chart along the higher disease plane. This indicates these corals got sicker during the project and could be good individuals to investigate for disease effects in other project datasets. Corals like 3420, 3446, 4503, and 88 moved towards the corals with less disease in the plot. This indicates they were healthier during the project and might also be good targets for determining disease differentials.

Discussion: This is a preliminary analysis of the disease history data. It supports the resistance categories and elucidates disease differences between regions. The Lower Keys corals require many more treatments and are more frequently diseased when visited than the ECA. More investigation is needed. Identifying corals that got sicker during the project can point researchers

to scrutinize those colonies more in hopes of finding associations to and markers of disease. These data also need exploration to uncover the disease patterns related to amount of live tissue, tissue loss, and environmental factors. These will be the focus of future analyses.

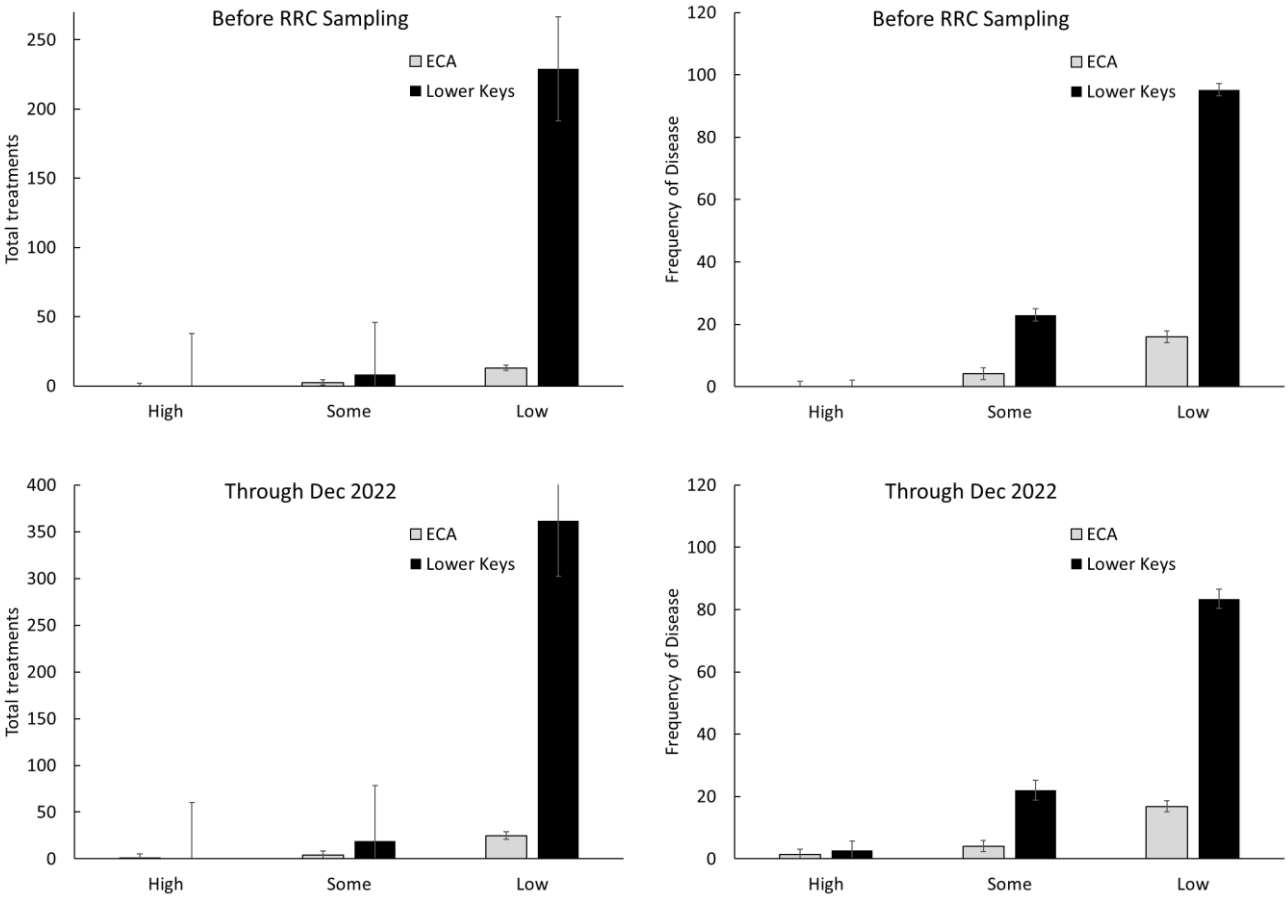

Figure 9. Mean total treatments (left) and frequency of visits with disease (right) for all RRC corals by region and resistance category before sampling (top) and as of December 2022 (bottom).

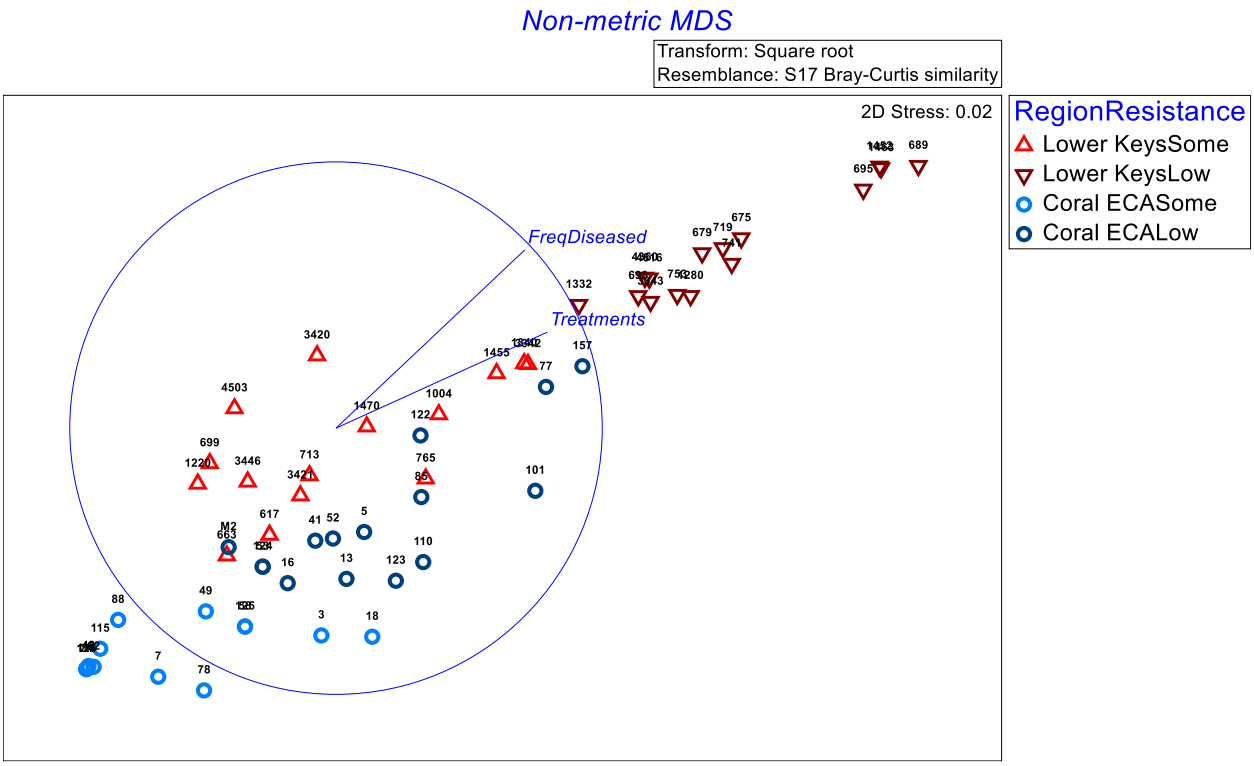

Figure 10. MDS of the frequency diseased and total treatments from all 90 RRC corals before sampling.

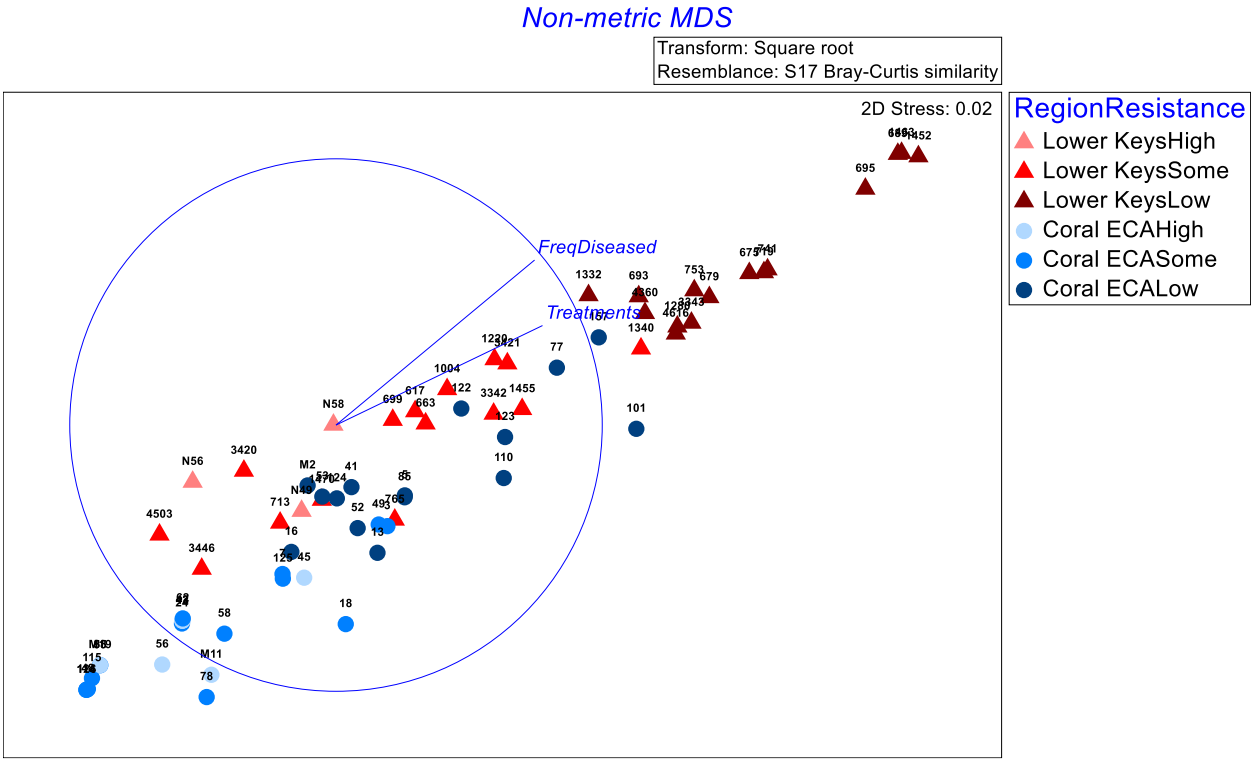

Figure 11. MDS of the frequency diseased and total treatments from all 90 RRC corals as of December 2022.

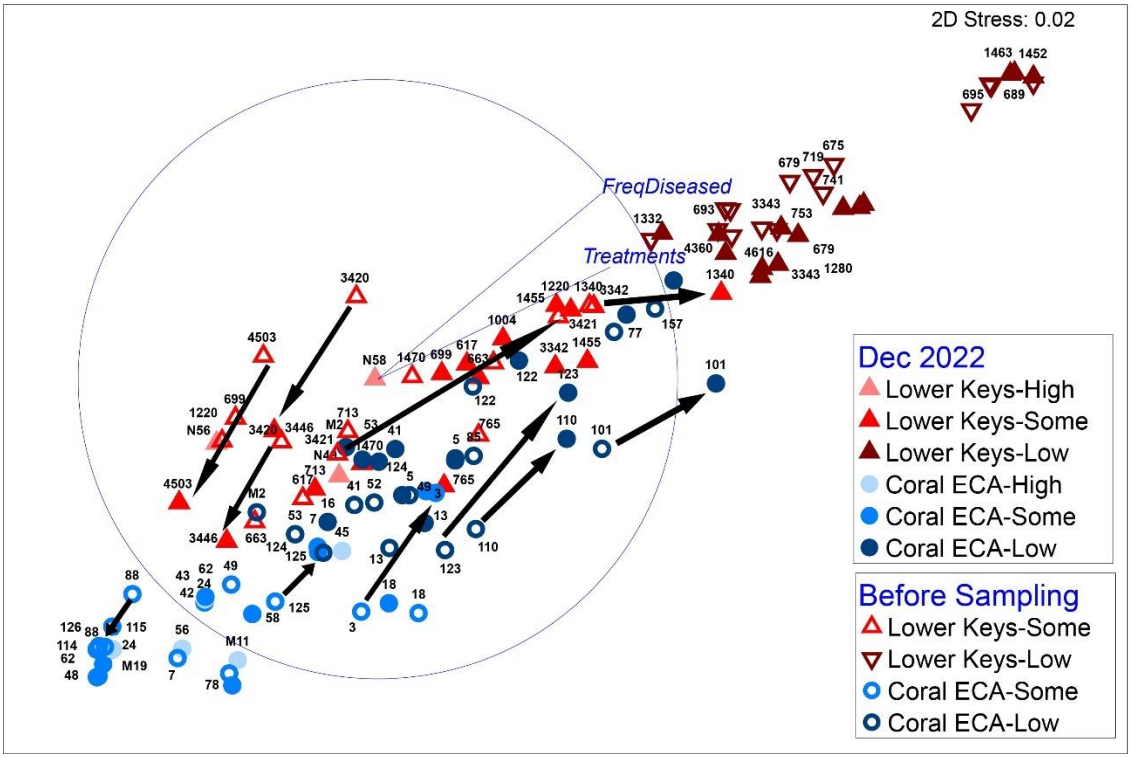

Figure 12. Combined MDS of the frequency diseased and total treatments from all 90 RRC corals before sampling and as of December 2022. Arrows indicate trajectories of certain corals from before sampling through 2022. Ones moving right had more disease and ones moving left had less.

3.2. **Histopathology (Hawthorn and Walker)**

Goal: Examination of gross cellular morphology to identify if disease pathology exists in visually apparent healthy tissue and differs by disease history, region, symbiont community, and time of year.

Significant findings: Histopathology scoring substantiated the SCTLD resistance classification. Pathology varied by time of year in the corals without previous disease lesions. Pathology temporal patterns varied by region.

Main results: Histopathological signs of disease were observed in all colonies (Figure 13). Lytic necrosis and degenerative Symbiodiniaceae varied in severity across samples and were scored accordingly (Figure 14 Figure 15). A permutational MANOVA (PERMANOVA) found significance in histopathology scoring between Sample Period, Region, and SCTLD affected/unaffected samples using lytic necrosis, mucous hyperplasia, and Symbiodiniaceae degenerative change scores as variables (Table 1). PERMANOVA tests on SCTLD affected/unaffected nested in region and did not yield any significance in sample period 1, but SCTLD affected/unaffected was significant for sample periods 2 and 3 ($p>0.01$). A MDS plot of coral samples by histopathology scores displayed by region and SCTLD affected factors illustrates these results (Figure 16). The Pearson correlation shows the variables directional influence on the plot.

Temporal differences in lytic necrosis and degenerative Symbiodiniaceae scores between SCTLD resistance categories had similar but different patterns in each region (Figure 17 Figure 18). In the ECA, the medium and high disease resistant corals had low scores in early summer (SP1), indicating a healthier state, whereas the low resistance corals had significantly higher lytic necrosis ($p>0.036$) and degenerative Symbiodiniaceae ($p=0.0766$) scores. In late summer (SP2), scores were similar with no significance across all resistance categories. In March (SP3), lytic necrosis ($p=0.0522$) and degenerative Symbiodiniaceae ($p=0.0835$) were again significantly lower in high resistance corals than low resistance corals.

Discussion: In the lower Keys, the low and medium disease resistant corals had high lytic necrosis and degenerative Symbiodiniaceae scores across all three sample periods, indicating a persistent unhealthier state. This was similar to the low resistance corals in the ECA. Unlike the ECA, the high resistance corals in the lower keys had significantly lower lytic necrosis and degenerative Symbiodiniaceae scores than the other resistance categories and in March (SP3), lytic necrosis and degenerative Symbiodiniaceae scores decreased to the healthiest state seen in any group.

In both regions, the low resistant corals always had significantly high scores that did not differ throughout the year. In the ECA, the medium and high resistance corals followed similar patterns dependent on time of year. The similarity between medium and high resistance corals in the ECA indicates that those categories are likely closer to the same state, but the medium ones in March did stay a little higher, although not significant.

In the Lower Keys, the low and medium resistance corals always had significantly high scores and the high resistant corals was always lower and drops much lower in March. This indicates that the medium and high resistance corals in the keys are a more similar state. Therefore, a new metric was to modify the resistance categories. This metric will be used in analyses throughout the project to see if they elucidate better relationships than the original three resistance categories.

The temporal patterns of histopathology scores in the high resistance categories is intriguing and potentially indicative of those corals being healthier. It also indicates the complexity behind identifying diseased corals through histology. All corals had varying levels of lytic necrosis and degenerative Symbiodiniaceae, which are some of the main indicators of SCTLD. However the more disease susceptible corals had consistently higher values compared to corals the have never had lesions, indicating that the magnitude of these indicators may be more important than just their presence.

Corals that have never had lesions were in the healthiest state in March, the period of lowest environmental stress and before gametogenesis. In the ECA in August, at the height of environmental stress, the corals exhibiting few or no previous disease showed a similar state as the diseased corals. These corals looked healthier in March and May/June. More research is needed to investigate the causes of this pattern to determine if it is environmentally driven or related to gametogenesis and spawning. In the ECA, the corals were sample right before spawning, whereas in the lower Keys they were sampled after, which could account for the differences of high resistance samples between regions in SP2.

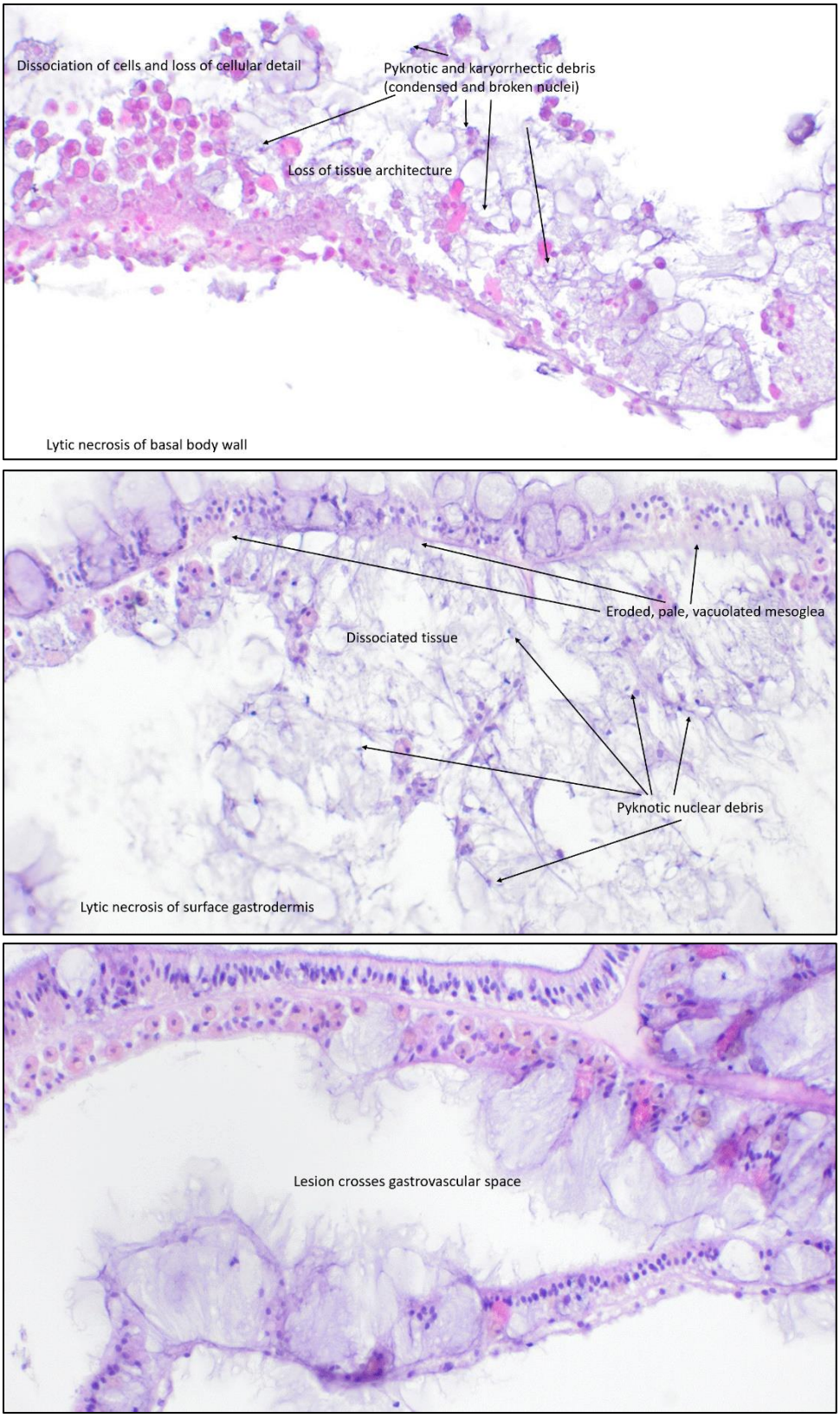

Figure 13. Histology slides illustrating pathologies.

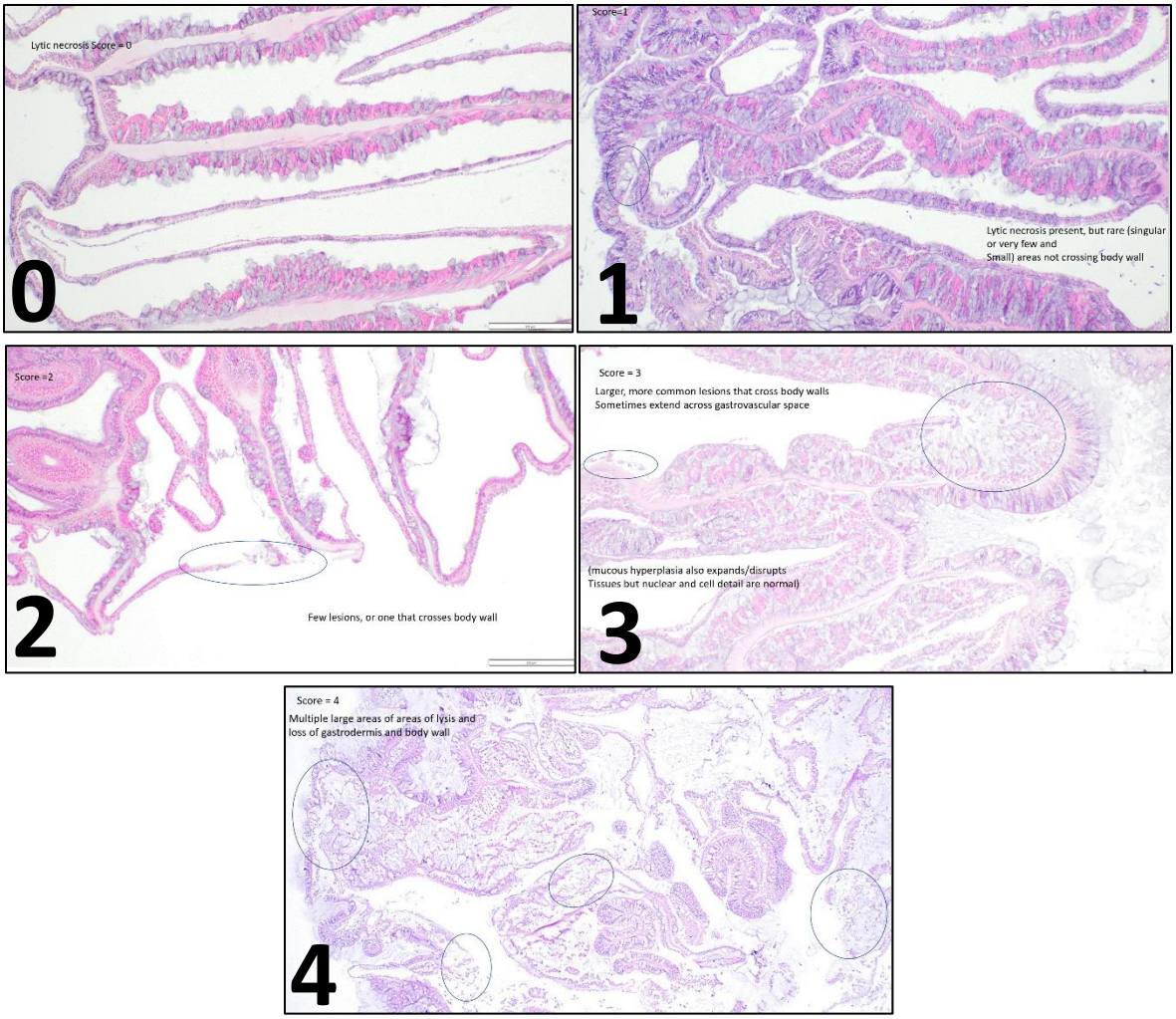

Figure 14. Histological examples of lytic necrosis scores.

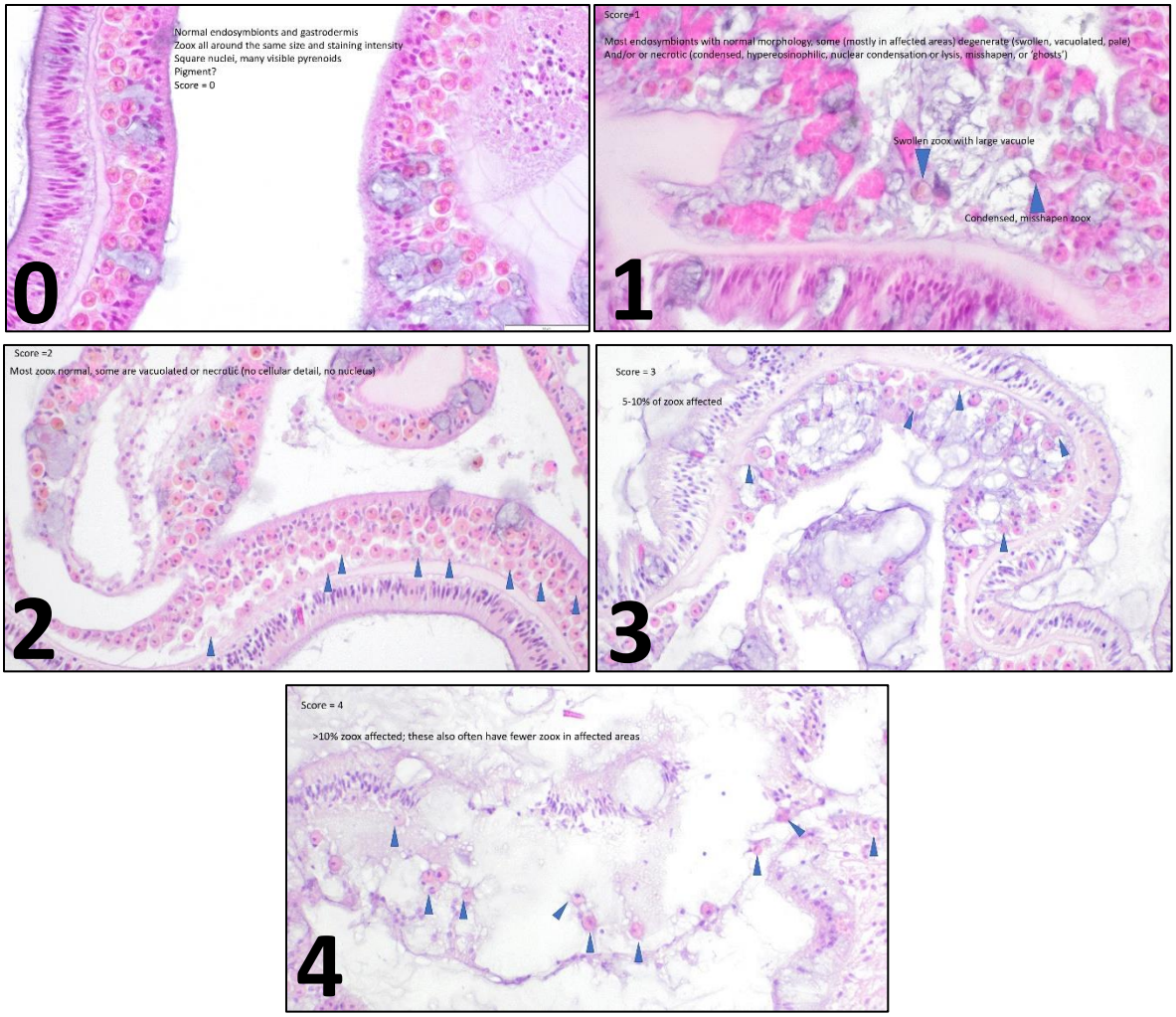

Figure 15. Histological examples of degenerative *Symbiodiniaceae* scores.

Table 1. PERMANOVA results. Bold text indicates significant tests.

Source	df	SS	MS	Pseudo-F	P (perm)	Unique perms
Sample Period (Sa)	**2**	**1669.2**	**834.6**	**5.4723**	**0.001**	**998**
Region (Re)	**1**	**589.39**	**589.39**	**3.8645**	**0.037**	**998**
SCTLD affected/unaffected (SC)	**1**	**2882.8**	**2882.8**	**18.902**	**0.001**	**999**
Sa x Re	2	454.32	227.16	1.4894	0.23	999
Sa x SC	**2**	**760.91**	**380.45**	**2.4946**	**0.051**	**999**
Re x SC	**1**	**807.83**	**807.83**	**5.2968**	**0.006**	**999**
Sa x Re x SC	2	263.77	131.88	0.86474	0.523	998

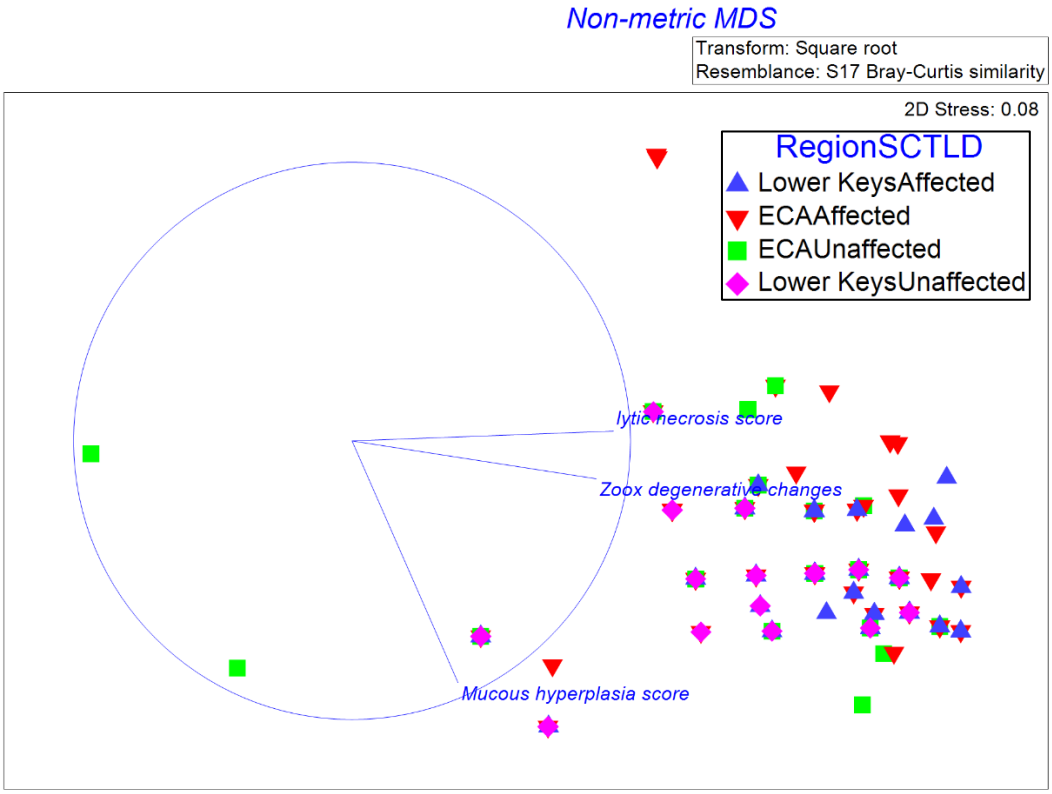

Figure 16. MDS plot of histopathology scores for each sample displayed by region and SCTLD affected factors. Pearson correlation shows the variables directional influence on the plot. The SCTLD affected colony samples had the highest lytic necrosis and degenerative Symbiodiniaceae scores.

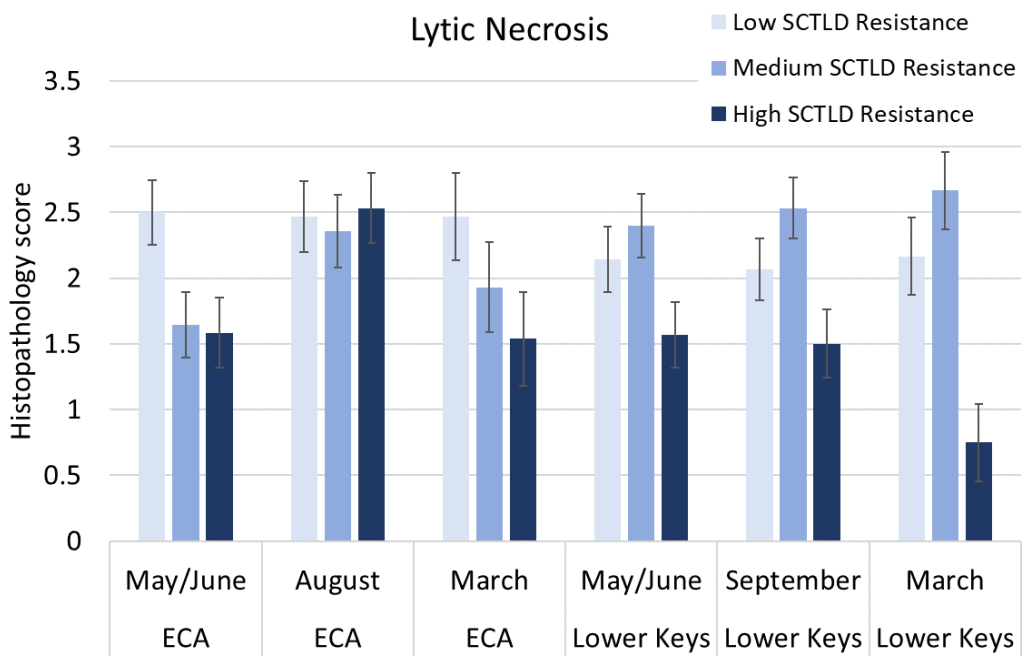

Figure 17. Mean histopathology scores for lytic necrosis between SCTLD resistance categories by region and sample period.

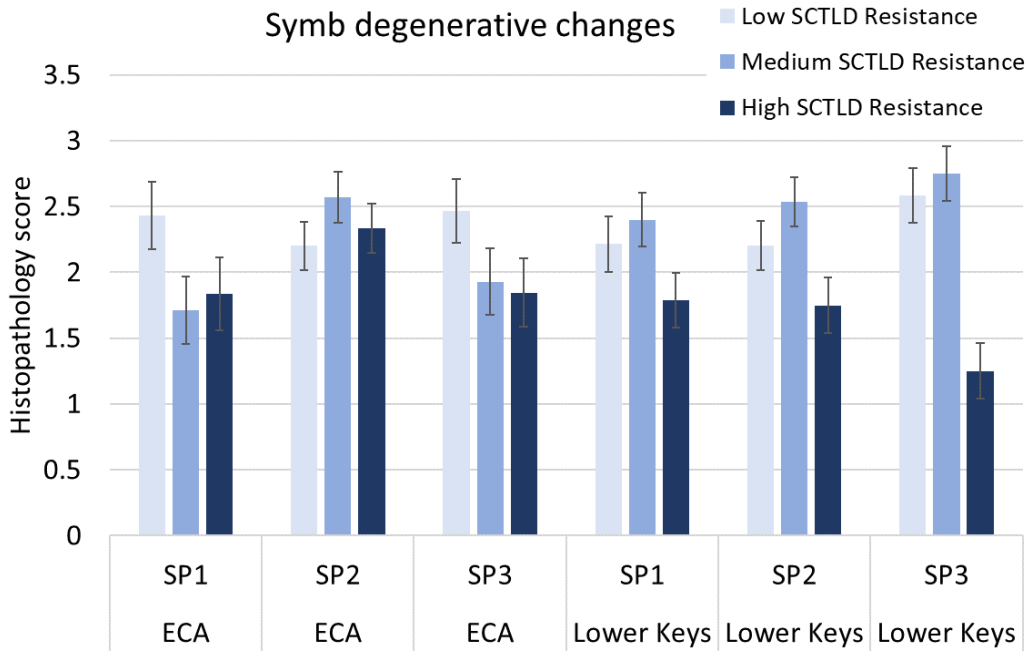

Figure 18. Mean histopathology scores for Symbiodiniaceae degenerative changes between SCTLD resistance categories by region and sample period.

3.3. **Transmission electron microscopy (Work)**

Goal: Compare lesion margin tissues and apparently normal tissues by electron microscopy examination on seven corals of varying SCTLD resistance.

Significant findings: Viral-like particles similar to those seen in previous Florida cases were present. These corals manifested evidence of significant pathology of endosymbionts associated with AVLP in both normal and abnormal tissues.

Results: Tissues were examined for deviations from expected normal morphology and changes classified as follows: For host cells, the following changes were graded as present/absent: Necrosis (Figure 19A) or mucus cell hyperplasia (Figure 19B) of gastrodermis. For endosymbionts, the following changes were graded as present/absent: Peripheral cytoplasmic vacuolation often associated with loss of detail of thylakoid membranes (Figure 19C) with enlargement of vacuoles leading to collapse of cell wall architecture (Figure 19D); variably sized intracytoplasmic cavities containing stellate anisometric viral like particles (AVLP) associated with granular matrix (Figure 19E-F) or stacks of membranes arranged in concentric laminae (Figure 20A-B). Electron dense bodies that were either homogenous (Figure 20C) or had a whorled or reticulated appearance (Figure 20D); necrotic endosymbionts (Figure 20E) or stacks of membranes dissecting between cell wall (Figure 20F).

Discussion: There was no evident pattern between non-lesion and lesioned fragments (Table 1). Both sets had notable pathology at light microscopy and ultrastructure level. The changes seen here mostly mirrored those from corals collected from Florida in 2016 and 2018 with some exceptions. Specifically, whilst stellate AVLP were evident often with accumulations of membranes in about 70% of non-lesion and lesioned fragments, we did not see coarse AVLP as in earlier studies (Work et al. 2021. Frontiers in Marine Science 8:750658) nor did we see as many instances of "putative early stage" viral infections in the form of smaller whorled electron-dense intracytoplasmic inclusions. Whilst loss of thylakoid membrane details was seen in these samples, gigantism of chloroplasts was less evident. Also, more evident in these samples in contrast to earlier studies (Frontiers 2021. 8:750658) was presence of peripheral intracytoplasmic vacuolation with more severe manifestations leading to deformation of cell wall of endosymbionts. Accumulation of membranes dissecting between cell wall of endosymbionts or accumulating in symbiosome space was less evident with this set of samples. As in previous studies (Frontiers 2021. 8:750658), coral host cell response seems limited to either necrosis or mucus cell hyperplasia mainly of gastrodermis, and host cells housing symbionts appear normal in spite of symbionts having various degrees of pathology suggesting as in earlier studies that the process seems to start with endosymbionts.

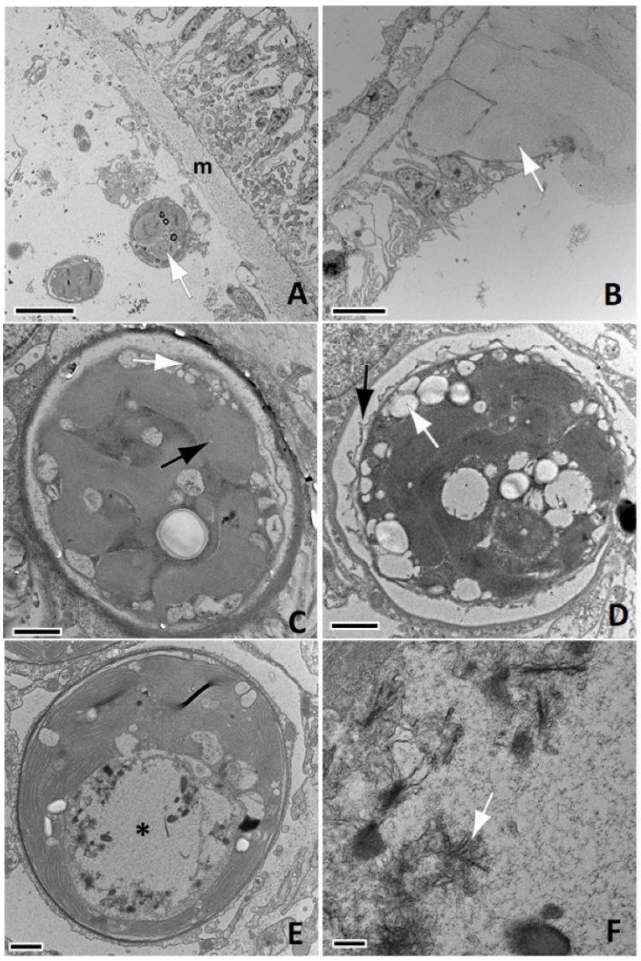

Figure 19. Ultrastructural pathology in *Orbicella faveolata*. A) Necrotic gastrodermis: Note loose endosymbionts among cell debris (arrow) with epidermis (upper right) on mesoglea (m); Bar 8 um. B) Mucus cell hyperplasia of gastrodermis (arrow); bar= 6 um. C) Peripheral cytoplasmic vacuolation (white arrow) with loss of thylakoid membrane details (black arrow); bar=1 um. C) More severe peripheral cytoplasmic vacuolation (white arrow) with crenelation and deformation of cell wall (black arrow); bar=1 um. E) Intracytoplasmic cavity (asterisk) containing stellate anisometric viral like particles (AVLP); bar=1 um. F) Detail of E; note AVLP (arrow); bar=200 nm.

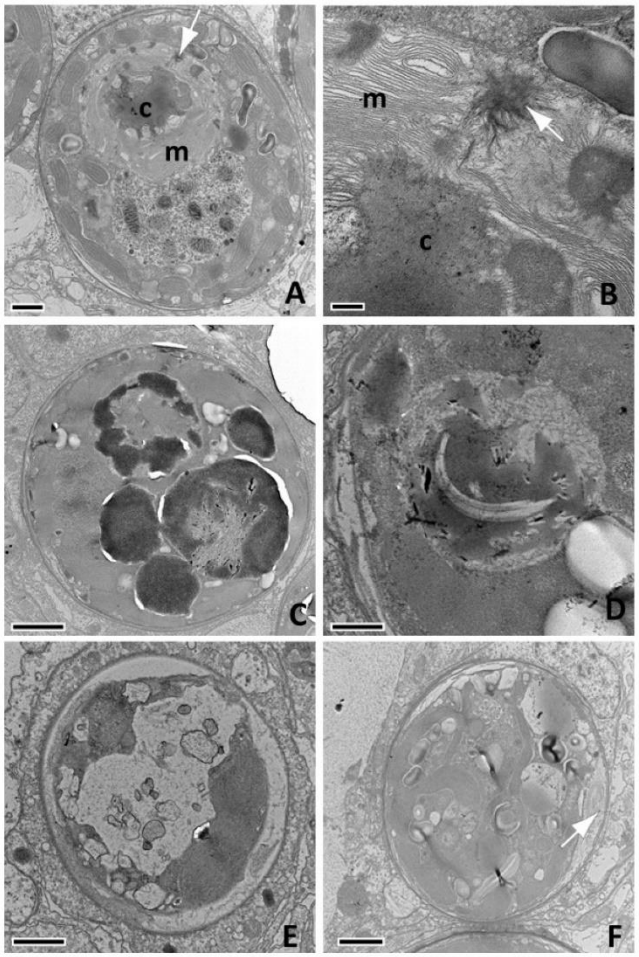

Figure 20. Ultrastructural pathology in *Orbicella faveolata*. A) Intracytoplasmic cavity containing an electron-dense core (c) surrounded by stacks of concentric membranes (m) with stellate AVLP (arrow); bar=1 um. B) Detail of A with AVLP (arrow), membranes (m) and electron dense core (c); bar=200 nm. C) Electron-dense bodies in cytoplasm; bar=2 um. D) Electron-dense bodies with whorled appearance; bar=600 nm. E) Necrotic endosymbiont; note cavity with cell debris and absence of nuclei; bar=1 um. F) Accumulations of membranes dissecting within cell wall of endosymbiont (arrow); bar=1 um.

3.4. **Genotype (Voss and Klein)**

Goal: Investigate the potential roles of individual genotypes in varying resistance to SCTLD observed among *O. faveolata* colonies on the FCR.

Significant findings: No significant genetic structuring among populations was observed indicating high connectivity and low genetic distinction between the Lower Keys and ECA *Orbicella*. A cluster of 13 colonies within 70 m near Fort Lauderdale were a clear distinct lineage from the rest of the population. There are neither uniquely SCTLD-susceptible nor SCTLD-resistant genetic lineages, even within clonal groups. Coral host genotype may not be a strong factor in SCTLD susceptibility however, we cannot rule out that other potential genetic components not captured with the streamlined 2bRAD method may underlie disease resistance status.

Results: To evaluate potential genotypic drivers for host resistant, high resolution analyses of >11,000 single nucleotide polymorphisms (SNPs) generated from 2bRAD sequencing was used. Samples that exhibited high levels of genetic similarity to one another near to the level of technical replicate groups were identified as naturally occurring genetic clones. We identified a total of 16 clones among six clonal groups (Figure 21A). There was one clonal group with five individuals, one clonal group with three individuals, and four clonal groups with two individuals (Figure 21A). Clonal groups occurred in both sample regions; within clonal groups, all samples were from the same study site, yet there was varying disease susceptibility status within some clonal groups (Figure 21A).

After the removal of clones and technical replicates, two outgroups remained (Figure 21B on the left). One group consisted of three colonies from Sand Key, which had the highest genetic distance from the rest of the samples. These samples were subsequently identified as colonies of the congener *O. franksi* based on further *in situ* observations. This information was passed along to the consortium with the guidance to remove these samples from analyses. The second outgroup cluster included colonies that were all from the ECA cluster collection site. This distinct lineage of *O. faveolata* colonies were closely related but were not genetic clones (Figure 21B).

After clones, technical replicates, and *O. franksi* samples were removed, ANGSD was re-run, and a total of 11,733 SNPs were identified. Two tight clusters were identified by PCoA, the first consisting of the North ECA outgroup and the second consisting of the remaining colonies from the other sites (Figure 22A). To better visualize potential differences among these other sites, a second PCoA was conducted with the ECA cluster outgroup removed and showed no distinct differentiation or clustering among individuals according to disease susceptibility (Figure 22B). The Analysis of Molecular Variance (AMOVA) indicated significant differentiation among sample region, explaining 5.93% of the total genetic variation across samples ($p = 0.01$). However, there was no significant differentiation among SCTLD affected and unaffected colonies.

Pairwise F_{ST} values also indicated that the ECA cluster site was significantly differentiated from all other regions (Figure 23), consistent with the clustering exhibited in the PCoA. Pairwise F_{ST} values demonstrated no significant differentiation among colonies of differing disease susceptibility status.

Both Clumpak and StuctureSelector *K* selection approaches identified the optimal number of genetic clusters as $K = 2$ (Figure 24). The genetic structuring among populations aligned with similarities found in the PCoA plots and pairwise F_{ST} analyses. The ECA cluster site was dominated by the genetic cluster indicated in yellow while all other sites were dominated by a second genetic cluster indicated in blue (Figure 24). The same analysis was re-run with the North ECA colonies removed as a quality check and no significant genetic structuring among populations was observed.

Discussion: Results from this study suggest that there are neither uniquely SCTLD-susceptible nor SCTLD-resistant genetic lineages within *O. faveolata* in South Florida. Rather, across the sampled populations, each genetic lineage we identified included both SCTLD-affected and SCTLD unaffected colonies. Even within clonal groups we observe both SCTLD affected and

unaffected colonies. Having genetically identical individuals with differing disease phenotypes suggests that coral host genotype may not be a strong factor in SCTLD susceptibility on the FCR.

It should be noted that the 2bRAD method is by design a rapid and reduced-representation approach which randomly targets a relatively small subset of the entire genome. Therefore, we cannot rule out that other potential genetic components may underlie disease resistance status which may not have been captured with the streamlined 2bRAD method. Future efforts could specifically target gene regions with known involvement in coral immunity or employ increasingly cost-accessible whole-exome or whole-genome sequencing approaches for genome-wide association studies.

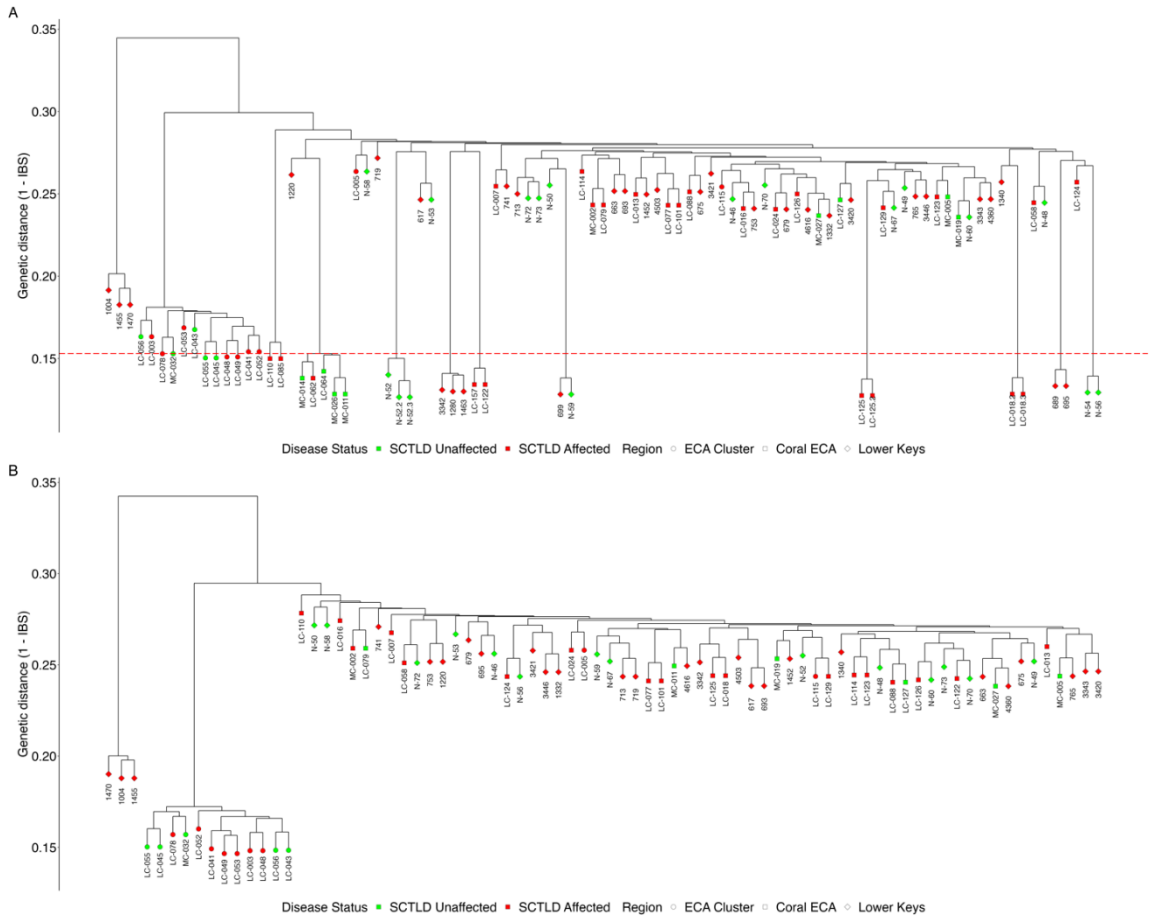

Figure 21. Dendrograms identifying clusters of samples based on Identity-by-State matrix calculations; **A** dataset with clones, **B** clones-removed dataset. Collection site is denoted by shape, disease susceptibility status is denoted by color. The dashed red line indicates the minimum genetic distance threshold for clonal groups. Technical replicates denoted by "*", clonal groups denoted by letter.

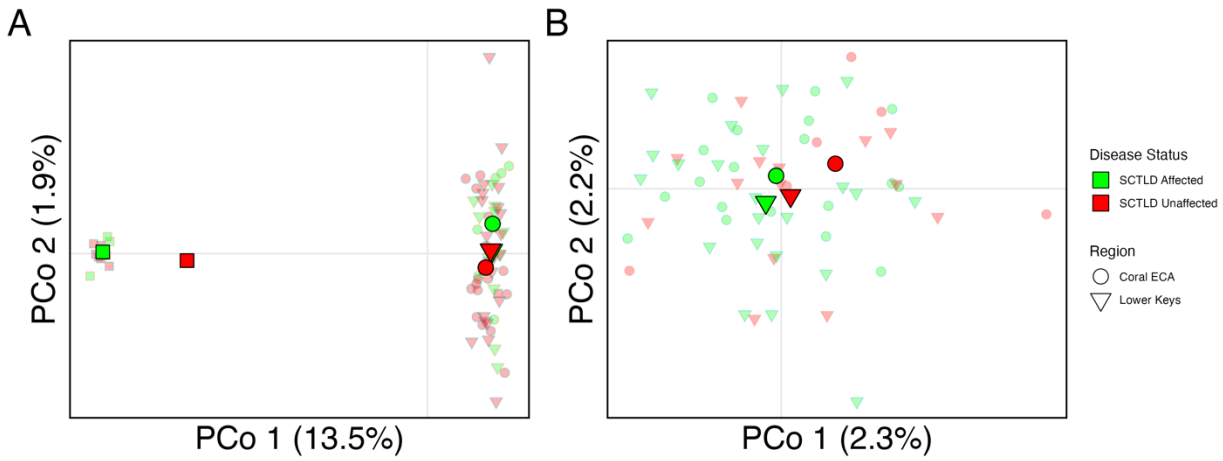

Figure 22. Principal coordinates analysis showing clustering of samples by disease susceptibility status (color) and region (shape). Individual samples are represented by transparent points. Population centroids are indicated by solid points. Percent variation is explained by each axis. "A" represents all samples, "B" showing outlier ECA cluster samples removed.

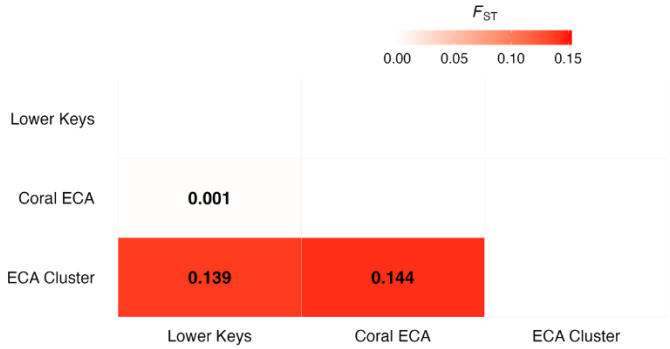

Figure 23. Pairwise fixation index values (F_{ST}) for all sample sites displayed as a heat map. Statistically significant values are bolded (post FDR-correction, $p < 0.05$).

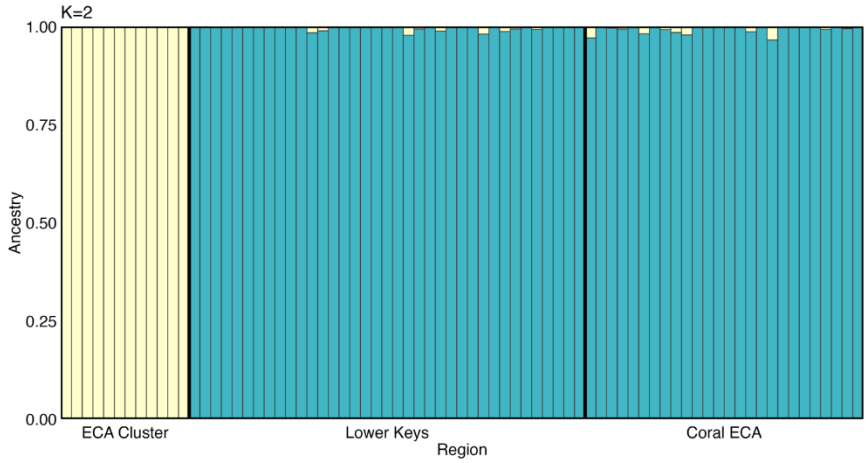

Figure 24. Population structure model (K = 2) generated by admixture analyses using genotype likelihoods. Genetic clusters are represented by the colors blue and yellow. Region denoted on x-axis.

3.5. **Symbiodiniaceae (Baker, Dennison, Voss, and Klein)**

Goal: Identify differences in Symbiodiniaceae between SCTLD resistance categories.

Significant findings: No significant differences were found in symbiont to host cell ratios (S:H) between SCTLD-affected and SCTLD-unaffected colonies. There was a significant relationship between S:H and dominant Symbiodiniaceae genus, with corals predominantly associating with *Breviolum* having higher S:H than those associating with *Cladocopium* or *Durusdinium*, perhaps due to the smaller cell size of *Breviolum*. Temporal changes in Symbiodiniaceae were minor and may have reflected small spatial differences in sampling rather than directional seasonal changes. 2bRAD analyses yielded different results from qPCR including the presence of Symbiodinium. To better resolve species-level Symbiodiniaceae community structure, a subset of samples were selected for ITS-2 sequencing. All 90 colonies from the first sample period and 14 samples from seven colonies in the unified sample dataset were chosen for analysis across all three sample periods. Depending on the ITS-2 results, the remainder of samples might need sequencing.

Results:

Algal Symbiont Analysis via qPCR (Baker and Dennison)

Extracted DNA was analyzed using an actin-based real-time PCR (qPCR) assay for algal symbiont identification (to the genus level) and quantification of *Symbiodinium*, *Breviolum*, *Cladocopium*, and *Durusdinium*. Symbiodiniaceae community composition and symbiont to host cell ratios were summarized for each sample period (SP). No *Symbiodinium* were detected in any coral samples over the course of the monitoring period. Of the N=90 coral colonies monitored for this project, 82 (>91%) predominantly associated with *Breviolum* across all sample points, with the remaining colonies associating with *Cladocopium* or *Durusdinium* (Figure 25,
Table *2*). Some low-level differences in Symbiodiniaceae community across sample periods were found. Two colonies that were originally dominated by *Breviolum* in the first sampling period changed to domination by other symbionts by the third sample period. Overall, changes in Symbiodiniaceae were minor and may have reflected small spatial differences in sampling (Table 3), rather than directional seasonal changes.

Symbiont to host cell ratios provided estimates of symbiont density (or "load") to better understand whether SCTLD dynamics (i.e., incidence, severity, etc.) were exacerbated by increased algal symbiont densities. No significant differences were found in S:H between SCTLD-affected and SCTLD-unaffected colonies (Figure 26). Additionally, temporal differences in S:H were not apparent, which has previously been suggested (Cunning & Baker 2013). However, there was a significant relationship between S:H and dominant Symbiodiniaceae genus, with corals predominantly associating with *Breviolum* having higher S:H than those associating with *Cladocopium* or *Durusdinium*, perhaps due to the smaller cell size of *Breviolum* (Figure 26).

Algal Symbiont Analysis via 2bRAD (Voss and Klein)

DNA from the genotyping also yielded algal symbiont DNA. Therefore, this was co-extracted and prepared into 2bRAD libraries. To isolate coral host sequences from algal sequences, high-quality 2bRAD reads were first mapped to a concatenated Symbiodiniaceae metagenome with the software package *Bowtie 2* (Langmead et al. 2009). These reads were then aligned to the *O. faveolata* genome (Prada et al. 2016). Sequence reads that mapped to both the Symbiodiniaceae

metagenome and the *O. faveolata* genome were discarded from subsequent analyses. Relative alignment rates to each of the four symbiont genomic references (*Symbiodinium microadriacticum, Breviolum minutum, Cladocopium goreaui, Durusdinium trenchii)* were used as a proxy for the relative abundance of the four algal symbiont genera associated with each colony. A permutational multivariate analysis of variance (PERMANOVA) was run to determine significance in beta diversity across differing disease susceptibility status as well as across sites. Abundances of each symbiont genera were square root transformed for this PERMANOVA to minimize influence of the most abundant symbiont group. A Welch's Two-Sided t-test was run to identify significance in differing abundance of the four symbiont genera among disease susceptibility status.

Overall, the majority of reads that aligned to the algal symbiont genomes aligned to *Breviolum* (Figure 27). However, all colonies dominated by *Durusdinium* (7) fell under the SCTLD-affected category (Figure 27a). A Welch's Two-Sided t-test found that *Durusdinium* was more abundant in SCTLD-susceptible colonies as compared to SCTLD-resistant colonies ($t = 3.478$ $p < 0.001$). There was no significant difference in abundance among the three other symbiont genera. Clonal groups also had variation in dominant symbiont taxa (Table 4). Clonal group 'a' had three individuals dominated by *Breviolum* and two samples dominated by *Cladocopium*. Clonal group 'e' had one individual dominated by *Breviolum* and one individual dominated by *Durusdinium* (Table 4).

ECA cluster samples were exclusively dominated by *Breviolum* while all other sites had a few colonies dominated by either *Cladocopium* or *Durusdinium* as well (Figure 27b). Site, disease status, and the interaction of the two all had a significant effect on algal symbiont beta diversity (PERMANOVA $F = 0.005, 0.24, 0.24$ respectively).

Discussion: More work is needed to understand the Symbiodiniaceae relationships in the unified core samples. Conflicting data between 2bRAD and qPCR were found. qPCR found small to no amounts of species other than *Breviolum* in the samples. More resolution was found with 2bRAD, but it was only run on the SP1 DNA from the genotype samples. The colony variability samples showed temporal differences in S:H ratios, but these were not as evident in the unified cores. Initial SCTLD resistance categories did not elicit any statistical relationships to specific symbionts. Therefore, more resolution in symbiont identification and quantification is needed.

Clonal *O. faveolata* groups harboring different dominant symbiont genera suggest that symbiotic communities rather than coral host may be driving SCTLD susceptibility in *O. faveolata.* Genetic clones would be hypothesized to have similar disease responses, however in this study, some members within clonal groups had variable disease susceptibilities. Clones harboring different dominant algal symbiont taxa may be linked to variation in disease status, however further investigation into this hypothesis is needed. *Orbicella faveolata* has been known to harbor multiple algal symbiont genera simultaneously across different areas of the colony. Ongoing research within the RRC is investigating how a mosaic algal symbiont community structure may be impacting SCTLD susceptibility in *O. faveolata* and further characterizing algal symbiont community structure with ITS2 markers.

Table 2. Number and percentage of samples predominantly associated with *Breviolum*, *Cladocopium*, and *Durusdinium* across all three sample points (SP1, SP2, SP3).

	# of colonies	% of colonies
Breviolum	242	90.6
Cladocopium	11	4.1
Durusdinium	14	5.2

Table 3. Number and percentage of colonies associating with *Breviolum*, *Cladocopium*, and *Durusdinium* across all three sample points (SP1, SP2, SP3).

	SP1	SP2	SP3
Breviolum	84	80	78
% Breviolum	93.3	89.9	88.6
Cladocopium	2	4	5
% Cladocopium	2.2	4.5	5.7
Durusdinium	4	5	5
% Durusdinium	4.4	5.6	5.7

Figure 25. Symbiodiniaceae associations across the 90 RRC unified coral colonies. Each panel represents a coral colony within which there are three sampling periods defined SP1, SP2, and SP3. Each bar represents the Symbiodiniaceae community composition. The majority of colonies across all sample points predominantly associate with *Breviolum*.

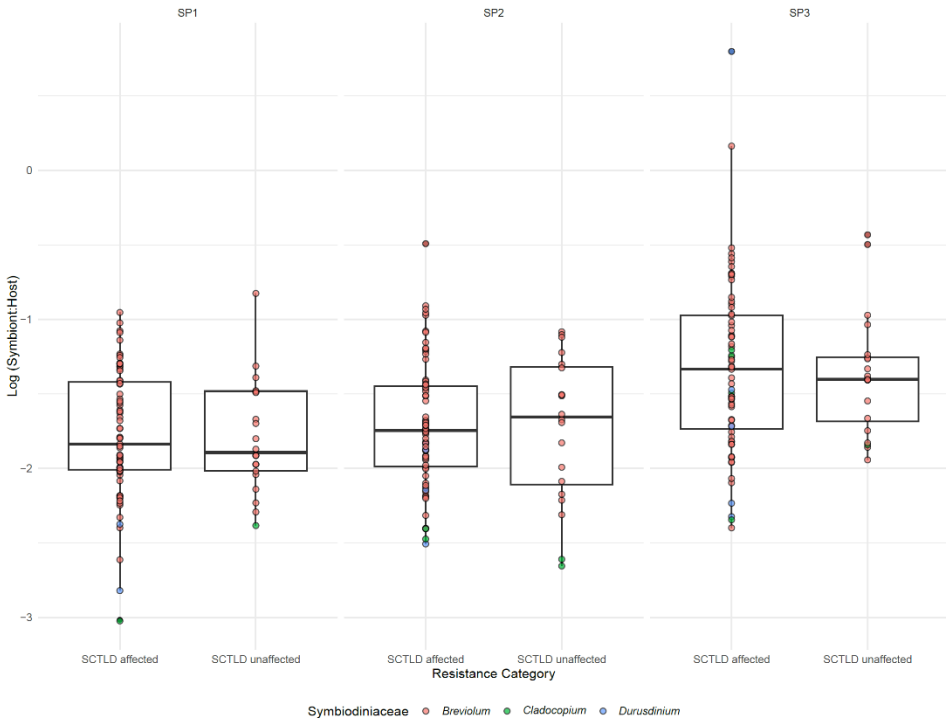

Figure 26. Symbiont to host (S:H) cell ratios across all 90 RRC unified coral colonies. S:H was compared both across sample periods (SP1, SP2, and SP3) between SCTLD affected and unaffected colonies. The resistance category (affected vs unaffected) was defined by the presence of SCTLD lesions of the entire monitoring period of each coral, which precedes the monitoring and sample period of this project.

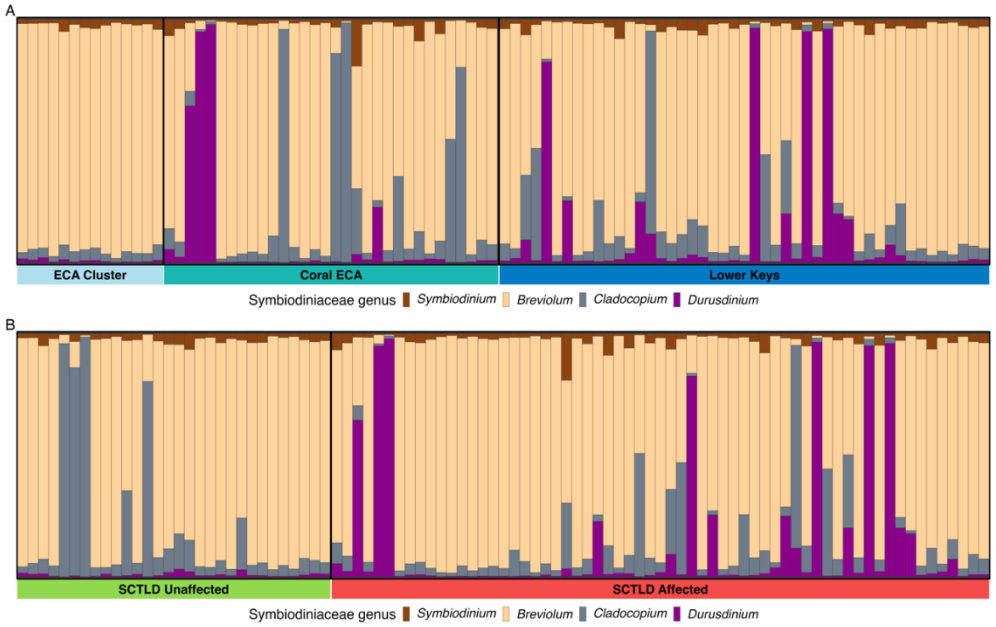

Figure 27. Bar plot representing the proportion of algal symbionts for each coral sample based on mapped reads to genomes of four different genera of algal symbionts, *Symbiodinium*, *Breviolum*, *Cladocopium*, and *Durusdinium*. Groupings are separated out by region **A** and disease susceptibility status **B**.

Table 4. Table displaying six identified clonal groups with disease status, collection site, and dominant symbiont taxa for each individual noted.

Clonal Group	Sample ID	Disease Status	Region	Dominant Symbiont
a	OF_029	SCTLD Unaffected	Coral ECA	*Breviolum*
	OF_037	SCTLD Unaffected	Coral ECA	*Breviolum*
	OF_038	SCTLD Unaffected	Coral ECA	*Breviolum*
	OF_044	SCTLD Affected	Coral ECA	*Cladocopium*
	OF_045	SCTLD Unaffected	Coral ECA	*Cladocopium*
b	OF_071	SCTLD Affected	Lower Keys	*Breviolum*
	OF_076	SCTLD Affected	Lower Keys	*Breviolum*
	OF_078	SCTLD Affected	Lower Keys	*Breviolum*
c	OF_002	SCTLD Affected	Coral ECA	*Breviolum*
	OF_025	SCTLD Affected	Coral ECA	*Breviolum*
d	OF_053	SCTLD Affected	Lower Keys	*Breviolum*
	OF_069	SCTLD Unaffected	Lower Keys	*Breviolum*
e	OF_050	SCTLD Affected	Lower Keys	*Durusdinium*
	OF_052	SCTLD Affected	Lower Keys	*Breviolum*
f	OF_066	SCTLD Unaffected	Lower Keys	*Breviolum*
	OF_067	SCTLD Unaffected	Lower Keys	*Breviolum*

3.6. **Microbiome (Voss and Klein)**

Goal: Investigate the microbial community composition in varying resistance to SCTLD observed among *O. faveolata* colonies in South Florida.

Significant findings: Initial analyses of the microbial community from SP3 did not show community structure related to region or SCTLD resistance. Sequencing for SP 1 and 2 did not yield usable data. We are working towards resequencing extracted DNA for all sample periods at a different facility with consistent extraction methods.

Results: Sample periods 1 and 2 were sequenced together and sample period 3 was sequenced later. There was variation among the produced read quality between the two sequencing runs. After trimming off sequence adapters and locus primers, there was an average of 77,197 reads per sample for SP 1 and 2. The errors for this sequencing run were unusually high and an average of only 264 reads per sample passed through filtering parameters. In this run, there were a lot of shorter sequences that clustered to the sequencer. This made it difficult to merge forward and reverse reads as there was limited to no sequence overlap resulting in only an average of 121 reads per sample. All reads from this sequencing run were deemed unsuitable for further downstream analyses.

SP 3 samples were library prepped and sequenced independently. After trimming off sequence adapters and locus primers, there was an average of 133,839 reads per sample. Errors for this sequencing run were better than SP 1 and 2 but still high. However, longer higher quality reads were present resulting in an average of 14,660 reads after filtering, and 11,812 reads after merging forward and reverse reads.

After quality filtering and merging of sequences, microbiomes were characterized for 86 of the 90 samples. The program phyloseq calculated 791 taxa from 79 different Families and 47 unique Orders.

Microbial community structure did not appear to correlate to disease susceptibility status or sample region (Figure 28). Relative abundances of amplicon sequence variants (ASVs) did not vary between SCTLD-affected and SCTLD-unaffected corals (Figure 29). Dispersion of beta diversity was examined according to SCTLD affectedness and across regions (Figure 30). Analysis of variance of the linear model indicated that beta diversity dispersion was not significantly different between SCTLD affectedness ($p= 0.53473$), sample region ($p= 0.23105$), or the combination of these factors ($p=0.07329$).

Discussion: Initial analyses of the microbial community from SP3 did not show community structure related to region or SCTLD resistance. Investigations are ongoing as to how to proceed with SP 1 and 2 samples. The goal is to use the extracted DNA and re-sequence the samples. Continued collaborative work within the RRC will help determine if specific microbial taxa are related to SCTLD susceptibility. Ongoing discussions with RRC partners, sequencing facilities, and DEP, will determine if resequencing for all three timepoints is warranted and beneficial.

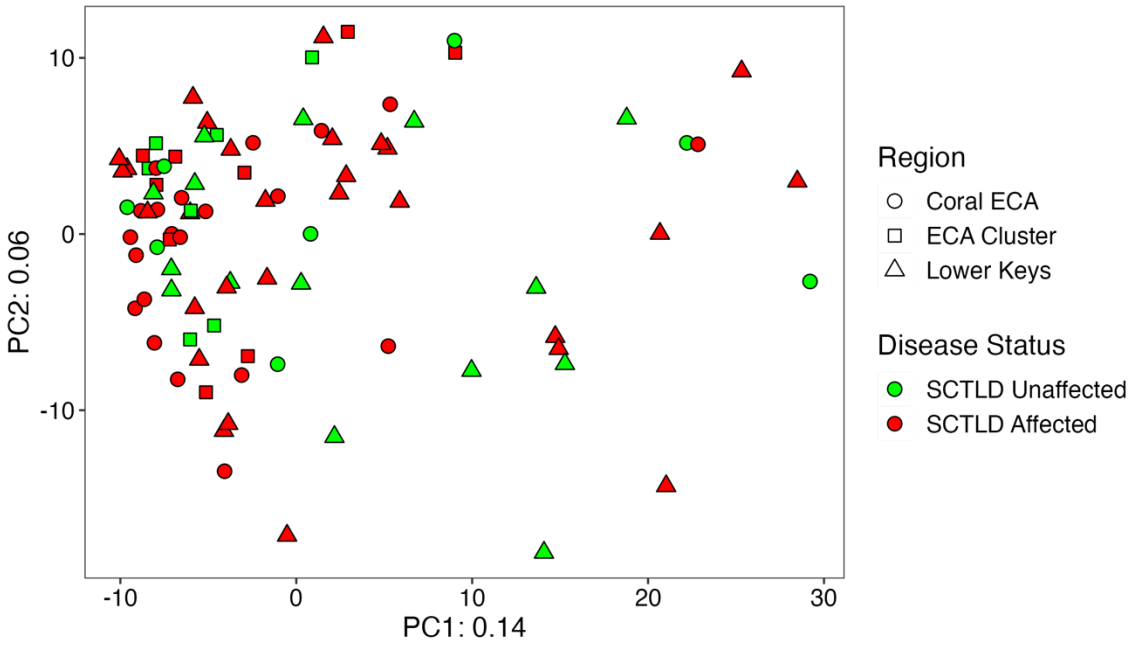

Figure 28. Principal component analysis of microbial community structure. Disease susceptibility status is indicated by color, sample region is indicated by shape.

Figure 29. Relative abundance of amplicon sequence variants, colored by Order, in each sample region. (A) Represents SCTLD Unaffected corals, and (B) represents SCTLD affected corals.

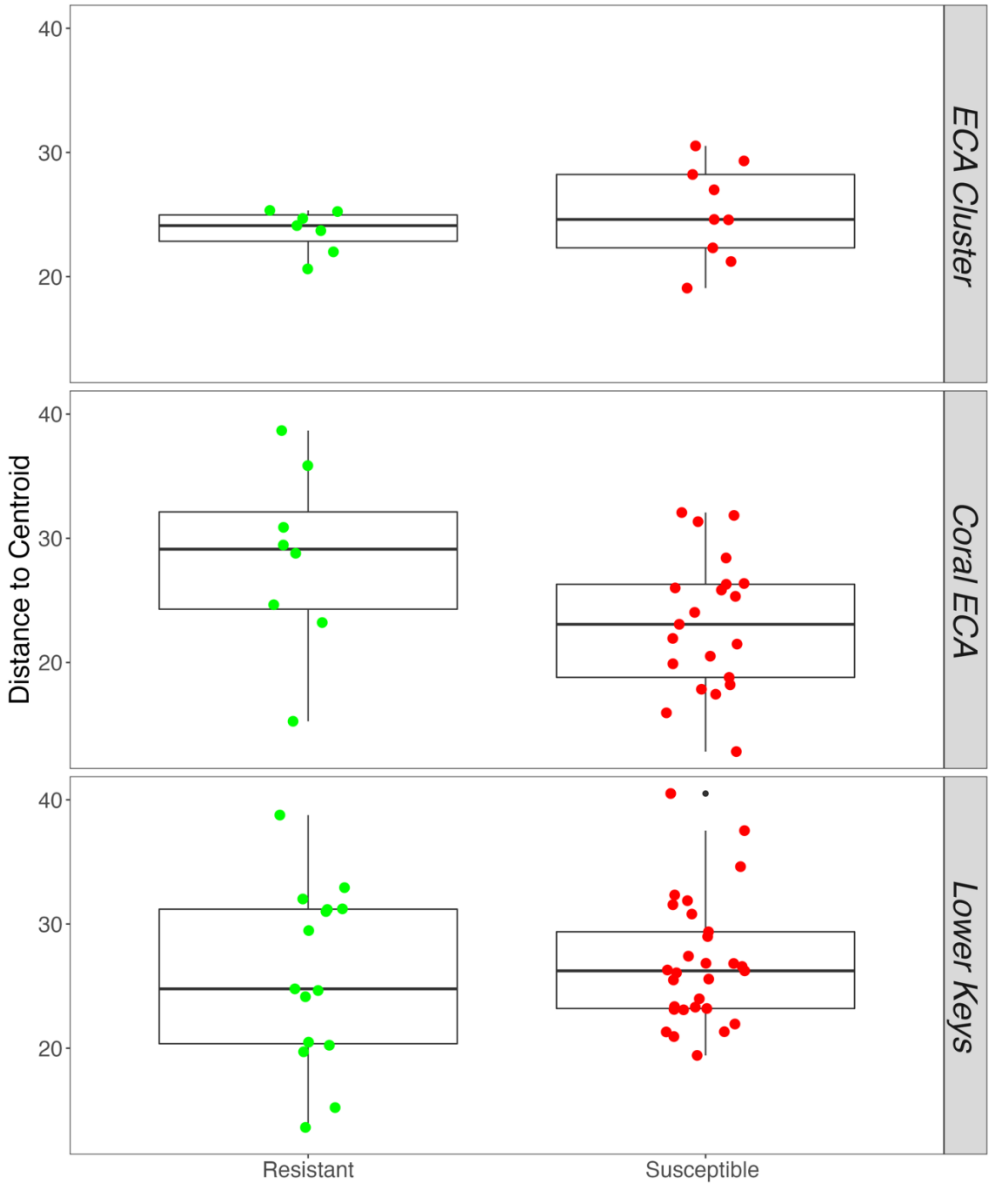

Figure 30. The dispersion of beta diversity shown as the distance to the centroid in microbial communities from resistant and susceptible corals from all sample regions.

3.7. **Bacterial metagenome (Meyer and Cauvin)**

Goal: Characterize functional genes of microbial communities.

Significant findings: None. The data are still being processed.

Results: Metagenomic libraries were successfully sequenced for 89 out of 90 samples collected during sample period 1 (May/June 2021). One high resistance sample (N-49) from Sand Key had an insufficient quantity of DNA for sequencing. An average of 123 million reads were obtained for each library (~2 Tb of data total). The original sequencing reads are publicly available in NCBI's Sequence Read Archive under BioProject PRJNA925892.

After sequencing, libraries go through a series of bioinformatics steps that include: 1) quality-filtering of the reads, 2) mapping of the reads to the publicly available *O. faveolata* genome (GCA_001896105.1) and removing the *O. faveolata* reads from the libraries, 3) mapping of the non-*O. faveolata* reads to the publicly available *Breviolum* genome (GCA_000507305.1) and removing the *Breviolum* reads from the libraries, and 4) assembly of the reads remaining after removal of *O. faveolata* and *Breviolum* reads. For this dataset (~ 2 Tb of data), the first step takes about 1 hour per library, the second step takes about 4 hours per library, the third step takes about 15 hours per library, and the fourth step takes about 2.5 days per library. These steps and additional assessments to examine the data quality at each step result in a minimum computational time of roughly 4 days per library. Some processes may be run concurrently to reduce the total computational time, but memory-intensive steps like the assembly will likely need to be run consecutively, requiring months to complete.

The 89 libraries were randomly divided into four equal groups and the first three steps described above have been completed for the first quarter of samples (22 total). After removal of *O. faveolata* and *Breviolum* reads, the phylogenetic composition of the remaining reads was assessed and showed that 4-6% of reads were bacterial, consistent with our mini sequencing run results. This translates to roughly 3 million 150-bp bacterial reads per library or approximately 10X coverage of 10 bacterial genomes per library. The remaining unclassified and eukaryotic reads are likely part of the *O. faveolata* and *Breviolum* genomes that were not effectively removed. While our methods enriched the bacterial content of the metagenomic libraries, this clearly did not eliminate all or even most eukaryotic reads in the sequenced libraries. Therefore, the dataset produced can also be useful for additional applications and analyses, including the improvement of *O. faveolata* and *Breviolum* genome assemblies or comparisons of genetic differences across eukaryotic hosts.

At the Disease Advisory Committee meeting on 3/22/23, NOAA researchers Michael Studivan and Ben Young presented their results for a greatly improved genome assembly for *O. faveolata.* We will therefore use this improved genome assembly for mapping and removing *O. faveolata* reads before metagenomic assembly of bacteria-enriched reads. The final metagenomic assemblies will be deposited in the IMG database.

3.8. *Vibrio coralliilyticus* presence and concentration (Meyer and Cauvin)

Goal: Quantify the presence of *Vibrio coralliilyticus* and look for associations to SCTLD resistance.

Significant findings: It is likely that SP 1 and 2 in these results are inaccurate due to the issues described in the microbiome section above. We are taking steps to check the validity of the data and redo this aspect if necessary.

Results: *Vibrio coralliilyticus* abundance did not coincide with colony resistance levels. The concentration of the vibriolysin gene *vcpA* was not significantly different among *a priori* resistance categories (Figure 31) or SCTLD affected and unaffected (Figure 32), regardless of sample period. This suggests that disease susceptibility is not being driven by the presence of the coral pathogen *Vibrio coralliilyticus* in these coral colonies.

Vibrio coralliilyticus abundance was highest in sample period 3. The vibriolysin gene *vcpA* was present in very low levels across most samples in sample period 1 and 2. In contrast, copies of the *vcpA* gene were present in significantly higher levels during sample period 3 (February - March 2022) ($p < 0.001$) (Figure 33). The increased abundance of the vibriolysin gene *vcpA* was higher during sample period 3, regardless of whether the colonies were affected by SCTLD during the study period (Figure 32).

We previously demonstrated that while *V. coralliilyticus* can exacerbate SCTLD infections, it is not the primary pathogen of SCTLD. Here, we found that the abundance of *V. coralliilyticus* was very low in two of three sample periods and did not coincide with observations of SCTLD. However, the increased abundance of *V. coralliilyticus* did coincide with observations of increased antimicrobial activity against vibrios in sample period 3 (see Task 8 by Dr. Paul). Further analysis and interpretation of these findings for sample period 3 will be pursued and will likely result in a peer-reviewed publication.

Discussion: Given the low presence and absence of *V. coralliilyticus* in SP 1 and 2, it is unlikely that the results are valid. We will work towards a resolution to this before moving forward with more analyses.

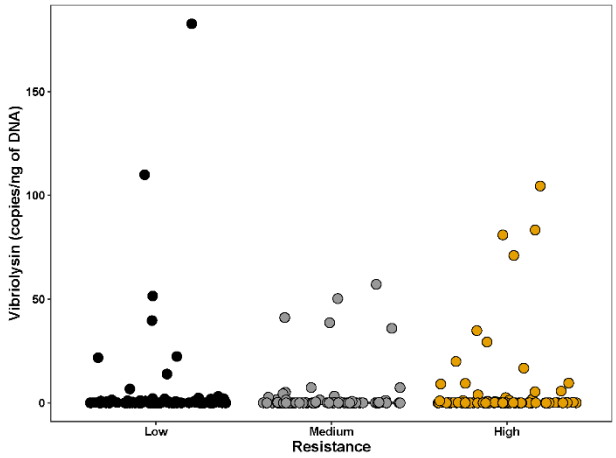

Figure 31. The concentration of the vibriolysin gene vcpA was not significantly different among corals of differing resistance to SCTLD (Kruskal-Wallis chi-squared = 0.61274, df = 2, p-value = 0.7361).

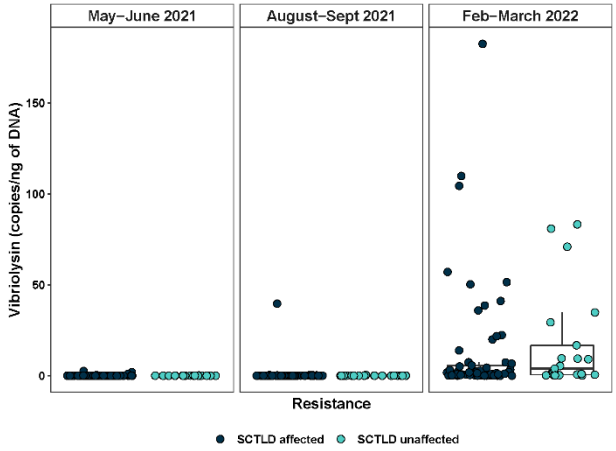

Figure 32. The concentration of the vibriolysin gene vcpA was not significantly different among corals affected by SCTLD versus unaffected during the study period. (Wilcoxon rank sum test with continuity correction of affected versus unaffected corals in period 3 only, W = 544, p-value = 0.1408).

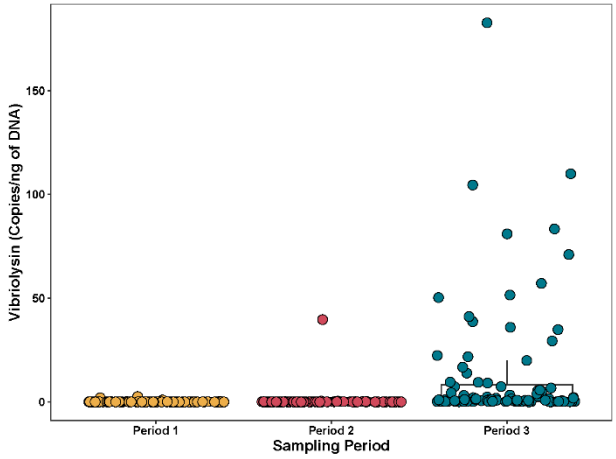

Figure 33. The concentration of the vibriolysin gene vcpA was significantly higher (Friedman chi-squared = 122.8, df = 2, p-value < 2.2e-16) during sample period 3 (February - March 2022), regardless of disease resistance level.

3.9. **Chemical Defenses (Paul)**

Goal: Chemical extraction, antimicrobial assays, and compound characterization to understand the level of antimicrobial defenses in each coral sample for each period.

Significant findings: The highest antimicrobial activity coincided with the period of lowest thermal stress (SP3) and was highest in SCTLD unaffected corals. Zones of inhibition were lowest in May/June (SP1). The differences between affected and unaffected corals were not significant in SP1 and increased and widened between sample periods.

Results: Temporal changes in the bioactivities of the nonpolar ethyl acetate (EtOAc) partition significantly increased with each sample period. Sample period 3 had the highest antimicrobial activity for the nonpolar partition (Figure 34). The corals that had been previously affected by SCTLD had lower antimicrobial activity than those that had never been affected.

Discussion: Zones of inhibition are indicative of the corals' ability to fight infection. Times of low inhibition indicate that the coral is less able to fight infections than times with high inhibition. The temporal variation of inhibition requires further research to relate them to environmental stressors or other aspects of the RRC. The partitioning of the extracts was an important first step in the bioassay-guided separation process. Further separations and testing with *Vibrio coralliilyticus* have been done on a subset of ~ 6 of the EtOAc partitions. These will be examined further for compounds of interest that show antimicrobial activity.

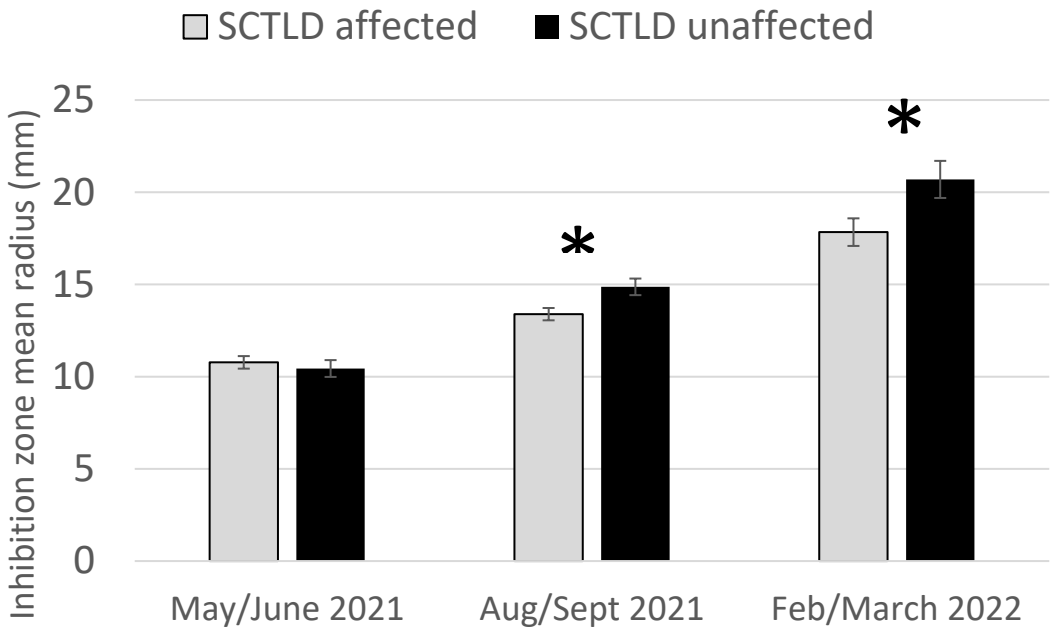

Figure 34. The zone of inhibition from disk diffusion assays with *Vibrio coralliilyticus* OfT6-21 of nonpolar partitions of the extracts of *Orbicella faveolata* were significantly different between SCTLD affected and SCTLD unaffected. The differences between affected and unaffected corals widened between sample periods.

3.10. **Transcriptome (Traylor-Knowles and Andrade)**

Goal: Process and analyze the transcriptomic response of the coral host in each coral for each period.

Significant findings: These preliminary results suggest that corals with low and some resistance to SCTLD have a fingerprint of the effects in their gene expression that might contribute to recurrent infections. We obtained 50 unique genes differentially expressed amongst all the comparisons. These genes could play a role in the type of response to SCTLD that these colonies have had. 25 of the 50 DEG have unknown functional annotations. More analysis is needed, especially with regard to region and sample period, to determine how the whole transcriptome is involved with the regulation of these genes.

Results: We used DEseq2 (version 1.38.3, Love et al., 2014) to model the data and obtain genes differentially expressed between the different categories used to characterize the phenotypic response to SCTLD exposure. Considering the complexity (different sample periods and phenotypic categories) and genetic diversity (2 populations of *O. faveolata*, different regions) of this data set, we performed several models to set the best fit of our data. The model that best fit our data corresponded to the one using the combination of the resistances categories as a factor "Both_Resistance" as well as the "Species" (distinguishing the distinct lineage group identified in the genetics task) and "Sample_Period", this model was then modified in DEseq2 by collapsing the sample periods as replicate samples of each colony. After plotting the PCA of the rlog transformation of the reads, we could observe that colonies N56 and LC053 were outliers. These colonies were eliminated from the analysis and the model was rerun showing a better dispersion of the samples (
Figure *35*). We can observe in Figure 35 that samples are separated by "Species" (or population) in the PC2 axes, however each population has a mix of susceptibilities to SCTLD that suggests the genetic distance between these populations has no effect on their susceptibility.

We performed six contrast analyses to compare the different susceptibilities to SCTLD and obtained differential genes expressed (DEG) that might be involved in determining those phenotypes. In total, we obtained 50 unique genes differentially expressed amongst all the comparisons. These genes could play a role in the type of response to SCTLD that these colonies have had. 25 of the 50 DEG have unknown functional annotations. This is a common issue in coral biology and it is imperative to improve our understanding of coral gene functions in order to better interpret the results of gene expression analysis (Cleves et al., 2020). However, from the genes that have been annotated, we found that ctenidin-3-like, a potential antimicrobial peptide, was down-regulated in colonies with low and some resistance to SCTLD compared to the highly resistant ones. Considering that SCTLD seems to be a disease driven partially by an unbalance in the microbiome (Rosales et al., 2023), it is crucial to better understand the consequences of colonies down-regulating this type of peptide.

Most of the DEG when comparing colonies with low and some resistance to the high resistance once (SCTLD_unaffected and SCTLD_affected) were up-regulated and involved in DNA/RNA binding/packing or transcription. For example, a protamine-like codifying gene and a putative maintenance chromosome element. Protamine-like proteins have been associated with spermatogenesis DNA packing and regulations might have epigenetic consequences (Putnam, 2021). There was also up-regulation of immune-related genes like putative codifying genes for macrophage erythroblast attacher-like and interferon alpha-inducible protein potentially involved in apoptosis (Pretti et al., 2023; Riesgo et al., 2022). Most of the literature on SCTLD involving gene expression has shown an up-regulation of genes involved in apoptosis, which is assumed to be related to the coral cellular response to the rapid tissue necrosis happening during infection (Traylor-Knowles et al., 2021). Having genes related to apoptosis regulated in corals that are visually healthy can suggest that the dysregulation of the immune system is apparent at a genetic level even if disease is not yet observed.

Discussion: More analyses are needed, especially with regard to region and sample period. These preliminary results suggest that corals with low and some resistance to SCTLD have a fingerprint of the effects in their gene expression that might contribute to recurrent infections. More analysis is needed in this data set to determine how the whole transcriptome is involved with the regulation of these genes.

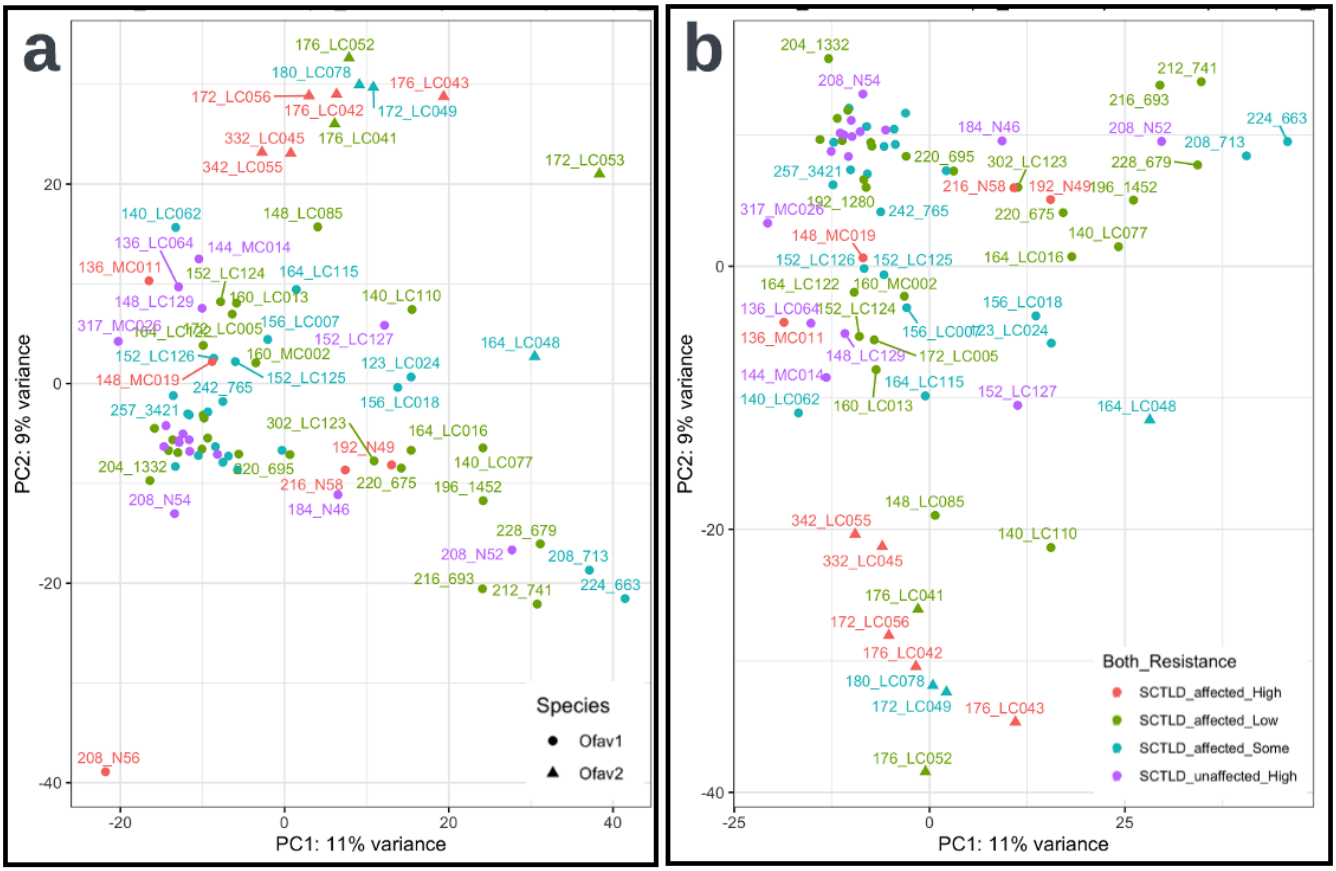

Figure 35. Principal component analysis (PCA) plots of read counts transformed with rlog transformation. **a** PCA with two colony outliers N56 and LC053, **b** PCA after elimination of the outliers.

3.11. **Metabolome (Garg, Deutsch, and Walker)**

Goal: Analyze the organic extracts using in-house ultra-high-resolution mass spectrometer (QqTOF) coupled to an ultra-high-performance liquid chromatography to obtain a comprehensive metabolome of coral species.

Significant findings: Metabolites varied by Sample Period, Region, and Histopathology-supported resistance categories. Every sample period and region were different from each other; however, resistance was only significant in the lower Keys in Sample Periods 1 and 2. High levels of Lyso-lipids were found within two different sampling periods from both locations within the Florida Keys, supporting a connection between SCTLD resistance and the biochemical pathways in which these lipids are involved. Polyunsaturated fatty acids, indicators of healthy symbiosis between the coral and the zooxanthellae, were detected at lower intensity in the low resistance corals compared to the some or high resistance corals. Understanding how fecundity effects the metabolome could help differentiate gametogenesis factors from disease factors.

Results and Discussion: Metabolites varied by Sample Period, Region, and resistance (Figure 36). The bootstrap averages MDS plot illustrates the relationships with Sample Period, Region, and resistance in the metabolite data. A regular MDS plot is akin to looking at the raw data, whereas the bootstrap illustrates the means and confidence intervals between group factors. PERMANOVA analyses found that sample period ($p=0.001$), region ($p=0.001$), and Histopathology-supported resistance categories ($p=0.03$) were significant. Every sample period and region were different from each other; however, resistance was only significant in the lower Keys in Sample Periods 1 ($p=0.025$) and 2 ($p=0.052$). Another interesting pattern was that the bootstrap averages for low resistance in the ECA were more varied than the high resistance corals evidenced by the broader confidence intervals.

A supervised multivariate partial least squares-discriminant analysis (PLS-DA) was performed to identify metabolite features that explain variation attributable to sample period and region. For all PLS-DA models, the top 10 metabolites on the Variable Importance in Projection plot for the first component were compared. Many of these top metabolites were identified on several models (Table 5). GNPS spectral library matching was used to identify several of these top differentiating metabolites as diacylglyeryl-carboxyhydroxymethylcholine (DGCC) betaine lipids, phosphocholines (PC), platelet-activating factors (PAF), and carnitines. MolDiscovery aided the annotation of phosphocholines, in-lab databases facilitated the annotation of DGCC betaine lipids and where metabolite annotations could not be made, CANOPUS on the SIRIUS platform was used to predict the chemical class. DGCCs, PCs, and PAFs have been reported as differentially detected by coral health state, and DGCC betaine lipids were variably detected between apparently healthy and SCTLD-affected *Montastraea cavernosa*. **The selection of metabolites that are differentially detected by coral health state in the**

PLS-DA models suggests that there are region-specific and sample period-specific responses to SCTLD that should be carefully characterized.

UpSet plots were generated to visualize the distribution of metabolite features by season and location (Figure 37). The UpSet plot analysis enables rapid identification of unique metabolite features that can be prioritized for annotation. It is interesting to note that SP1 corals contain the greatest number of unique metabolite features, followed by SP3 corals and then SP2 corals (Figure 37A). This may indicate SCTLD is associated with reduced metabolite diversity over time, although if this were the only explanation for the observed trend, then metabolite feature uniqueness should decrease across the sample periods, which is not observed in this study. This trend may also reflect the response to the unique stressors that the corals are experiencing during each sample period. Corals from each region/location also displayed unique metabolites (Figure 37B). It is interesting to note that the second largest intersection of metabolite features is shared between Sand Key and Looe Key, the locations closest in physical proximity.

Coral samples from Sand Key collected in SP1 (labeled as SP1_Sand Key) were evaluated to target metabolites driving significance in disease resistance. Careful assessment of the metabolomes of the corals from Sand Key collected in the SP1 will aid the analysis of the remaining groups, as the intragroup variation may obscure metabolite variation attributable to *a priori* resistance within the other groups. Indeed, when analysis of variance (ANOVA) was performed to analyze the differences between the means of the detection intensity of the metabolites using MetaboAnalyst, only the model built on samples from Sand Key collected in the SP1 (labeled as SP1_Sand_Resistance) returned statistically significant results. These metabolite features are included in

Table *6*, along with the chemical class identifications predicted by CANOPUS. One metabolite feature was a library hit to a macrolactone natural product, Valactamide E (putative) on the GNPS platform (Figure 38).

Lists of the metabolite features identified through the Kruskal Wallis Test as statistically differentiating (adjusted $p<0.05$) were identified. An UpSet plot was used to visualize the distribution of these statistically significant features across groups since each group was assessed individually (Figure 39). Interestingly, the largest subsets were those of the metabolite features uniquely detected within each Sample Period_Region group. This might be explained by the observation that each location and season have a large influence on the metabolomic signature; however, it is simultaneously possible that the metabolite features within these unique sets belong to the same chemical class. Some of these features may also belong to the same metabolic pathways; thus, while there are unique metabolites identified for each site, the same processes may be disrupted over time. Indeed, there were many identical chemical classes predicted across the groups.

Several metabolite features were annotated as (Lyso)-phosphocholines (PCs), Lyso-platelet activating factors (PAFS), carnitines, xanthophylls, vitamin E derivatives, hydroxyeicosatetraenoic acids and (Lyso)-DGCC betaine lipids. For metabolite features annotated as Lyso-PCs and analogues, a trend emerged wherein these metabolites were detected at a higher intensity in the high resistance samples from SP1_Sand Key compared to some resistance (n=9 metabolites annotated, Figure 40). Certain analogues were also at a higher intensity in high resistance compared to low resistance. This same trend was observed for metabolite features annotated as Lyso-PCs and analogues for coral samples from SP2_Looe Key (n=5 metabolites identified, including one sodiated adduct, Figure 41). This trend is perhaps unsurprising, as Lyso-PAF lipids have been reported at higher abundance in healthy phenotypes in various stress models. It remains to be investigated whether these Lyso-lipids are directly involved in the defense against coral stressors, or if the presence of these lipids is indicative of additional underlying immune mechanisms that provide resiliency to diseases. It is encouraging that this trend is captured within two different sampling periods from both locations within the Florida Keys, as such **this observation supports a connection between SCTLD *a priori* resistance and the biochemical pathways in which these lipids are involved.**

Metabolite features annotated as acyl carnitines that statistically differentiated the SP1_Sand Key corals by *a priori* SCTLD resistance also showed a trend wherein the detection was higher in the high resistance corals compared to some resistance corals (n=5 metabolites identified, Figure 42). Interestingly, some of these metabolites were detected at a higher intensity in the low resistance corals compared to some resistance; although most of the features were always at highest abundance in the high resistance corals. The biochemical pathways of acyl carnitines in corals is understudied. In mammals, carnitines are considered a conditionally essential nutrient and in the microalgae diatom *Phaeodactylum tricornutum*, the short chain propanoyl-carnitine and butanoyl-carnitine accumulate under nitrogen-starvation. Carnitines have also been reported as a biomarker of frailty in humans, where particular analogues, including stearoylcarnitine, were downregulated in the frail population. Stearoylcarnitine was detected at a lower abundance

in the corals classified with some *a priori* SCTLD resistance, perhaps indicating these corals are frail. It is interesting to note that stearoylcarnitine was detected at statistically higher abundance in the low resistant corals compared to the some resistance corals, which contradicts the hypothesis of frailty. It is important to remember that the resistance categories were *a priori* and the tissue sampled was apparently healthy. Continued monitoring of the corals may help link the presence of carnitines at the time of sampling with the eventual fate (SCTLD-affected vs SCTLD-unaffected). **The detection pattern observed of the acyl carnitines within the SP1_Sand Key corals is intriguing, and the biochemical role of acyl carnitines within corals should be further queried to elucidate the connection with SCTLD history and lesion presence.**

Finally, we annotated polyunsaturated fatty acids (PUFAs) within the metabolite features that statistically differentiated the groups by resistance (

Table 7). PUFAs are indicators of healthy symbiosis between the coral and the zooxanthellae. These polyunsaturated fatty acids tended to be detected at lower intensity in the low resistance corals compared to the some or high resistance corals. The observed trend for the PUFAs holds regardless of sample period or region (

Table 7). **Many of these PUFAs the detection pattern of these lipids may indicate either an ongoing breakdown in symbiosis, or a weaker symbiosis occurring in apparently healthy coral tissue collected from corals have low resistance.**

Discussion: Differences found in the lower Keys in SP1 and SP2 are important indicators. More research is needed to investigate connections between the effects of fecundity and disease on the metabolomics data. SCTLD affected lower Keys colonies were the least fecund. Understanding how fecundity effects the metabolome could help differentiate gametogenesis factors from disease factors. One important clue is that in the Lower Keys, SP2 was collected after spawning. Does their separation indicate a role outside of fecundity? Does the lower degree of separation indicate a fecundity effect?

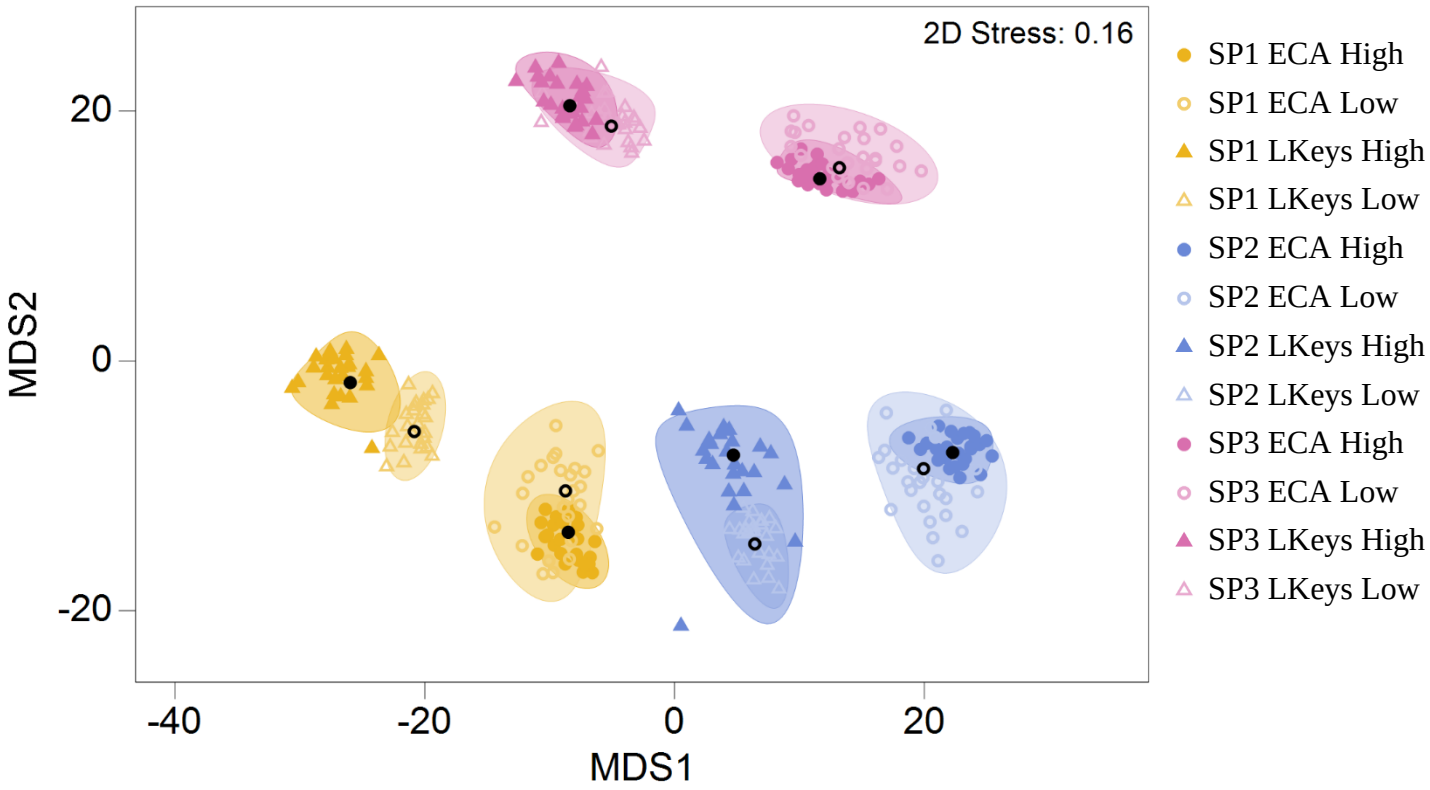

Figure 36. Bootstrap averages plot of metabolomics data by sample period, region, and resistance.

Table 5. Top Differentiating Metabolites Selected Through PLS-DA Models.

***m/z*_RT**	**Putative Annotation or Chemical Class**	**Method of Annotation**	**Summer**	**Fall**	**Winter**	**Looe**	**Sand**	**ECA**
220.112_12.8	*N*-Phenyl-2-naphthylamine	GNPS Library Hit	X					X
282.221_16.5	Benzene and derivatives	CANOPUS						X
305.247_15.8	Eicosatetraenoic acid	GNPS Library Hit			X			
344.352_17.5	1,2-aminoalcohols	CANOPUS					X	
372.383_20.2	Secondary alcohols	CANOPUS				X	X	X
372.383_20.5	1,2-aminoalcohols	CANOPUS						X
372.383_20	Lipids and lipid-like molecules	CANOPUS			X	X	X	
372.383_21.8	1,2-aminoalcohols	CANOPUS				X	X	
400.342_14.4	Hexadecanoylcarnitine	GNPS Library Hit			X			
400.342_14.8	Hexadecanoylcarnitine	GNPS Library Hit	X			X	X	
447.383_20.3	Diisodecyl phthalate	GNPS Library Hit						X
466.329_14.5	Lysophophatidylethanolamines	CANOPUS	X	X	X			
482.36_13.1	Lyso-PAF C-16	GNPS Library Hit	X	X	X			
490.373_13.9	Lyso-DGCC (16:0)	GNPS Library Hit		X				
496.339_12.8	Lyso-PC (16:0)	GNPS Library Hit	X					X
502.292_12.2	Amino acids and derivatives	CANOPUS	X	X	X	X	X	X
510.391_14.5	Lyso-PAF C-18	GNPS Library Hit	X		X	X		
524.371_14	Lyso-PC (18:0)	GNPS Library Hit			X		X	
526.313_13.6	Glyercophosphoserines	CANOPUS		X	X			
562.374_13.3	Lyso-DGCC (22:6)	GNPS Library Hit		X				
750.586_21.1	DGCC (34:3)	Literature Search*				X		
766.573_18.5	Eicosapentaenoyl PAF C-16	GNPS Library Hit	X					
766.573_18.6	Eicosapentaenoyl PAF C-16	GNPS Library Hit	X					
766.573_19	Eicosapentaenoyl PAF C-16	GNPS Library Hit		X				
768.587_17.5	PC(16:0/20:4)	MolDiscovery		X				
768.588_16.4	PC(16:0/20:4)	MolDiscovery		X				
792.588_19.8	Docosahexaenoyl PAF C-16	GNPS Library Hit				X		X
800.602_21.3	DGCC (38:6)	GNPS Library Hit			X		X	
800.602_21.7	DGCC (38:6)	GNPS Library Hit	X	X		X	X	X
872.601_20.3	DGCC (44:12)	Literature Search*				X	X	X
		*Deutsch *et al*., 2021						

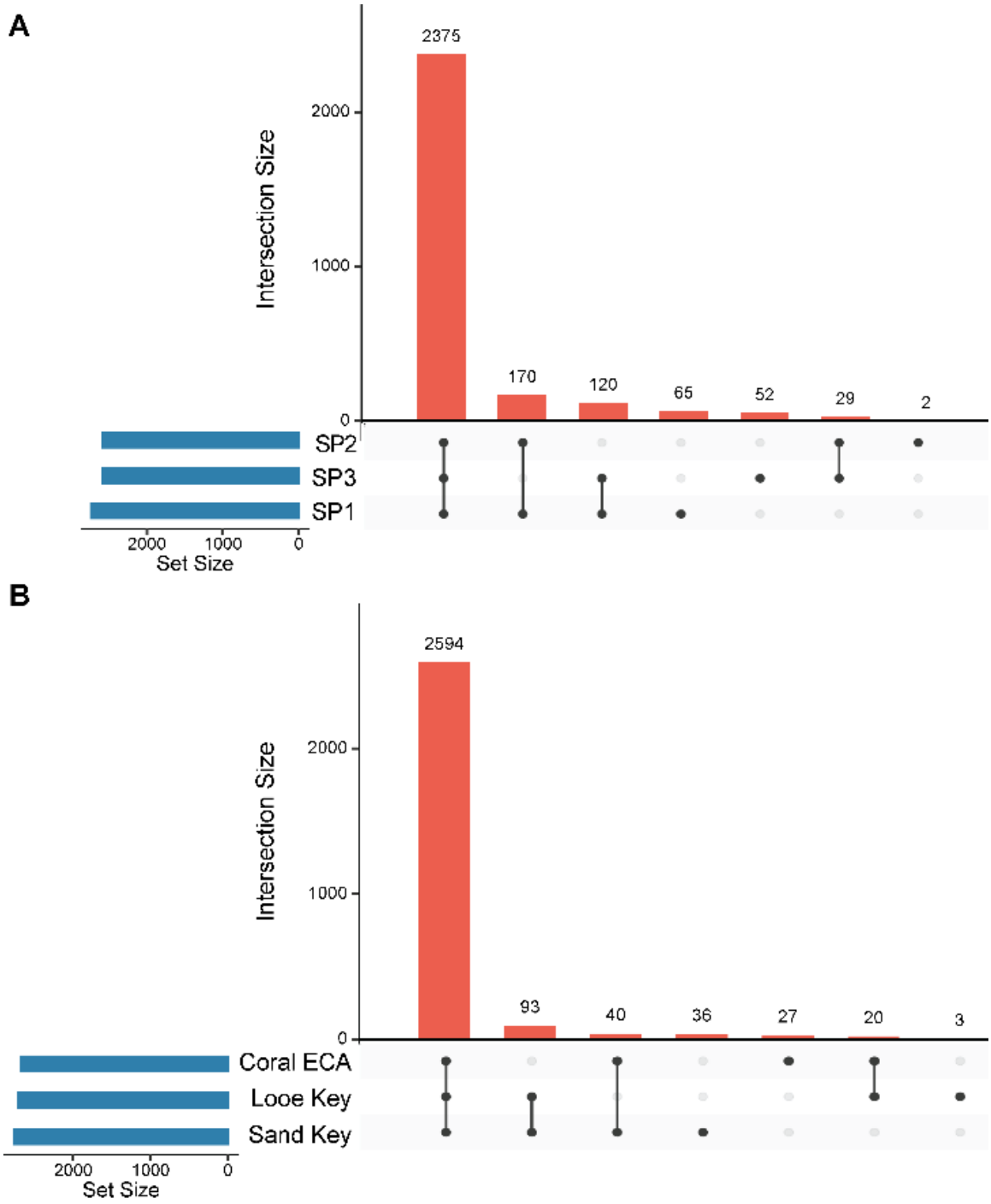

Figure 37. UpSet Plot Analysis. Shows the distribution of metabolite features by (A) sample period and (B) region/location. (Sample period 1= SP1, sample period 2= SP2, sample period 3= SP3).

Table 6. SP1_Sand Key Statistically Differentiating Metabolites from ANOVA.

***m/z*_RT**	**Chemical Class (CANOPUS)**
316.321_16.3	1,2-aminoalcohols
404.352_16.5	1-hydroxy-2-unsubstituted benzenoids
682.561_20.5	Amino acids and derivatives
724.643_20.4	Ceramides
427.36_18	Cholesterols and derivatives
849.674_17	Diterpenoids
425.341_16.6	Ergostane steroids
598.504_20.4	Fatty acid esters
344.279_11.6	Fatty acid esters
624.519_20.4	Fatty acyl glycosides
680.581_21.2	Fatty acyl glycosides of mono and disaccharides
545.493_23.5	Fatty Acyls
404.352_16.1	Fatty Acyls
702.566_20.6	Glycosyl *N*-acyl sphingosines
749.575_21.1	Lipids and lipid-like molecules
425.341_17	Macrolactone Natural Product**
628.514_19.4	Triacylglycerols
917.577_20.5	-
917.577_20.2	-
917.577_19.8	-
887.566_23.1	-
887.566_21.8	-
543.252_9.5	-
542.918_9.5	-
489.524_9.7	-
450.801_23.7	-
450.801_19.1	-
450.801_18.1	-
400.239_7.2	-
367.831_6	-
358.368_19.1	-
357.279_16.6	-
334.558_13.1	-
310.113_16.3	-
294.187_14.1	-
287.197_14.5	-
281.662_14.1	-
280.171_12.8	-
274.672_14.5	-
273.181_13.1	-
265.166_14.6	-
260.657_13.2	-
252.641_14.5	-
199.618_10.4	-
	**GNPS Library Match

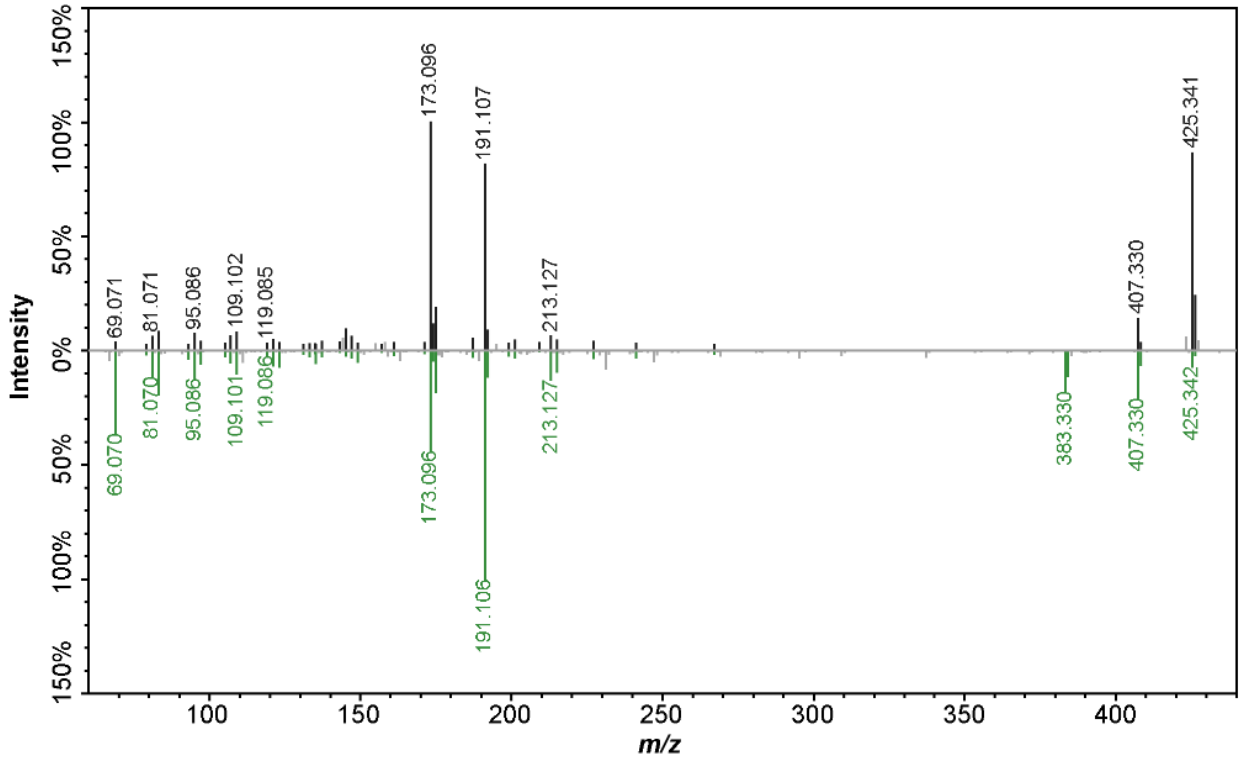

Figure 38. MS^2 mirror plot for a macrolactone natural product. The spectrum from the experimental data (top) is compared to the spectrum is available in the GNPS library (bottom).

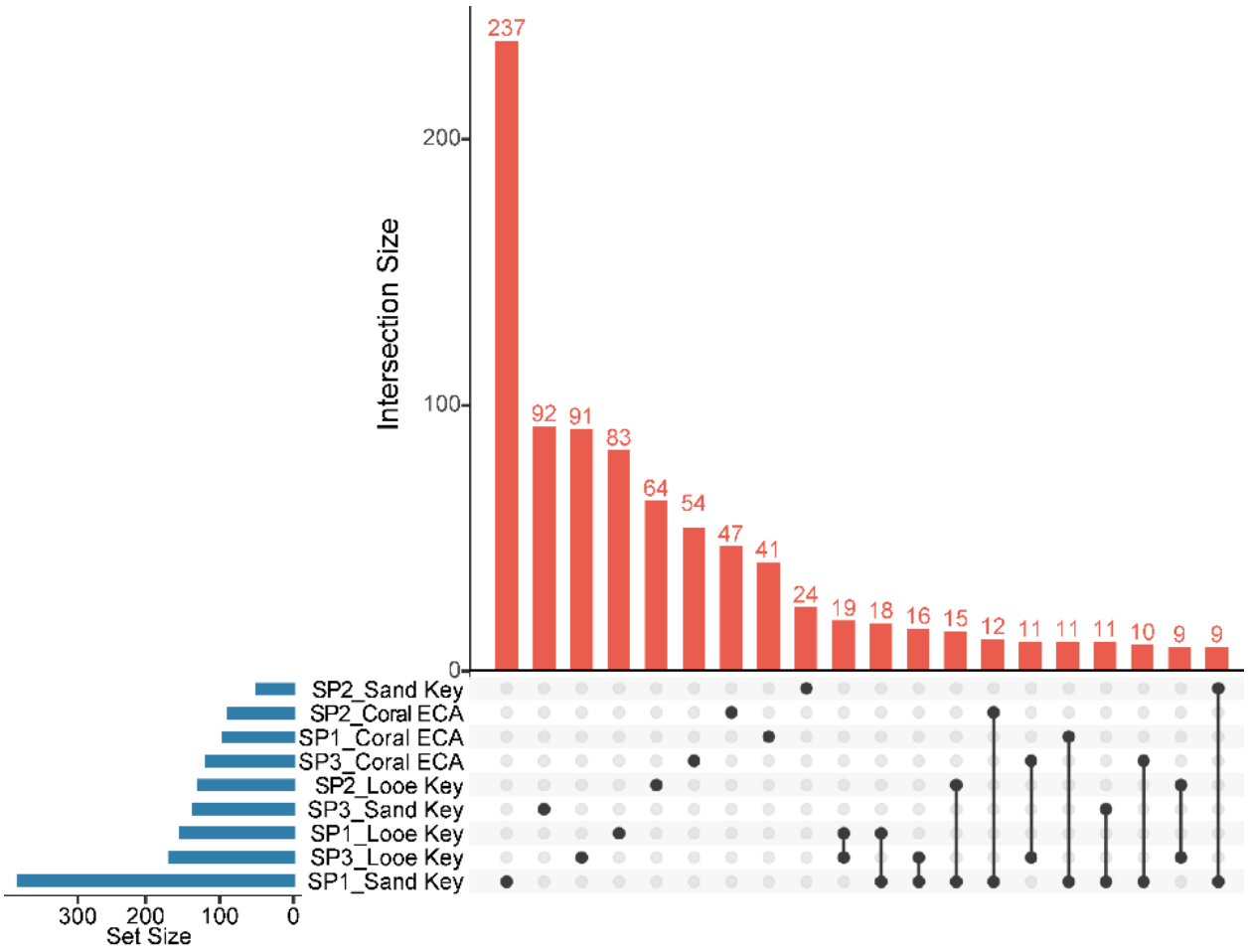

Figure 39. UpSet Plot howing the distribution of statistically differentiating metabolite feature as determined by the Kruskal-Wallis with Dunn's Post Test (adjusted $p<0.05$) across the Sample Period_Region/Location categories. (Sample period 1= SP1, sample period 2= SP2, sample period 3= SP3)

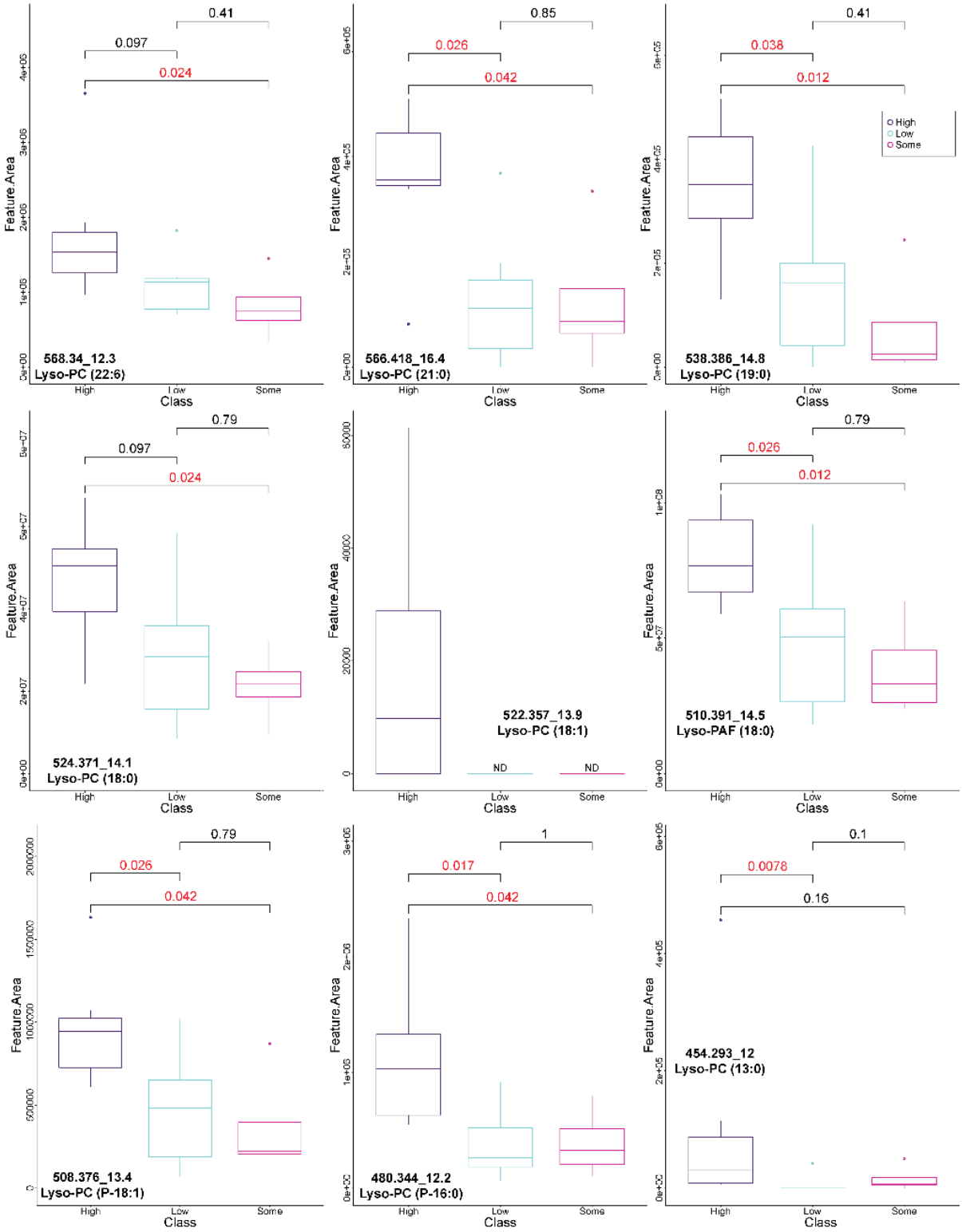

Figure 40. Box plots of statistically differentiating metabolite features in SP1_Sand Key corals by a priori SCTLD resistance annotated as Lyso-phosphocholines and analogues. Kruskal-Wallis was used to compare the means of the detection intensity ("Feature.Area"). Significant differences ($p<0.05$) are indicated in red text. The metabolite identification is included on each plot. (ND= not detected).

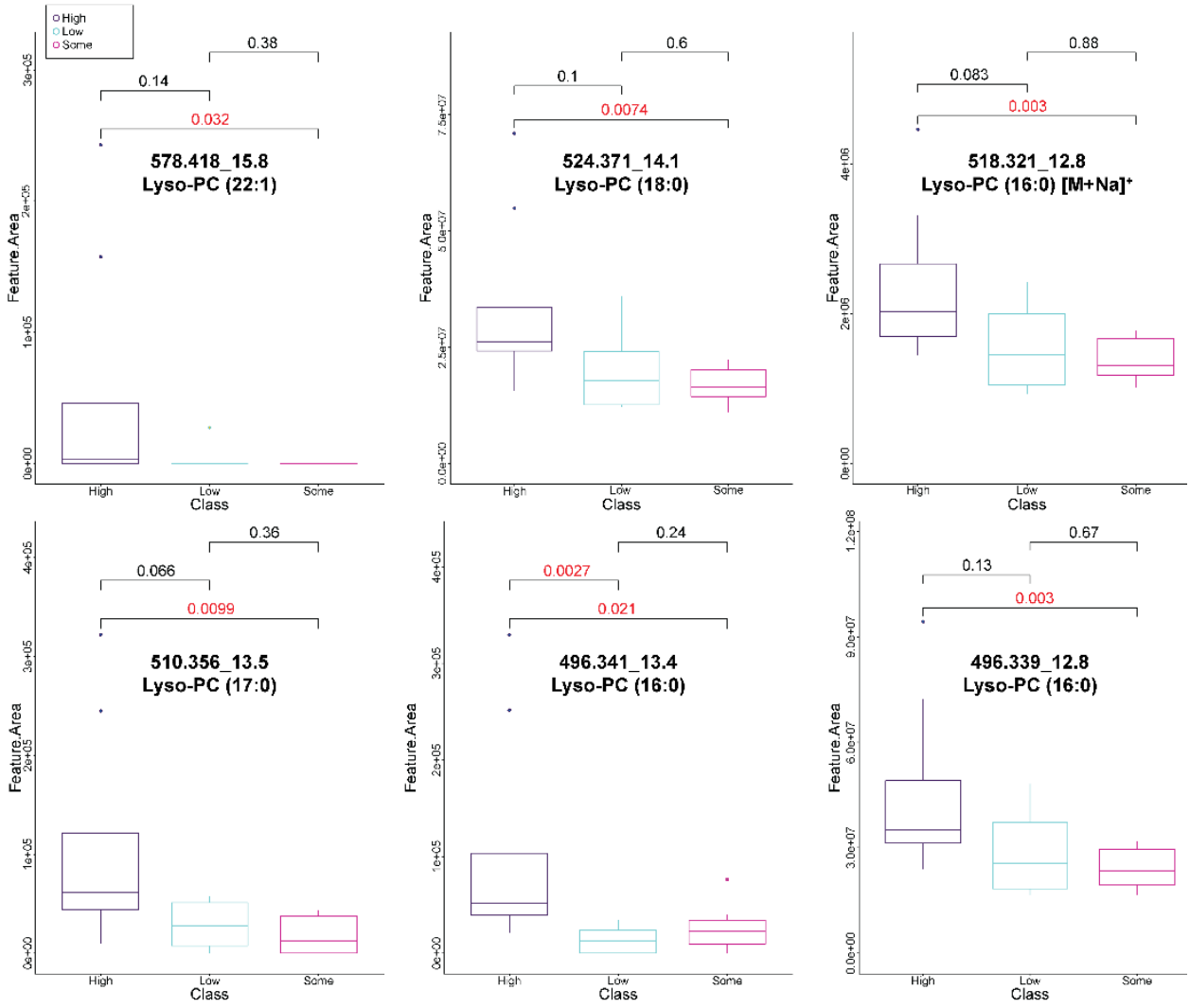

Figure 41. Box plots of statistically differentiating metabolite features in SP2_Looe Key corals by a priori SCTLD resistance annotated as Lyso-phosphocholines and analogues. Kruskal-Wallis was used to compare the means of the detection intensity ("Feature.Area"). Significant differences ($p<0.05$) are indicated in red text. The metabolite identification is included on each plot.

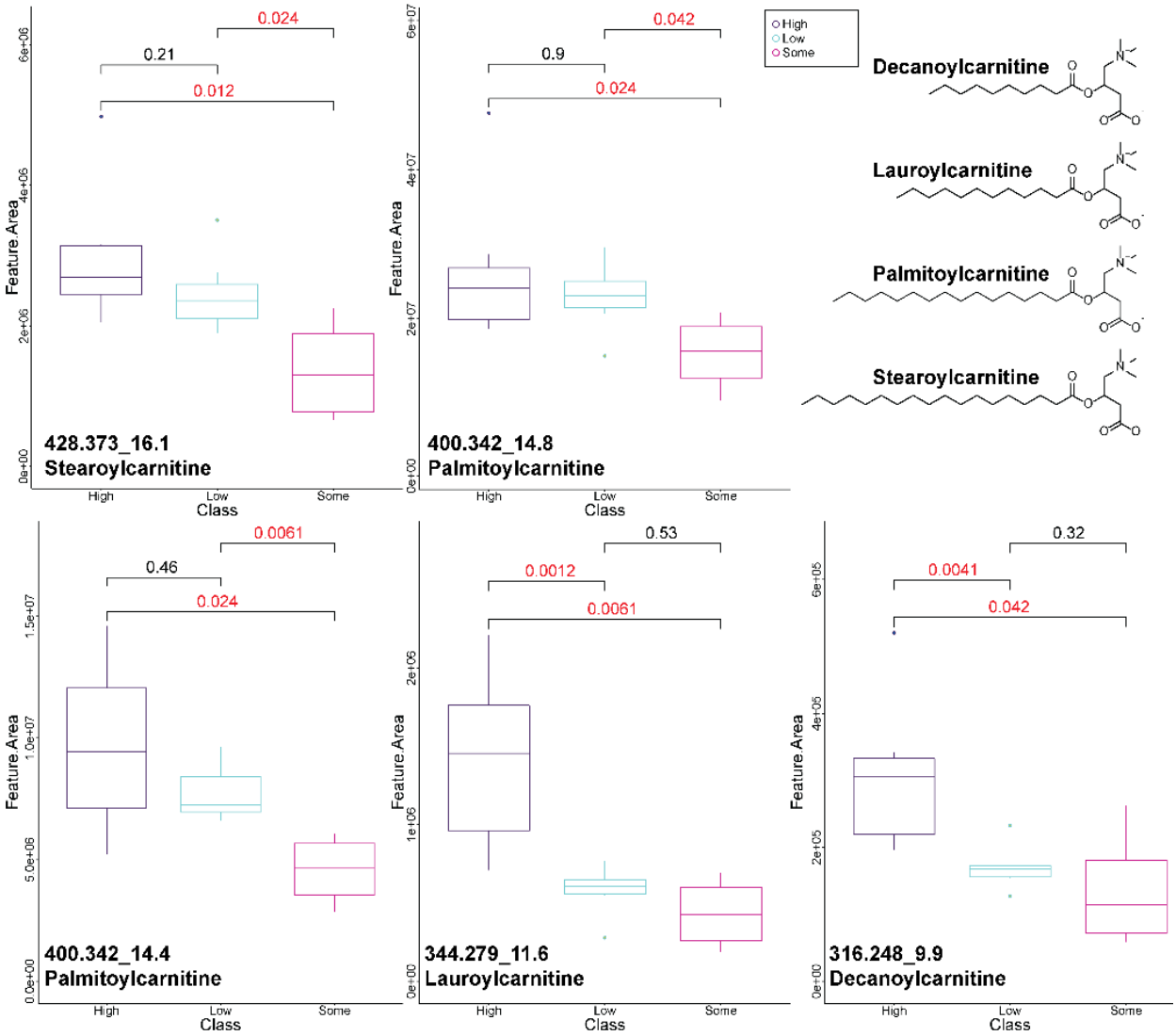

Figure 42. Box plots of statistically differentiating metabolite features in SP1_Sand Key corals by a priori SCTLD resistance annotated as acyl carnitines. Kruskal-Wallis was used to compare the means of the detection intensity ("Feature.Area"). Significant differences ($p<0.05$) are indicated in red text. The metabolite identification is included on each plot.

Table 7. Fatty acids that statistically differentiate Sample period_Region groups by a priori SCTLD resistance.

m/z_RT	Annotation	Tail Length	Statistical Significance in Groups (p<0.05)
277.216_14.4	Stearidonic acid	(18:4)	SP3_ Coral ECA
279.232_15.2	Linolenic acid*	(18:3)	SP3_Looe Key
303.232_15	Eicosapentaenoic acid	(20:5)	SP1_Sand Key, SP3_Looe Key
305.247_15.8	Arachidonic acid	(20:4)	SP1_Sand Key
307.263_16.5	Eicosatrienoic acid	(20:3)	SP1_Sand Key, SP1_Looe Key, SP3_Looe Key
329.245_16.5	Docosahexaenoic acid	(22:6)	SP1_Sand Key, SP1_Looe Key, SP2_Looe Key
331.263_16.1	Docosapentaenoic acid	(22:5)	SP1_Sand Key, SP2_Looe Key
333.278_16.9	Docosatetraenoic acid	(22:4)	SP1_Sand Key

*or γ-Linolenic acid

3.12. **Lipidome (Garg, Deutsch, and Paul)**

Goal: To provide a lipidome analysis on the RRC samples and investigate data associations with other available data collected during the RRC project.

Significant findings: Differences in lipids were found between all sample periods and regions. Differences between resistance classes in the lower Keys were found in SP1 and SP3. More analysis is needed.

Preliminary Results: A global fixed effects permanova model of relative positive mode lipids between all samples for sample period, region, and resistance found a significant difference in sample period and region (p=0.001). The bootstrap averages plot illustrates this well (Figure 43). The bootstrap plot illustrated that SP2 was much more variable than SP1 or SP3 as well. In SP1, a MDS plot revealed that N-54 and 1455 were outliers. Once removed, a fixed effects permanova model of relative lipids found that the combination of region and resistance was a significant factor (p=0.042) (Figure 44). The Lower Keys low and high resistance corals were significantly different (p=0.017). The Lower Keys some and high resistance corals were almost significantly different (p=0.068). In SP1, no significance was found between the ECA resistance classes. In SP2, region was the only significant factor (p=0.001) (Figure 45). In Sp3, a MDS plot revealed that 1470 was an outlier. Once removed, region and resistance were significant factors (p=0.001, p=0.37) and the Lower Keys some and high resistant corals were different (p=0.01) (Figure 46). In SP3, no significance was found between the ECA resistance classes.

Discussion: Lipidomics data became available in late June, thus preliminary analyses occurred on June 29. Differences were found between all sample periods and regions indicating that all future analyses should include these classifiers. Differences in lipids between resistance classes in the lower Keys were found in SP1 and SP3. Further investigations are needed to identify lipids that differed and their biological context.

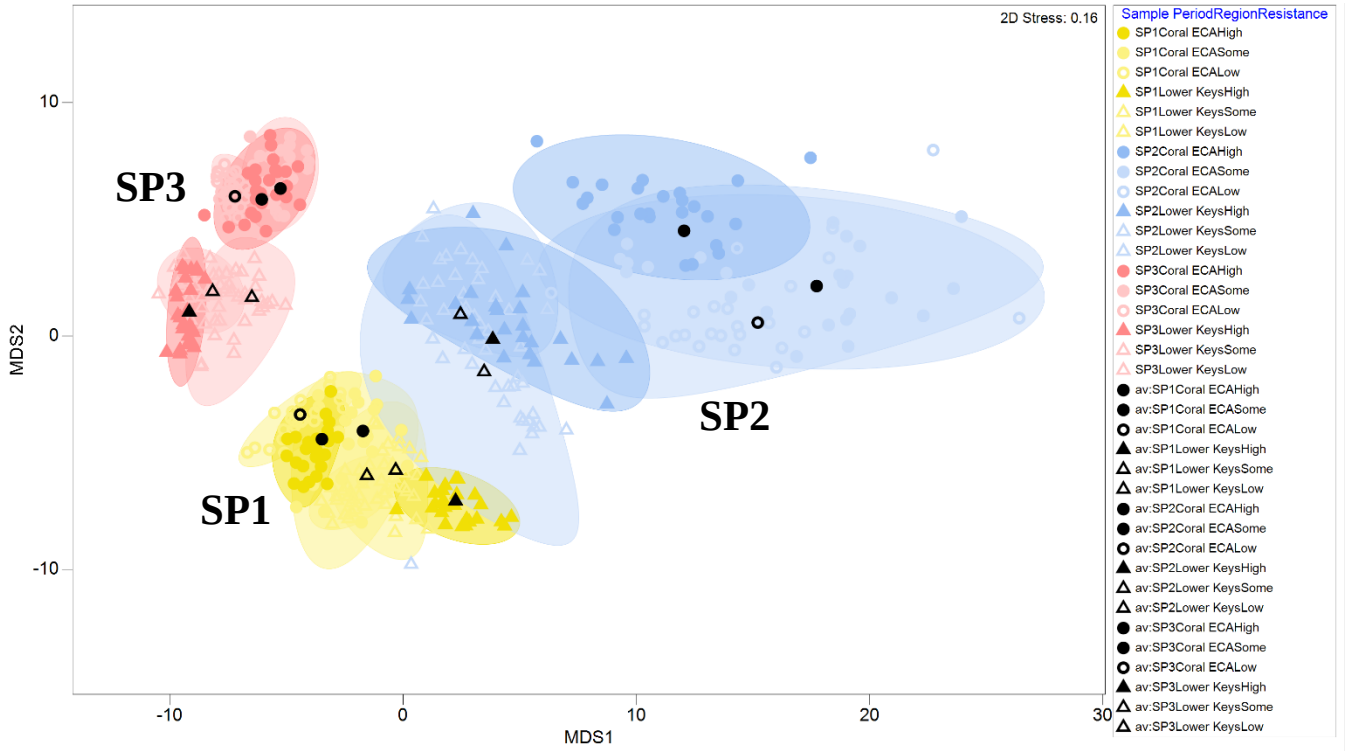

Figure 43. Bootstrap averages plot of lipidomics data by sample period, region, and resistance.

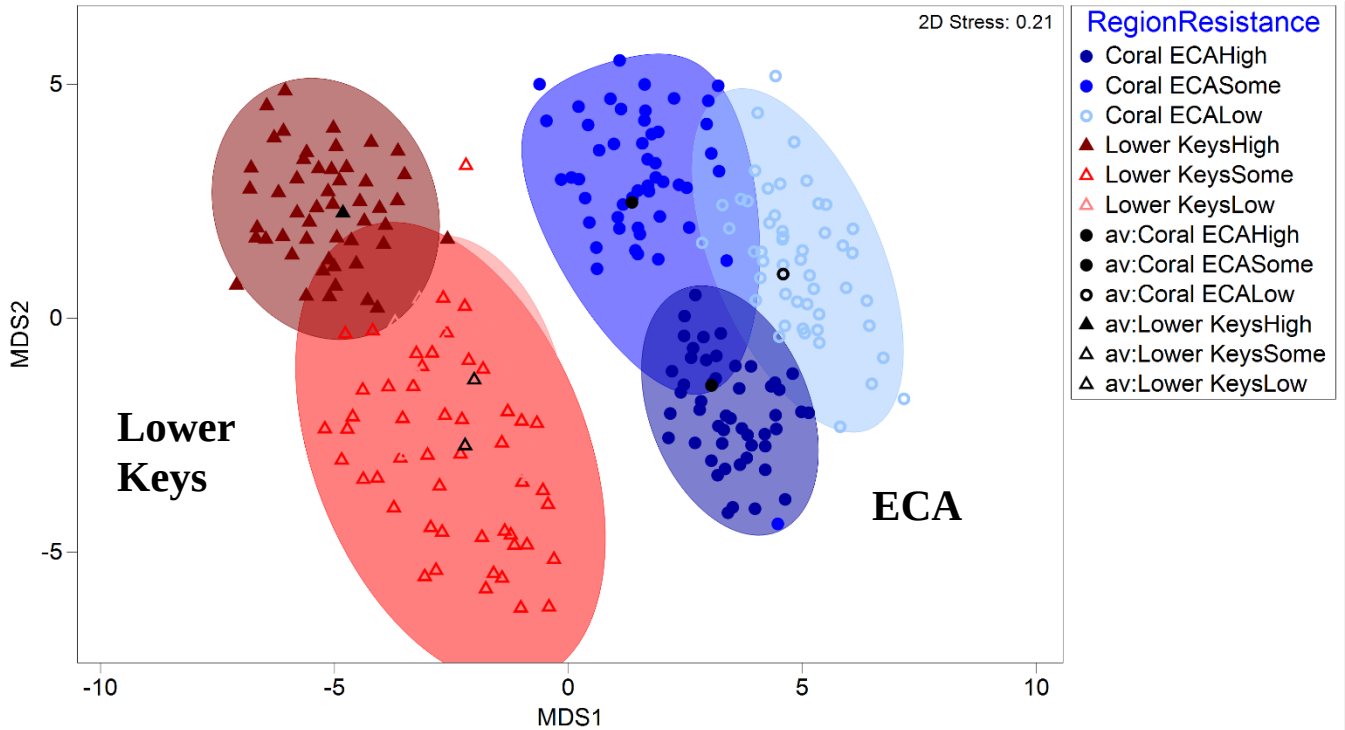

Figure 44. Bootstrap averages plot of lipidomics data across all SP1 samples between region and resistance.

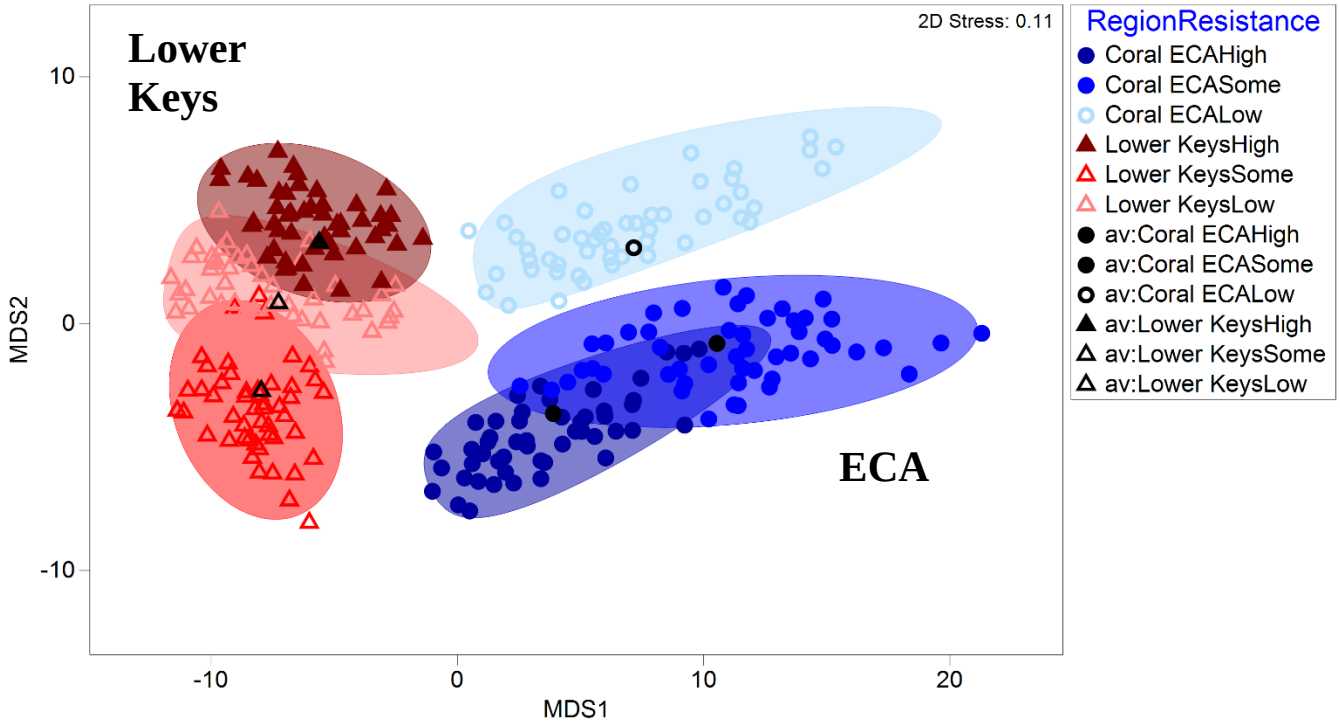

Figure 45. Bootstrap averages plot of lipidomics data across all SP2 samples between region and resistance.

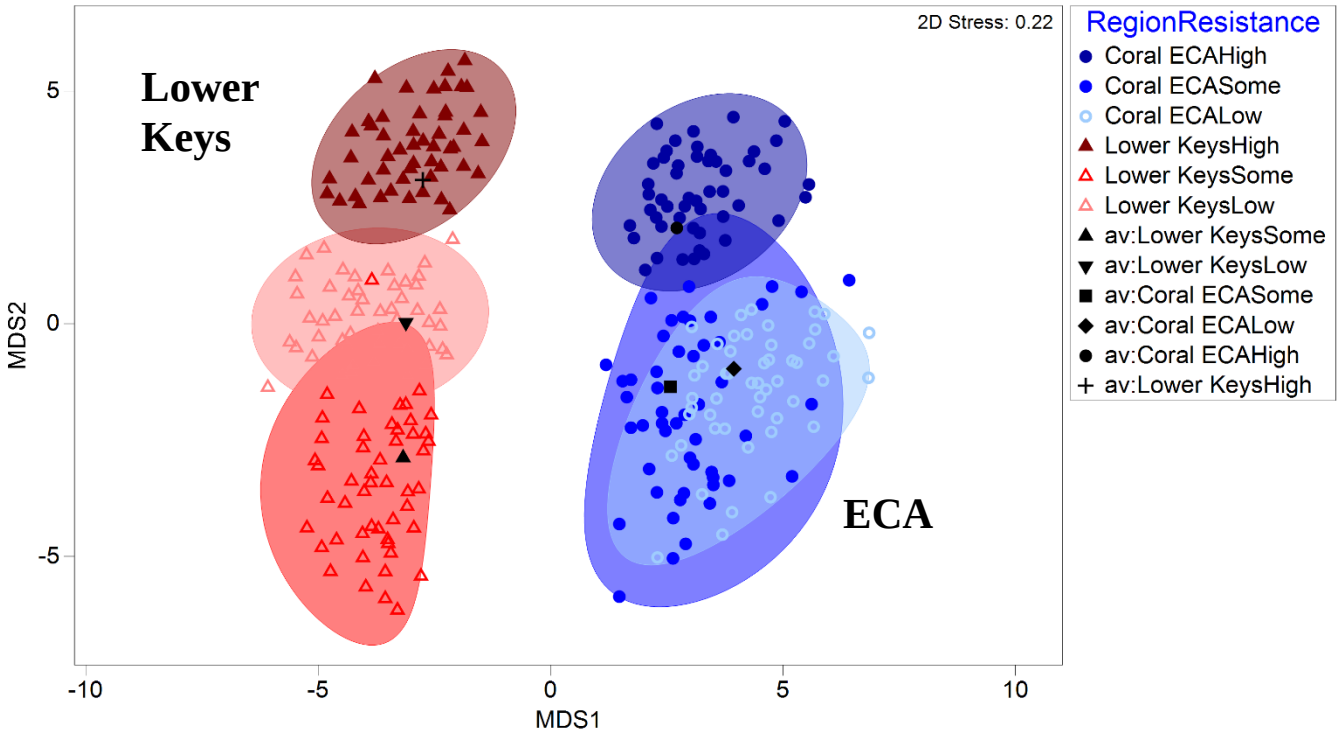

Figure 46. Bootstrap averages plot of lipidomics data across all SP3 samples between region and resistance.

3.13. **Proteome (Woodley, Saunders, Janech, and Duselis)**

Goal: Process and analyze the proteome of the coral host in each coral for each period to investigate intraspecific associations with disease resistance.

Significant findings: Expressed proteins between sample periods were significantly different. In Sample period 1, the Lower Keys proteins significantly differed from the ECA and between resistance classes. In Sample period 3, there were no significant differences between region or resistance. This indicates that expressed proteins are dynamic over time and may be associated with gametogenesis, environmental stress, and other factors. Continued investigation is into the health trajectories of specific corals immediately before sampling could be key to understanding which proteins are related to disease.

The appearance of so many metabolism-related proteins in the list of significant proteins indicates that energy production could be an influential factor of SCTLD resistance. Structural and bioadhesion proteins are likely indicative of differing cellular structural integrity between high resistance and low resistance samples. The 11 differentially abundant ECA proteins and 80 differentially abundant Lower Keys proteins could indicate different degrees of stress or susceptibility of the coral.

Results: A total of 86 samples from SP1 were re-purified with an updated protocol and re-sequenced. 84 samples from SP1 and 87 samples from SP3 (due to three poor quality spectra) were included in statistical analysis.

A global fixed effects permanova model of relative proteins between all samples for sample period, region, and resistance found a significant difference in sample period ($p=0.001$). The bootstrap averages plot illustrates this well (Figure 47). In SP1, a fixed effects permanova model of relative proteins between all samples found that the combination of region and resistance was a significant factor ($p=0.013$). In SP1, the low and high resistance corals were significantly different between ECA and the Lower Keys ($p<0.041$) (Figure 48). The low resistance class was significant from the some and high resistance in the Lower Keys ($p<0.027$) but no differences between resistance classes were found in the ECA. In SP3, no significance was found between regions of resistance factors (Figure 49).

In total, 5,093 peptides were identified in Period 1 samples and 5,179 in SP3 samples with 5,035 proteins being common in Periods 1 and 3 (Figure 50). 169 proteins appeared in all 84 samples from Period 1, 129 proteins appeared in all 87 samples from SP3, and 79 proteins appeared in all samples in both collection periods (Figure 51).

Of the 169 proteins identified in all samples, there were nine proteins in SP1 that were more abundant (Mann-Whitney t-test, $p<0.05$) in the low resistance colonies than SCTLD high resistance (Table 8). Nine proteins decreased in relative abundance ($p<0.05$) when comparing the some resistance samples to the high resistance group in Period 1.

There were less differentially abundant proteins overall in SP3. None of the 129 proteins identified in all samples were significantly different between the low and high resistance colonies. Two proteins, ferric-chelate reductase and transmembrane protease serine-9-like, decreased in abundance in the some and high resistance colonies.

The two regions had 10 protein changes between SP1 and SP3 in common (Figure 52). In Lower Keys, 90 proteins were significantly different in the low resistance samples during SP1. These proteins functioned in metabolism, iron transport and regulation of adhesion-dependent cell spreading, calcium binding, endocytosis pathways, protein transport, GTPase activity, and biosynthetic pathways. In the ECA, relative protein abundances among the low resistance samples decreased as compared to the high resistance samples. The Lower Keys had the opposite pattern, where the low resistance samples had a higher protein abundance compared to the high resistance corals (Table 9). The differentially abundant proteins in ECA are involved in cell-cell adhesions, cell motility, other processes involving epidermis formation, metabolic cell processes, and transport. The differentially abundant proteins in the Lower Keys samples were iron transport and regulation of adhesion-dependent cell spreading, calcium binding, protein transport, and biosynthetic pathways.

In the ECA, nine proteins were significantly different in the some resistance corals during SP1 (Figure 53). Eight proteins decreased in relative abundance and one increased. In the Lower Keys, five proteins changed significantly between the some resistance during SP1. There were four proteins that decreased in relative abundance and one that increased (Table 10). These proteins were involved in similar pathways as noted in the low resistance corals.

In SP3, there was one protein, transmembrane protease serine 9-like involved in proteolysis, that decreased in abundance in the some resistance Lower Keys corals versus the high resistance.

The Lower Keys region data was divided into Looe and Sand Keys and analyzed individually to evaluate whether differential abundances existed in protein expression between sites even though the colonies were in the same general region (Lower Keys). There were 21 proteins in low resistance corals that changed significantly from SP1 in ECA, 84 proteins that changed significantly in Looe Key, and nine proteins changed significantly in Sand Key (Figure 54). Nine proteins were common between ECA and Looe Key (Table 11), and seven were common between Looe and Sand Key (Table 12). There were no common proteins between ECA and Sand Key.

In the some resistance corals, there were 7, 6, and 0 proteins differentially abundant with respect to high resistance corals in ECA, Looe Key and Sand Key, respectively, during SP1. There were no common proteins that were differentially expressed in both ECA and Looe Key (Table 13).

In SP3, there was a completely different pattern of changes in all the groups, with Sand Key showing the greatest number of differentially expressed proteins. The low resistance corals compared to high resistance corals had no change in ECA, one protein (ferric-chelate

reductase 1-like) was decreased in Looe Key and 43 proteins were differentially expressed in Sand Key; one protein (integumentary mucin A.1-like increased in abundance, while the other 42 proteins were decreased). The top ten proteins that showed differential abundances are listed in Table 14.

Interestingly, the some resistance corals when compared to high resistance corals showed no proteins that were differentially abundant in ECA or Looe Key and 47 proteins that were differentially abundant in Sand Key, while 46 proteins decreased and one (integumentary mucin A.1-like) increasing in abundance relative to the high resistance corals.

Discussion: These results provide a unique view into the protein expression landscape of diseased and resistant *Orbicella faveolata* corals helping to elucidate some of the mechanisms behind the SCTLD. Previous studies have mainly focused on changes within the genome and transcriptome, citing changes in genes associated with apoptosis, immune related and extracellular genes (Traylor-Knowles et al., 2021; Traylor-Knowles et al., 2022). Understanding the disease mechanism can assist management in multiple ways. First, understanding how the disease progresses can lead to developing more effective treatment targets to halt the disease faster and more efficiently. Secondly, understanding the disease mechanism can lead to identifying potential biomarkers for earlier detection of SCTLD. Lastly, understanding the disease mechanism can lead to the development of preventative measures to protect coral from SCTLD.

Proteomic Changes and Molecular Pathways: In the initial limited analysis of SP1, there were 28 proteins identified as having differential expression in low resistance compared to high resistance samples. **The appearance of so many metabolism-related proteins in the list of significant proteins indicates that energy production could be an influential factor of SCTLD resistance** in *O. faveolata*. Some significant proteins were not annotated by gene ontology (GO), such as those associated with antioxidants and peroxidase activity. **Structural and bioadhesion proteins are likely indicative of differing cellular structural integrity between high resistance and low resistance samples.**

Ten common proteins were differentially abundant between ECA and Lower Keys. Interestingly, the differentially abundant proteins increased in Lower Keys and decreased in ECA, which may have contributed to these proteins not being identified when looking at the overall averages. The proteins that showed changes involved ion and protein transport, endocytosis, biosynthetic pathways, DNA folding, cell signaling, enzyme activity and other metabolic processes. **The other 11 differentially abundant ECA proteins and 80 differentially abundant Lower Keys proteins could indicate different degrees of stress or susceptibility of the coral.** Likewise, the patterns in the protein expressions could correspond to antibiotic treatments. More investigation is needed into specific corals with treatments and if their proteins indicate differences from those corals with less or no treatments (Figure 55). For example, proteins involved in epithelial formation, Sushi, von Willebrand factor type A, EGF and pentraxin domain-containing protein 1-like, were decreased in the ECA low resistance samples, which might be an early indicator of cytoskeletal changes. Comparing histology to the samples that had a decrease in this protein could reveal interesting correlations.

Antibiotics are known to affect calcium signaling (Gonzalez-Pleiter et al., 2017), although amoxicillin and other penicillin derivatives are more mild than other classes of antibiotics. Gonzalez-Pleiter et al. (2017) showed that after exposure to antibiotics, such as amoxicillin, cells undergo a quick Ca^{2+} release. It's reasonable to speculate that with amoxicillin paste treatment, coral cells experience a continuous Ca^{2+} release which triggers downstream signaling effects which can lead to a variety of cellular responses as well as protein changes. As calcium signaling changes could be caused by numerous factors, it would not be an ideal biomarker to use for stony coral tissue loss disease. Although it could provide clues to disease pathway mechanisms when looking at changes downstream of Ca^{2+} signaling.

Downstream of calcium regulation are pathways such as MAPK signaling pathway, apoptosis, phosphatidylinositol signaling pathway, cytoskeletal regulation, and others. As low resistance corals develop lesions, it would plausible to see cytoskeletal protein changes occur (Figure 56). Proteins associated with focal adhesions and cytoskeletal elements (filamin, talin, calpains) were differentially abundant in low resistance samples. It could be informative to stain histological samples for actin to evaluate whether actin changes occur prior to lesion formation and determine if any cytoskeletal rearrangement can be observed.

Multiple proteins involved in endocytosis pathways were differentially abundant in low resistance samples compared to high resistance corals. Corals have an endosymbiotic relationship with dinoflagellates, so dysregulation of these pathways would explain the loss of symbionts seen with SCTLD and other coral diseases (Yuyama et al., 2018). Endocytosis can occur via clathrin-dependent or clathrin-independent pathways (Figure 57) and it would appear that proteins in both pathways are affected within low resistance corals. This mechanism could prevent the uptake of nutrients from symbionts that coral need for survival.

Finally, if a specific biosynthetic pathway is being altered with SCTLD as a result of metabolic disruption, identifying protein changes could help understand the mechanism of the disease as well as potentially identifying early biomarkers. The metabolites that change in response to different types of stress or disease would be a more specific source of biomarkers. Recently, a study found that Acropora spp. use an alternative pathway for cysteine biosynthesis, as they have lost cystathionine B-synthase, which is a key enzyme in this pathway (Salazar et al., 2022). It was proposed that this species relies on symbiosis with dinoflagellates to acquire cysteine; however, an alternative pathway for cysteine production was found. The presence of differing metabolic pathways may also explain why some corals are more susceptible to disease than others. Therefore, we plan to use the metabolomic data for validation of protein changes that might be associated with biosynthetic pathways that could potentially be used as biomarkers.

RRC data synthesis: Benefits from this proteomic study can also assist other areas of research in developing testable hypotheses to reconcile the data with gross and histological observations. For instance, knowing that proteins associated with cytoskeleton are changing with SCTLD presence could help explain histology data. Understanding

differential cytoskeleton protein expression in individual corals could explain why some corals might heal lesions quickly while others do not. The proteomic data for this project has shown that individual corals within the same susceptibility class and region, are responding differently to SCTLD and antibiotic treatments in a way that isn't easily explained solely by the metadata. If these differences could be related to changes detected in genomic, transcriptomic, or even metabolomic data, it could lead to more accurate predictions about which corals are most or least at risk for contracting SCTLD or associated diseases. It would also help to explain if the protein changes observed were due to genetic differences or environmental factors. If the differences in protein expression aren't shared in genetic data, then it would indicate the susceptibility is more environmentally driven or perhaps a disruption in transcriptomics.

Some studies have named zooxanthellae as the primary target of SCTLD, with pathological changes first occurring in basal body wall and surface body wall zooxanthellae and showing lesions first appearing in the gastrodermis of the basal body wall (Landsberg et al., 2020). The disruption of host-zooxanthellae symbiosis is then disrupted. Due to changes detected in endocytosis pathways, a more in-depth look at the proteomics of the zooxanthellae with and without SCTLD and also understanding the effects that amoxicillin treatments have on dinoflagellates and endocytosis would be worth investigating. Especially if some corals are relying on dinoflagellates for obtaining certain biosynthetic products.

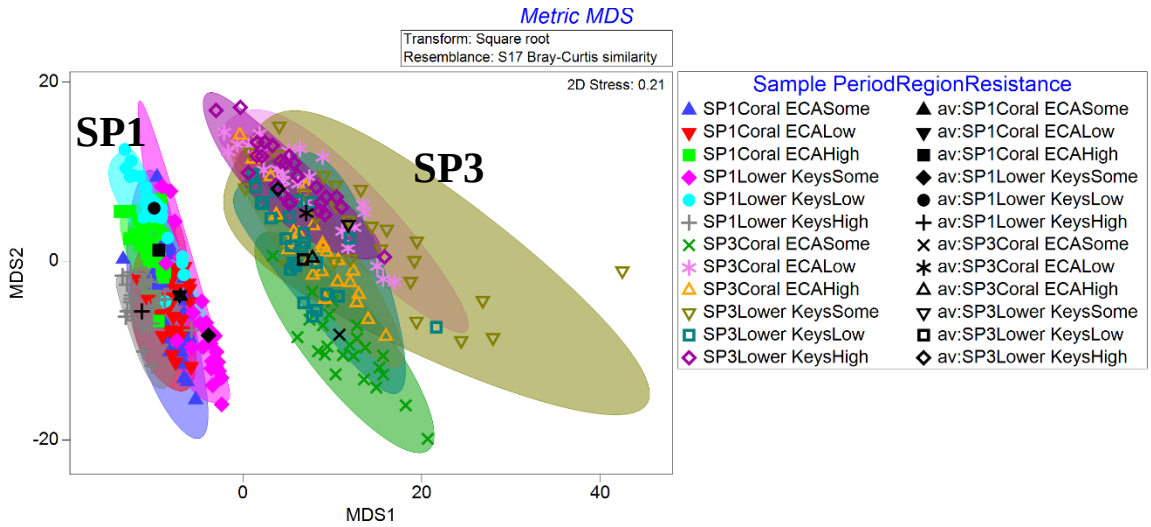

Figure 47. Bootstrap averages plot of proteomics data across all samples between sample period, region, and resistance.

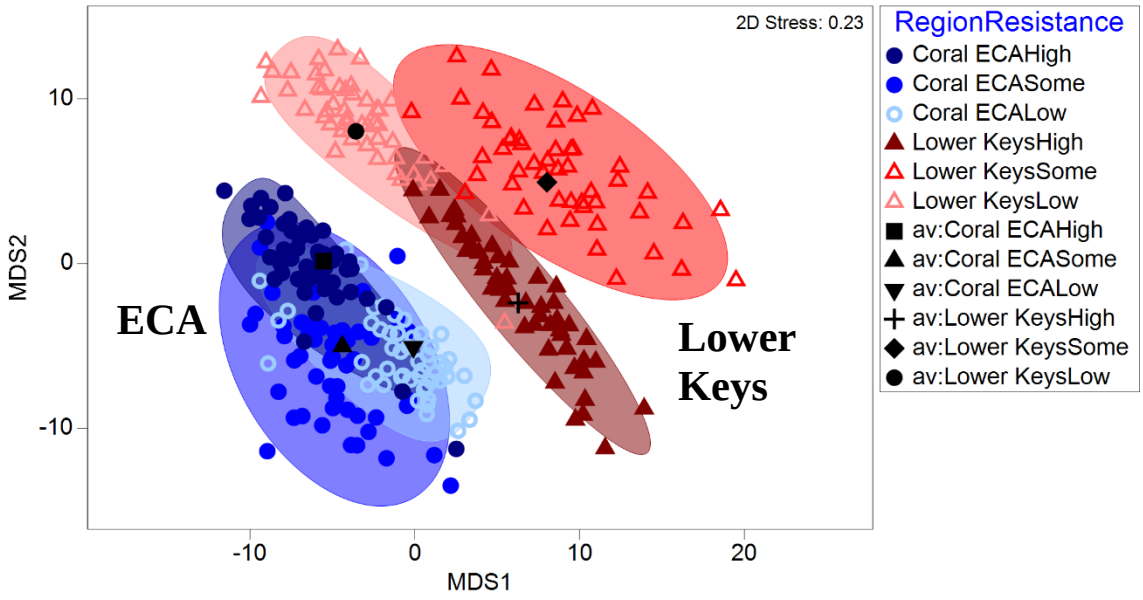

Figure 48. Bootstrap averages plot of proteomics data across all SP1 samples between region and resistance.

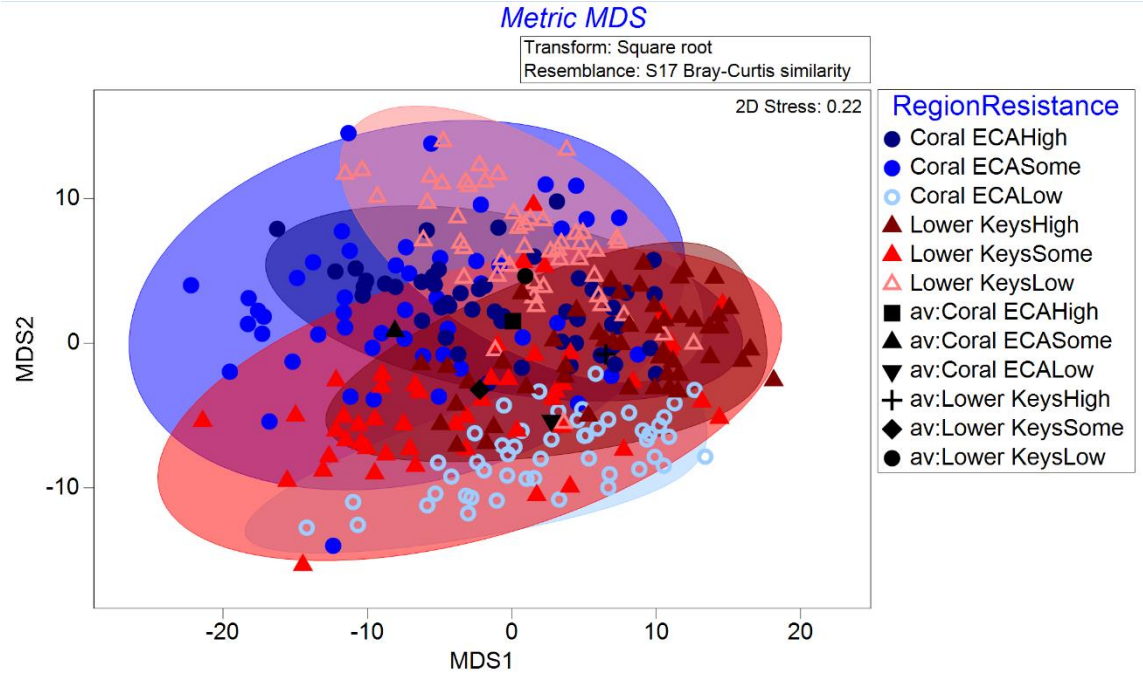

Figure 49. Bootstrap averages plot of proteomics data across all SP3 samples between region and resistance.

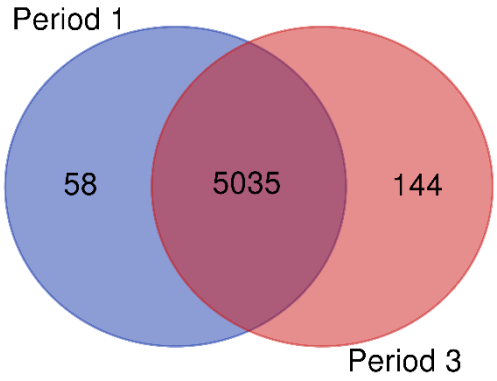

Figure 50. Venn Diagram showing the number of unique and common proteins identified in at least one coral sample in Periods 1 and 3.

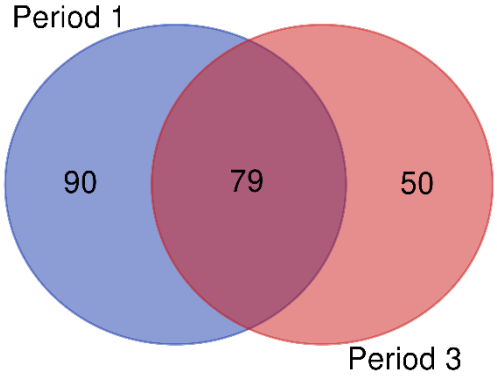

Figure 51. Venn Diagram showing the number of unique and common proteins identified in all coral samples in Periods 1 and 3

Table 8. Differentially abundant proteins during Period 1 in low resistance and some resistance corals when compared to high resistance corals.

Accession Numbers	Proteins differentially abundant in "susceptible"	Fold Change
XP_020600803.1	heat shock cognate 71 kDa protein-like	1.24
XP_020608140.1	glutamic acid-rich protein-like	1.51
XP_020613965.1	uncharacterized protein LOC110052179	1.11
XP_020615186.1	lamin-B1-like	1.46
XP_020630384.1	uncharacterized protein LOC110067397	1.27
XP_020607894.1	guanylate-binding protein 4-like	1.34
XP_020625412.1	pyruvate kinase PKM-like	1.26
XP_020630784.1	phosphatidylinositol-binding clathrin assembly protein LAP-like	1.15
XP_020627630.1	RAC-gamma serine/threonine-protein kinase-like	1.06

Table 8 continued.

Accession Numbers	Proteins differentially abundant in "medium"	Fold Change
XP_020601888.1	protein phosphatase 1 regulatory subunit 12C-like	0.71
XP_020615643.1	F-actin-capping protein subunit alpha-2-like	0.7
XP_020628332.1	staphylococcal nuclease domain-containing protein 1-like	0.76
XP_020632349.1	glycine-rich RNA-binding protein 1-like	0.77
XP_020601488.1	ubiquitin-conjugating enzyme E2 variant 2-like	0.76
XP_020617442.1	polyadenylate-binding protein 4-like	0.77
XP_020630784.1	phosphatidylinositol-binding clathrin assembly protein LAP-like	0.83
XP_020610915.1	tubulin polymerization-promoting protein family member 2-like	0.71
XP_020612008.1	protein NDRG1-like	0.78

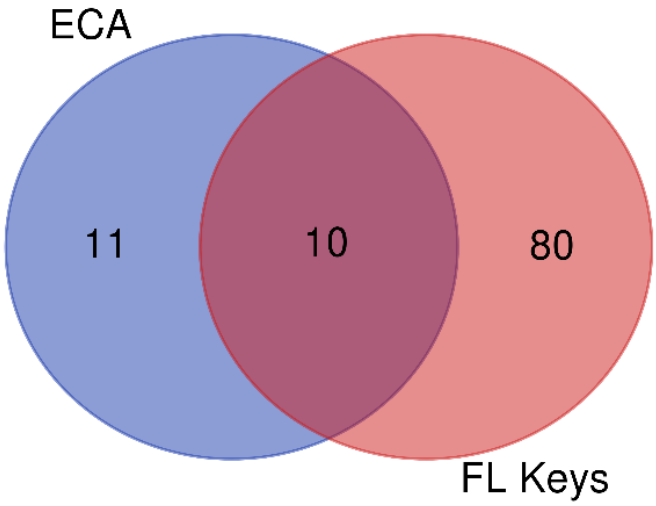

Figure 52. Venn diagram showing number of unique and common protein changes between ECA and Lower Keys low resistance group during SP1.

Table 9. Differentially abundant proteins that changed in both ECA and Lower Keys Regions in the low resistance group during SP1.

Accession Number	ECA & FL Key Common Differentially Abundant Proteins in Period 1 "Susceptible" group	Fold Change FL Keys	Fold Change ECA
XP_020600692.1	phosphatidylserine decarboxylase proenzyme 2-like	1.3	0.74
XP_020611348.1	uncharacterized protein LOC110049851	1.44	0.74
XP_ 020623408.1	histone H2B, gonadal-like	1.41	0.71
XP_ 020621203.1	melanotransferrin-like	1.56	0.75
XP_ 020630503.1	EF-hand domain-containing protein D2-like	1.32	0.8
XP_ 020604604.1	calnexin-like isoform X1	1.47	0.84
XP_ 020607175.1	uncharacterized protein LOC110045893 isoform X1	1.35	0.77
XP_ 020610726.1	sorting nexin-2-like	1.28	0.78
XP_ 020614642.1	cGMP-dependent protein kinase 1-like isoform X4	1.35	0.77
XP_ 020628335.1	protein-glutamine gamma-glutamyltransferase K-like	1.38	0.77

Table 9 continued

Accession Number	ECA Proteins that are differentially abundant in Period 1 in "Susceptible" group	Fold Change	Accession Number	FL Key Proteins that are differentially abundant in Period 1 in "Susceptible" group	Fold Change
XP_020613095.1	sushi, von Willebrand factor type A, EGF and pentraxin domain-containing protein 1-like	0.99	XP_020627630.1	RAC-gamma serine/threonine-protein kinase-like	2.09
XP_020623666.1	uncharacterized protein LOC110061165	1.14	XP_020608860.1	interstitial collagenase-like	1.88
XP_020628963.1	putative gastrointestinal growth factor xP4 isoform X2	1.13	XP_020600429.1	actin, cytoplasmic	1.69
XP_020629364.1	voltage-dependent anion-selective channel protein 2-like	1.25	XP_020609427.1	uncharacterized protein LOC110048010	1.67
XP_020630178.1	peroxiredoxin-5, mitochondrial-like	1.18	XP_020621108.1	receptor expression-enhancing protein 5-like	1.59
XP_020614762.1	prostatic acid phosphatase-like	0.97	XP_020607456.1	calcyphosin-like protein	1.58
XP_020615643.1	F-actin-capping protein subunit alpha-2-like	1.24	XP_020609442.1	uncharacterized protein LOC110048026	1.58
XP_020628093.1	sushi, von Willebrand factor type A, EGF and pentraxin domain-containing protein 1-like	0.99	XP_020609787.1	uncharacterized protein LOC110048345 isoform X1	1.57
XP_020608020.1	sushi, von Willebrand factor type A, EGF and pentraxin domain-containing protein 1-like	1.03	XP_020608140.1	glutamic acid-rich protein-like	1.56
XP_020618666.1	uncharacterized protein LOC110056510	1.26	XP_020621203.1	melanotransferrin-like	1.56
XP_020610820.1	sorting nexin-3-like	1.06	XP_020630384.1	uncharacterized protein LOC110067397	1.55

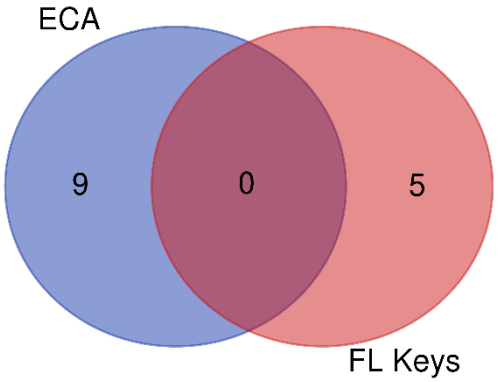

Figure 53. Venn Diagram showing differential protein abundances in ECA and Lower Keys (Sand and Looe Key) in some resistance coral samples compared to high resistance coral samples.

Table 10. Differentially abundant proteins that are unique changes in ECA and Lower Keys some resistance coral groups compared to high resistance corals during SP1.

Accession	ECA Proteins that are differentially abundant in Period 1 in "Medium" group	Fold Change	Accession	FL Key Proteins that are differentially abundant in Period 1 in "Medium" group	Fold Change
XP_020621203.1	melanotransferrin-like	0.72	XP_020601888.1	protein phosphatase 1 regulatory subunit 12C-like	0.71
XP_020628468.1	inorganic pyrophosphatase-like	1.45	XP_020615643.1	F-actin-capping protein subunit alpha-2-like	0.69
XP_020630846.1	mechanosensory protein 2-like	0.59	XP_020607894.1	guanylate-binding protein 4-like	0.69
XP_020632349.1	glycine-rich RNA-binding protein 1-like	0.71	XP_020608860.1	interstitial collagenase-like	1.97
XP_020625515.1	60S ribosomal protein L3-like	0.73	XP_020617442.1	polyadenylate-binding protein 4-like	0.76
XP_020610235.1	LOW QUALITY PROTEIN: AP-2 complex subunit mu-like	0.79			
XP_020614642.1	cGMP-dependent protein kinase 1-like isoform X4	0.72			
XP_020619702.1	glutathione peroxidase 1-like isoform X2	0.69			
XP_020610820.1	sorting nexin-3-like	0.73			

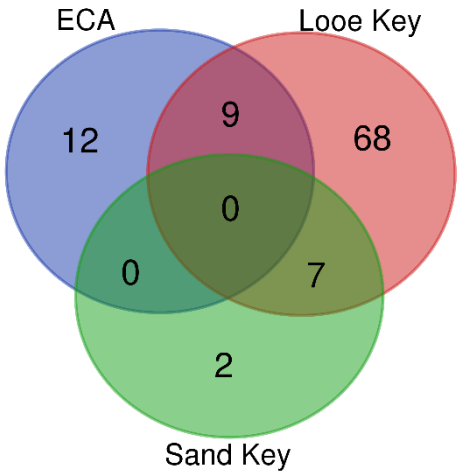

Figure 54. Venn Diagram showing common and unique differential abundances of proteins in ECA, Looe and Sand Key in the low resistance coral group compared to high resistance corals in SP1.

Table 11. Common differential abundances of proteins between ECA and Looe Key in low resistance coral group compared to high resistance corals in SP1.

Accession Numbers	ECA and Looe Key Proteins that are commonly differentially abundant in Period 1 "Susceptible"	ECA Fold Change	Looe Key Fold Change
XP_020611348.1	uncharacterized protein LOC110049851	0.74	1.60
XP_020623408.1	histone H2B, gonadal-like	0.71	1.76
XP_020621203.1	melanotransferrin-like	0.75	1.57
XP_020630503.1	EF-hand domain-containing protein D2-like	0.80	1.33
XP_020604604.1	calnexin-like isoform X1	0.84	1.50
XP_020607175.1	uncharacterized protein LOC110045893 isoform X1	0.77	1.54
XP_020610726.1	sorting nexin-2-like	0.78	1.29
XP_020614642.1	cGMP-dependent protein kinase 1-like isoform X4	0.77	1.46
XP_020618666.1	uncharacterized protein LOC110056510	0.71	1.53

Table 12. Common differential abundances of proteins between Sand and Looe Key in low resistance coral group compared to high resistance corals in SP1.

Accession Numbers	Sand and Looe Key Proteins that are commonly differentially abundant in Period 1 "Susceptible"	Sand Key Fold Change	Looe Key Fold Change
XP_020614358.1	calpain-9-like	1.47	1.38
XP_020630384.1	uncharacterized protein LOC110067397	1.60	1.34
XP_020609885.1	14-3-3-like protein C	1.47	1.53
XP_020609787.1	uncharacterized protein LOC110048345 isoform X1	1.80	1.27
XP_020630784.1	phosphatidylinositol-binding clathrin assembly protein LAP-like	1.43	1.45
XP_020610235.1	LOW QUALITY PROTEIN: AP-2 complex subunit mu-like	1.23	1.30
XP_020621108.1	receptor expression-enhancing protein 5-like	1.58	1.62

Table 13. Differentially abundant proteins that are unique to corals in ECA and Looe Key some resistance group relative to high resistance corals in SP1.

Accession Numbers	**ECA Proteins that are**	ECA Fold Change	Accession Numbers	**Looe Key Proteins that**	Looe Fold Change

	differentially abundant in Period 1 in "Medium" group			**are differentially abundant in Period 1 in "Medium" group**	
XP_020621203.1	melanotransferrin-like	0.72	XP_020600429.1	actin, cytoplasmic	2.13
XP_020632349.1	glycine-rich RNA-binding protein 1-like	0.71	XP_020612133.1	deleted in malignant brain tumors 1 protein-like	1.60
XP_020625515.1	60S ribosomal protein L3-like	0.73	XP_020618943.1	ras-related protein Rab-1A	1.74
XP_020610235.1	LOW QUALITY PROTEIN: AP-2 complex subunit mu-like	0.79	XP_020608860.1	interstitial collagenase-like	2.87
XP_020614642.1	cGMP-dependent protein kinase 1-like isoform X4	0.72	XP_020602028.1	ZP domain-containing protein-like	1.78
XP_020619702.1	glutathione peroxidase 1-like isoform X2	0.69	XP_020630784.1	phosphatidylinositol-binding clathrin assembly protein LAP-like	0.72
XP_020610820.1	sorting nexin-3-like	0.73			

Table 14. The top ten differentially expressed proteins in Sand Key low resistance group during SP3.

Accession Numbers	Sand Key Proteins that are differentially abundant in Period 3 “Susceptible”	Sand Key Fold Change
XP_020608772.1	integumentary mucin A.1-like	2.32
XP_020606936.1	myosin-8-like	0.72
XP_020628074.1	protein disulfide isomerase-like 2-2	0.67
XP_020606732.1	endoplasmin-like isoform X1	0.63
XP_020616450.1	EGF and laminin G domain-containing protein-like	0.61
XP_020615505.1	talin-2-like	0.61
XP_020609883.1	14-3-3 protein epsilon-like isoform X2	0.60
XP_020621224.1	nesprin-1-like isoform X2	0.59
XP_020610186.1	phosphoenolpyruvate carboxykinase [GTP], mitochondrial-like	0.59
XP_020611585.1	extended synaptotagmin-2-A-like isoform X1	0.58

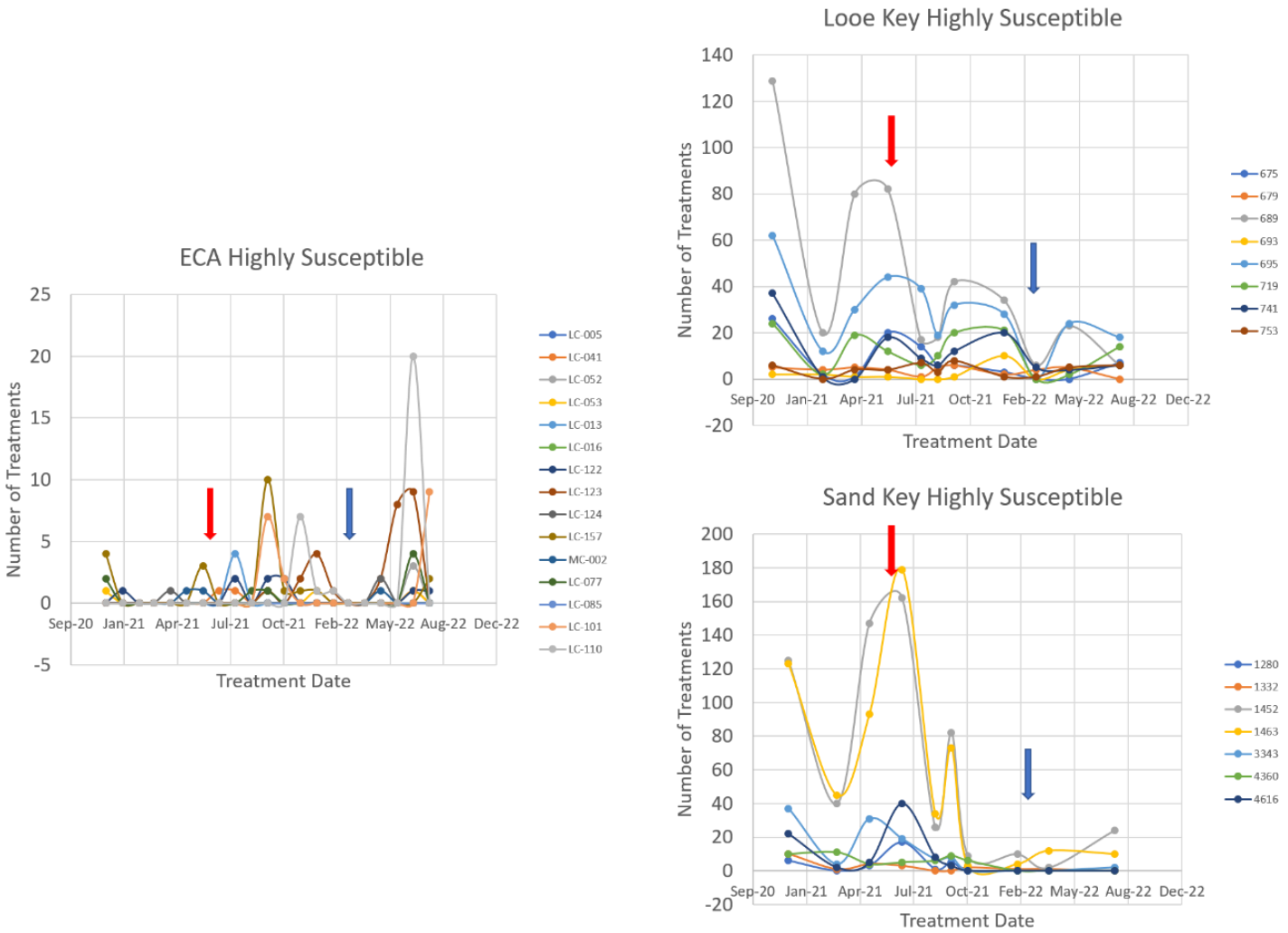

Figure 55. These graphs show the history of antibiotic treatments of low resistance ("Highly Susceptible") corals in the different regions. Red arrows indicate when SP1 samples were taken. Blue arrow indicates when SP3 samples were collected.

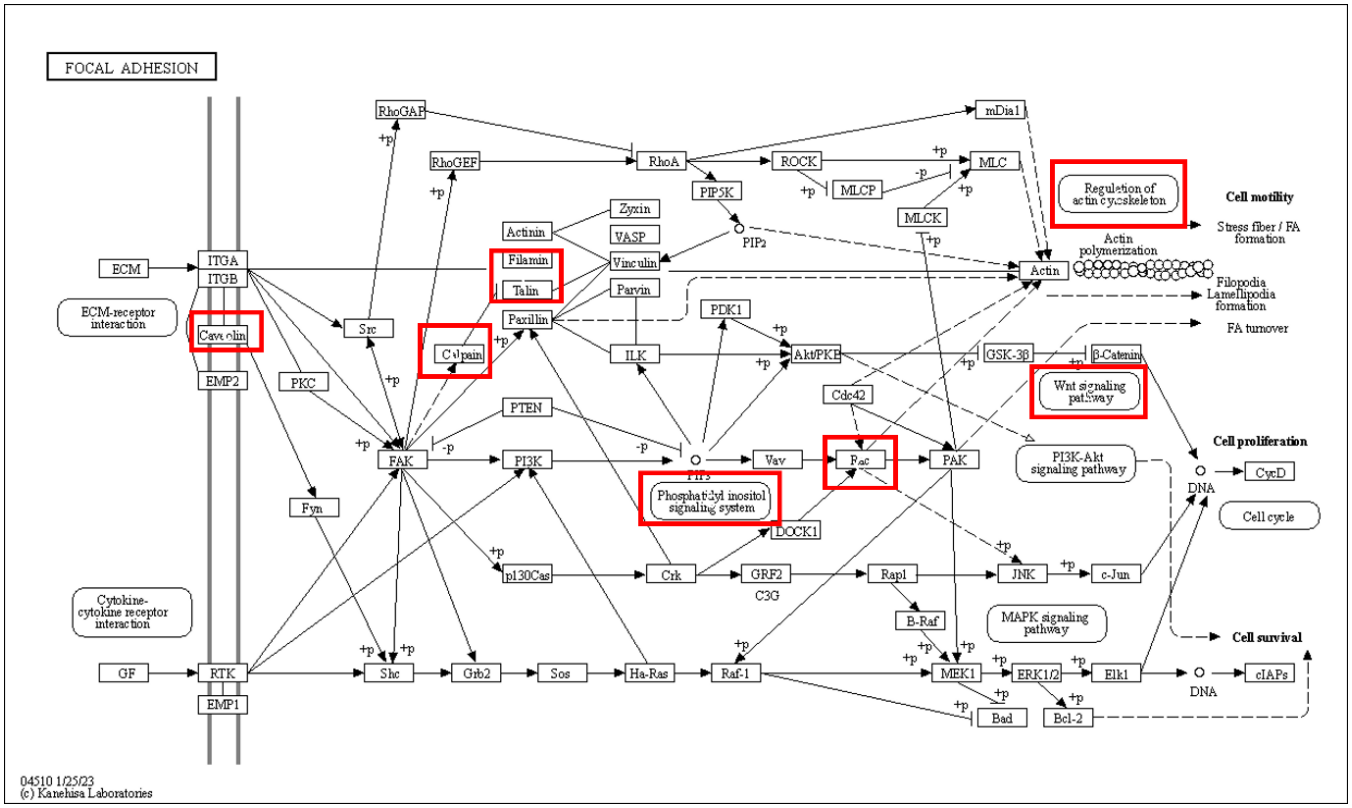

Figure 56. Focal Adhesion Pathways. Red boxes indicate changes seen in our data. With permission: KEGG https://www.genome.jp/pathway/hsa04144

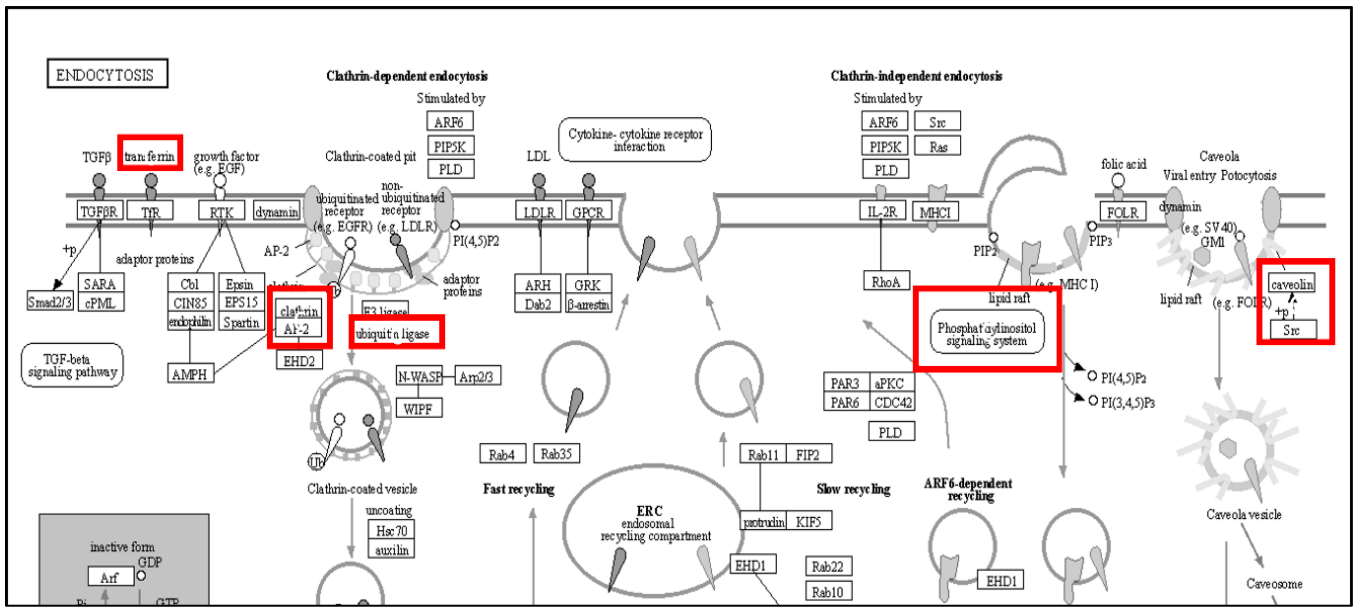

Figure 57. Endocytosis Pathways. Red boxes indicate changes seen in our data. With permission: KEGG https://www.genome.jp/pathway/hsa04144

3.14. **Fecundity (Renegar, Mazurek, and Walker)**

Goal: To quantify the amount of reproductive cells to understand if colony reproduction was being affected by location, environmental stressors, or SCTLD history.

Significant findings: Most colonies were fecund with developmentally appropriate stages for the time of sampling. Polyp fecundity and gamete metrics were lower overall in the Lower Keys region, particularly at Looe Key. SCTLD status (affected) and low resistance level were associated with lower polyp fecundity in the Lower Keys, particularly again at Looe Key. In the Coral ECA, SCTLD status (affected or unaffected) did not impact fecundity, gamete presence, or oocyte size.

Results: It is important to note that the Coral ECA colonies were sampled in August, right before spawning, and the lower Keys were sampled in June. Therefore, differences in oocyte development between regions were expected. However, it is not clear how this sampling difference affects fecundity. Sampling differences should not affect the presence of gametes.

Histology revealed that 91% of the 89 total colonies examined had ova and 85.4% had spermaries (Table 15). Of the 45 ECA corals, 93.3% had ova and 95.6% had spermaries (Figure 58). Of the 44 Lower Keys colonies, 88.6% had ova and 75% had spermaries. Of the 24 Looe Key colonies, 95.8% had ova and 62.5% had spermaries. Of the 20 Sand Key colonies, 80% had ova and 90% had spermaries.

The proportion of oocytes present was not significantly different between locations (Fisher Exact p=0.2058) (Figure 59A), however the proportion of spermaries present was significantly lower at Looe Key (Fisher Exact p=0.001332) (Figure 59B). No significant difference in the proportion of oocytes or spermaries present was found between affected and unaffected corals at each location (Fisher Exact, p=1, 1, 0.2487, 1, 0.657, and 0.5211) although affected corals typically had a lower percentage of gametes present at both locations in the Lower Keys (Figure 59C and Figure 59D).

Mean polyp fecundity (oocytes per gonad per polyp) was significantly higher in the Coral ECA compared to the Lower Keys region (One-way ANOVA, $p < 0.0001$) and to the Lower Keys sites, Sand Key and Looe Key (Figure 60). Polyp fecundity was not significantly different between Sand Key and Looe Key in the Lower Keys (One-way ANOVA, p=0.647). Post hoc analysis of polyp fecundity and location did not identify significant differences between Sand Key and Looe Key.

SCTLD affected colonies had significantly lower fecundity than the unaffected samples in the Lower Keys (One-way ANOVA, p= 0.0147), but not in the ECA (Figure 61). Differences between affected and unaffected corals only occurred at Looe Key (Figure 62). Differences in histopathology supported resistance levels were also found between regions and between low and high resistance in the Lower Keys (Figure 63).

Difference in sampling time, August for the Coral ECA and June for the Lower Keys, resulted in an understandably significant difference in oocyte size and counts by development stages. Significantly more stage 4 oocytes were counted in the Coral ECA, and the Lower Keys had a significantly higher number of stage 3 oocytes (Figure 64). Oocyte diameter was also significantly higher in the ECA for stages 3 and 4 (Figure 65). Interestingly, Looe Key had the smallest mean oocyte max diameter of all locations.

Discussion:

Histology revealed that the majority of colonies were fecund with developmentally appropriate stages for the time of sampling. Observed differences in polyp fecundity and gamete metrics indicate a degree of impact from SCTLD on coral reproductive status, with more significant effects observed in the Lower Keys. SCTLD status (affected or unaffected) did not impact fecundity, gamete presence, or oocyte size in Coral ECA. In contrast, polyp fecundity and gamete metrics were lower overall in the Lower Keys region, particularly at Looe Key. SCTLD status (affected) and low resistance level were associated with lower polyp fecundity in the Lower Keys, particularly again at Looe Key. Interpretation of differences in oocyte metrics was complicated by the difference in sampling time between Coral ECA and the Lower Keys, where the Coral ECA samples were collected close to spawning in August, and the Lower Keys samples were collected in June. This temporal aspect is the likely source of differences in gamete developmental stage and oocyte size between regions.

Table 15. Proportion of colonies with Ova and spermaries present. ECA n=45; Looe n=24; Sand n=20.

Proportion	Ova	Sperm
All corals	0.910	0.854
ECA	0.933	0.956
Lower Keys	0.886	0.750
Looe	*0.958*	*0.625*
Sand	*0.800*	*0.900*

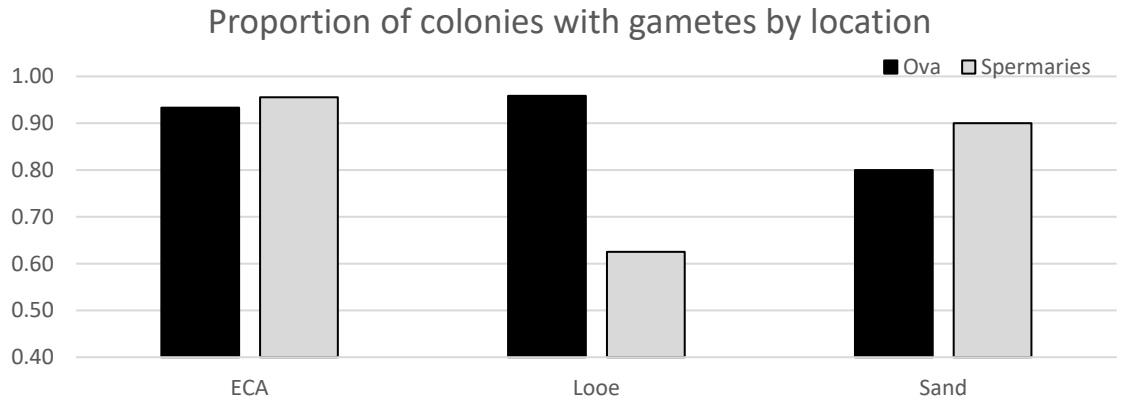

Figure 58. Chart of the proportion of colonies with Ova and spermaries present by location. ECA n=45; Looe n=24; Sand n=20.

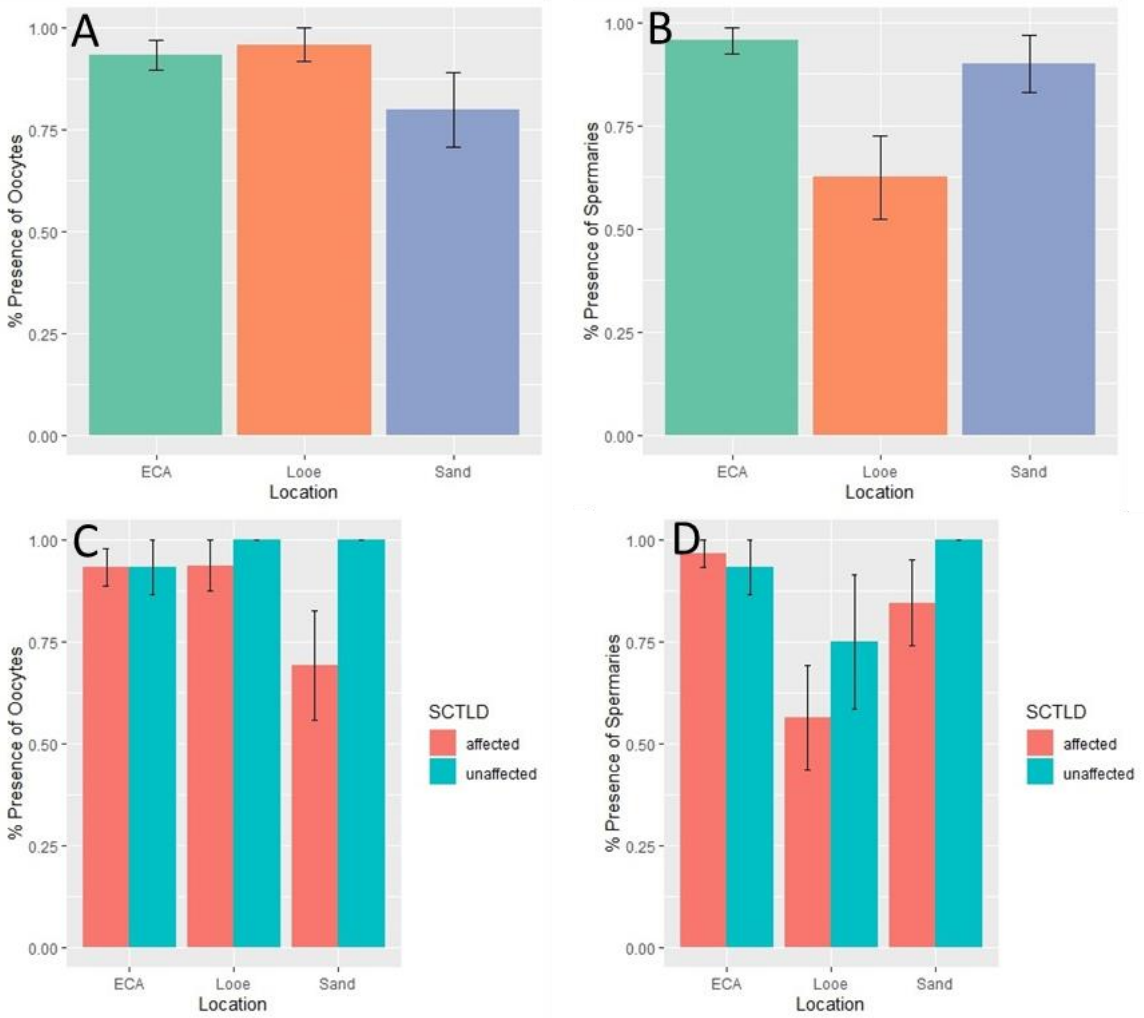

Figure 59. *Orbicella faveolata* gamete % presence (mean +- se). A), oocyte % presence across locations, B) spermary % presence across locations, C) oocyte % presence in affected and unaffected corals across locations, and D) spermary % presence in affected and unaffected corals across locations.

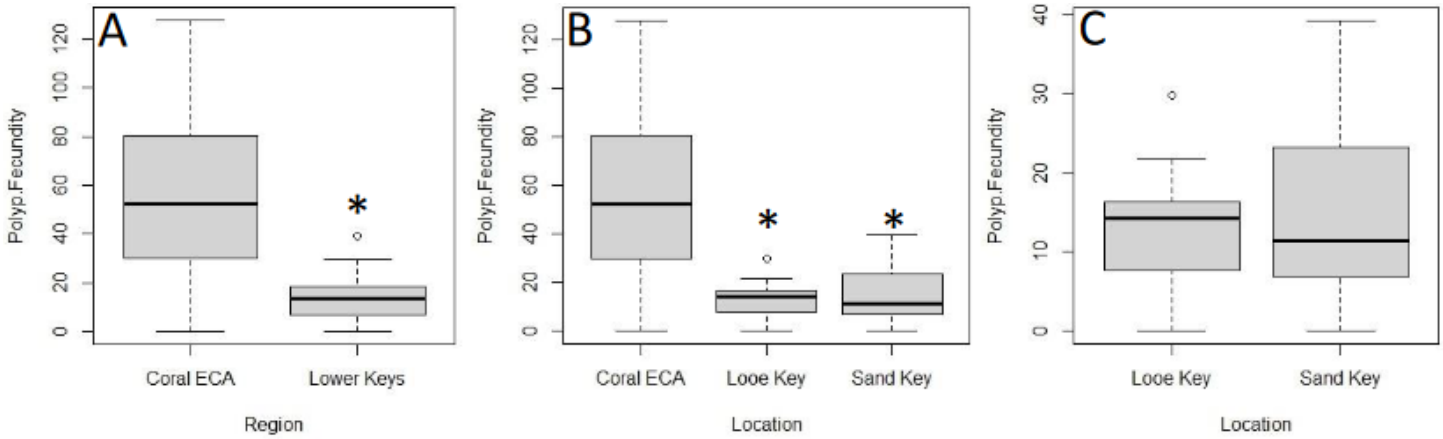

Figure 60. *Orbicella faveolata* polyp fecundity and region or location. A) the Coral ECA and Lower Keys regions B) all sites, and C) locations in the Lower Keys.

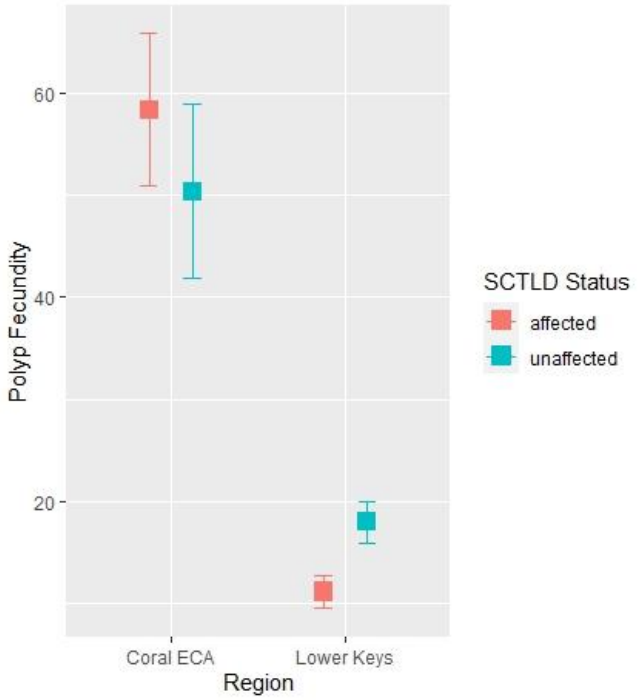

Figure 61. Polyp fecundity (±se) between SCTLD affected and unaffected colonies in the Coral ECA and the Lower Keys.

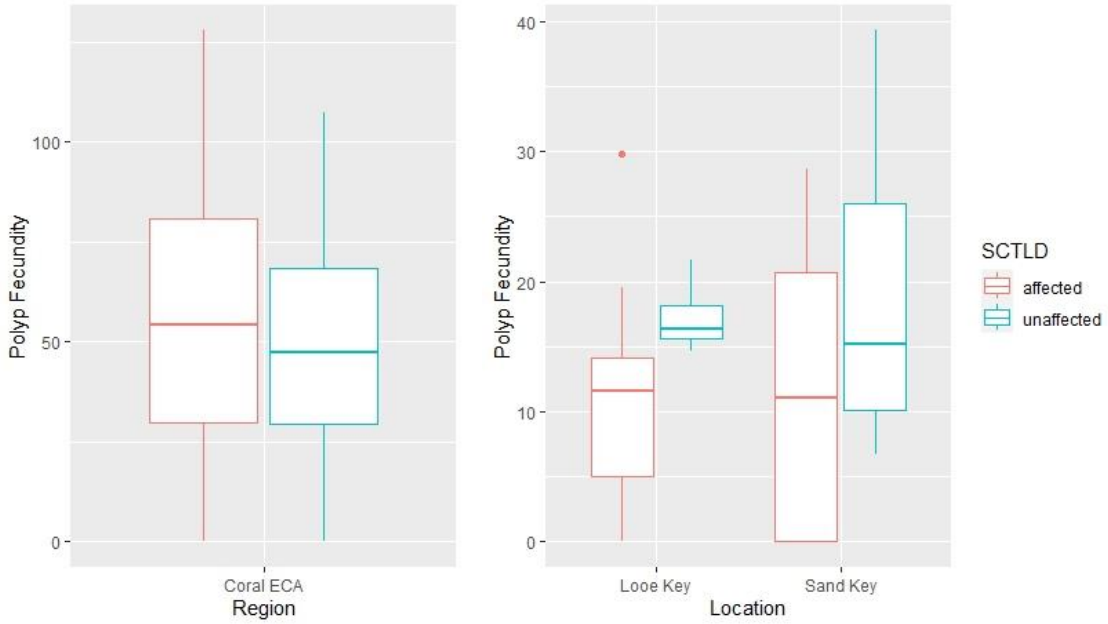

Figure 62. Polyp fecundity between SCTLD affected and unaffected in the Coral ECA (left) and Lower Keys locations Looe and Sand Key (right).

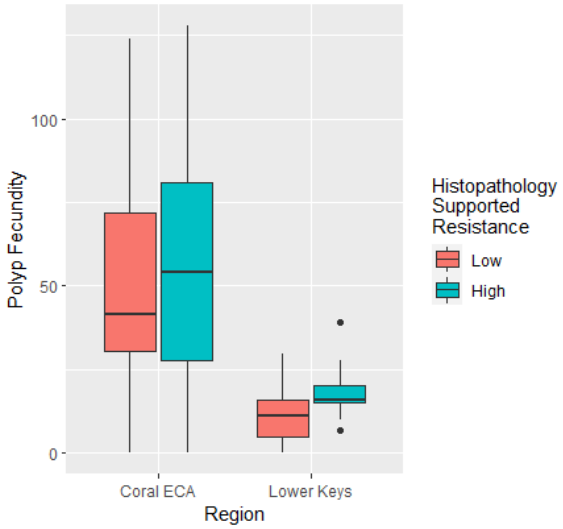

Figure 63. Polyp fecundity between histopathology supported resistance factors in the Coral ECA and Lower Keys.

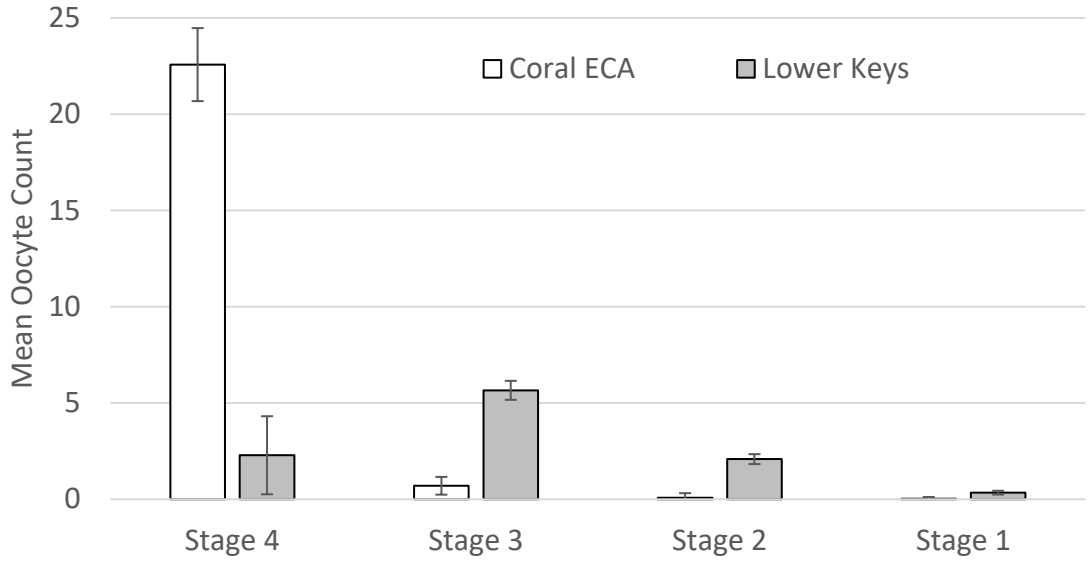

Figure 64. Mean oocyte counts by Region for all four development stages.

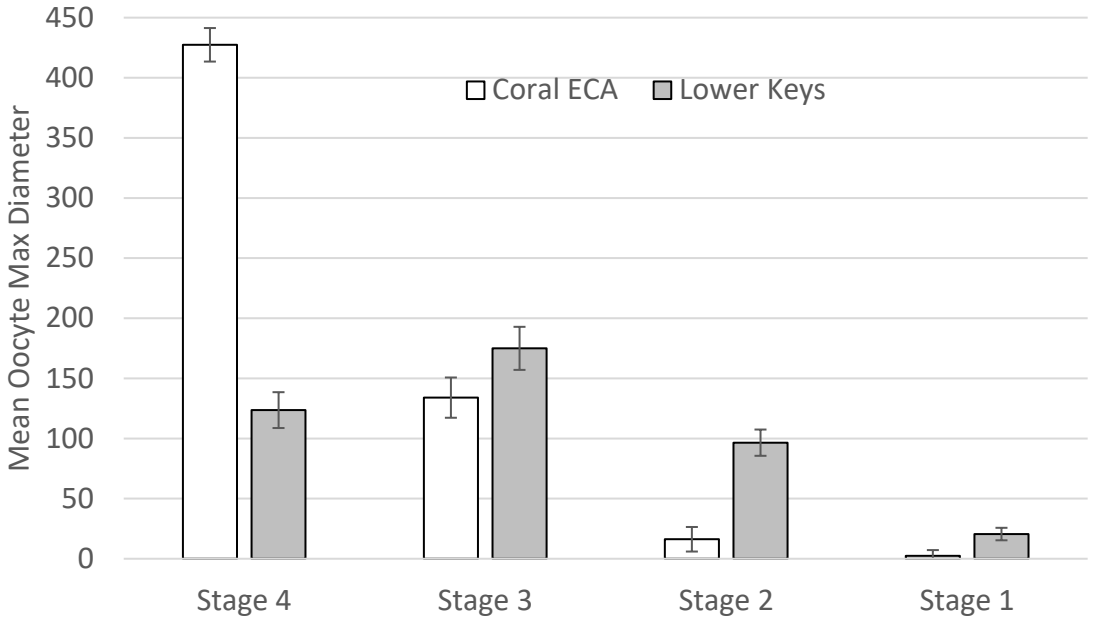

Figure 65. Mean maximum diameter (±se) for stage 3 oocytes (left) and stage 4 oocytes (right) by Region.

4. CONCLUSIONS AND NEXT STEPS

The SCTLD Resistance Research Consortium's (RRC) integrated approach to understanding the underpinnings for SCTLD resistance and susceptibility among Florida *O. faveolata* populations has been a success. The synchronized core sampling across time of year, regions, and disease resistance classes of a statistically robust number of corals has given many insights into the genetic, biochemical, and physiological underpinnings in the holobiont of individuals.

Genetic analyses identified three colonies of a separate species, several clones, and a distinct lineage in the Coral ECA. It discovered a highly connected population throughout the reef tract with no evidence of regionality or associations to disease resistance. Using size as a proxy for age, the genetics of these large colonies indicates that the *Orbicella* populations were once successfully recruiting throughout the reef system. Something that happens very rarely if at all today.

Disease was evident in all coral samples at varying levels. Histopathology scoring supported the resistance categories by showing increased lytic necrosis and degenerative Symbiodiniaceae in the low resistance colonies, but only over certain times of year. Histopathology scores were highest at the end of summer before and after releasing gametes and were lowest in the March. More investigation of these data is needed to determine the role of gametogenesis and environmental stress on the amount of lytic necrosis and degenerative Symbiodiniaceae throughout the year. No clear associations of Symbiodiniaceae with disease resistance were found. This prompted additional sample

analyses using ITS2 to identify Symbiodiniaceae species. Once complete, the ITS2 will be used to look for associations in disease resistance and histopathology differences.
Coral disease was dynamic during the study with some corals getting more disease, some for the first time, and others having less. While all corals were sampled in healthy-looking tissue away from any disease, tracking these disease states facilitated identifying specific corals with recent disease to investigate resistance and possible disease markers. More research is needed to understand what specific aspects of these corals differed.

Metabolite, lipid, and protein data all provided evidence that a coral's state is dynamic over time and varied by region. Differences in resistance were found only in specific regions at specific times of the year. In the Lower Keys, resistance classes differed by metabolite species in June and September, by lipid species in June and March, and by protein species in June. In the ECA, no significant differences were found in all metabolite, lipid, or protein species between resistance classes. Although as a whole certain patterns were seen, there were differences in specific metabolites, lipids, and proteins that warrant further investigation. Research is needed into the specific compounds causing these differences and their functions inside the cell to determine if they are related to gametogenesis, environmental stress, or disease resistance/susceptibility.

Most colonies were fecund with developmentally appropriate stages for the time of sampling. Polyp fecundity and gamete metrics were lower overall in the Lower Keys region, particularly at Looe Key. SCTLD status (affected) and low resistance level were associated with lower polyp fecundity in the Lower Keys, particularly again at Looe Key. In the Coral ECA, SCTLD status (affected or unaffected) did not impact fecundity, gamete presence, or oocyte size. More research of these data is needed to understand the role of gametogenesis in cell functioning, histopathology, associations with disease, and associations with amoxicillin treatments.

A key piece missing thus far in the project is the microbial data. Bad sequencing runs inhibited the timely ability to analyze the microbial communities. The chemical defense analyses showed that the highest antimicrobial activity coincided with the period of lowest thermal stress (SP3) and was highest in SCTLD unaffected corals. Zones of inhibition were lowest in May/June (SP1). The differences between affected and unaffected corals were not significant in SP1 and increased and widened between sample periods. The differences in antimicrobial activity over the year could be indicative of colonies putting more resources into reproduction, environmental stress, or high microbe loads. More research is needed to determine associations here. Steps have been taken to re-sequence extracted DNA in the coming months to help understand the role microbe play in these colonies. Furthermore, the microbial metagenomics is a painstakingly slow process to build the libraries and annotate. Progress on this in the coming year will help elucidate the functions the microbial communities are expressing across time, regions, and resistance.

The transcriptomics data have not been fully analyzed, however preliminary results suggest that corals with low and some resistance to SCTLD have a fingerprint of the effects in their gene expression that might contribute to recurrent infections. We obtained 50 unique genes differentially expressed amongst all the comparisons. These genes could play a role in the

type of response to SCTLD that these colonies have had. 25 of the 50 DEG have unknown functional annotations. More analysis is needed, especially with regard to region and sample period, to determine how the whole transcriptome is involved with the regulation of these genes.

In conclusion, the analyses of the many various components in this investigation, genomics, transcriptomics, metabolomics, proteomics, lipidomics, histopathology, microbiomes, endosymbionts, tissue regeneration, and fecundity, have elicited many future research leads to gain a wholistic understanding of the coral's condition. This project was successful in obtaining the data to realize the goal of understanding and determining SCTLD resistance and susceptibility factors in *Orbicella faveolata* on Florida's Coral Reef. There is much work remaining to uncover the many statistical associations and pathways across the various components.

Appendix 1. Additional sample processing details.

1. HISTOPATHOLOGY

270 *Orbicella faveolata* 20mm diameter samples preserved in z-fix with at least 1:20 ratio of tissue to z-fix were cataloged and photographed over three sampling periods. Tissue plugs were trimmed into tissue cassettes, decalcified with EDTA, and embedded in paraffin blocks. Core trimming was such that there was a sagittal section the width of the sample and two coronal sections with one embedded oral side up and the other oral side down, and all tissue is embedded. The sections are 4um thick. They were then cut and stained with hematoxylin and eosin for detailed tissue description and analysis. Tissue sections were examined and classified as SCTLD affected or unaffected. Affected samples received a description, and semiquantitative scoring of characteristic lesions, with comparison of lesion development over the course of the study where available.

Slides were prepped, evaluated, and scored by Aine Hawthorn. Scoring consisted of identifying conditions present in each slide and ranking its severity on a scale from 1 to 4. One being the least severe and four being the most. Sample Period 1 and 2 scored the following eight features: Lytic necrosis, Zoox degeneration, Mucocyte hypertrophy/ hyperplasia, Pyknotic necrosis, Skeletal (endolithic) suspect fungal hyphae, Calicodermis condition. The presence of ova and spermaries and other organisms were noted. These features were chosen based on Esther Peters in white plague investigation and Landsberg et al. 2019 that described lytic necrosis and symbiont degeneration as an indicator of SCTLD. After extensive meeting and coordination with the SCTLD Histopathology working group, only three features were scored for sample period 3: Clear evidence of lytic necrosis (minimum score 2), symbiont degeneration, and mucocyte hyperplasia. Data were analyzed across all 270 samples in Primer with lytic necrosis, symbiont degeneration, and mucocyte hyperplasia scores as variables.

Histopathology scoring definitions.

Score	Lytic necrosis	Mucoid Hyperplasia	Septal Tissue Loss	Calicodermis Condition	Symbiodiniaceae Condition
0	No lytic lesions in section	Not hypertrophic, no increase	None, tissue over costae intact	Cells squamous and cover mesoglea	No changes; healthy zooxanthellae
1	Rare, small area(s) of lytic necrosis within gastrodermis and not crossing body wall	Mild hypertrophy	Fewer than 1/4 of costae exposed	Cells slightly attenuated or hyperplasitc in some foci	Occasional swollen and pale, vacuolated or hypereosinophilic zoox
2	Lesion that crosses body wall and/or small but multiple areas of lysis	Moderate hypertrophy, mucous release	1/4 to 1/2 of costae exposed	Prominent hyperplasia and/or attenuation	Degenerate (pale/swollen/vacuolated) or necrostic (misshapen. Shrunken, Hypereosinophilic) zoox present

3	Larger, more common lesions that cross body wall and/or extend across the gastrovascular space	Marked hypertrophy, some ruptured and necrotic mucocytes	1/2 to 3/4 costae exposed	Extensive attenuation or hyperplasia, coral acid protein, small foci of sloughing and/or necrosis	5% to 10% of zoox degenerate or necrotic
4	Large, multiple areas of lytic necrosis with loss of gastrodermis and/or body wall	Extensively hypertrophic and ruptured mucocytes, poor tissue integrity	More than 3/4 costae exposed	Necrosis and loss or sloughing present, and/or abundant coral acid protein	>10% of zoox degenerate or necrotic

2. TEM

Samples were decalcified with disodium EDTA (pH=8), rinsed in 0.1 M sodium cacodylate buffer containing 0.35 M sucrose and postfixed with 1% osmium tetroxide in 0.1 M sodium cacodylate buffer. Tissues were dehydrated in a graded ethanol series, the ethanol replaced with propylene oxide and embedded in LX112 epoxy resin. Ultrathin (60 to 80 nm) sections were obtained on an RMC Powertome ultramicrotome, double stained with uranyl acetate and lead citrate, viewed on a Hitachi HT7700 TEM at 100 kV, and photographed with an AMT XR-41B 2k-by-2k charge-coupled device (CCD) camera.

Electron micrographs were taken of the main tissue layers of corals including the calicodermis, gastrodermis, and epidermis. Morphology of cells and their organelles within these layers were characterized and compared and contrasted between normal and diseased tissues to evaluate any anomalies. Particular attention was paid to host cells and algal symbionts and their associated organelles including morphology of nucleus, pyrenoids, thylakoids, and symbiosomal membrane. Lesions were graded subjectively as to severity depending on morphological changes and any evidence of non-coral structures (viruses, inclusions, infectious agents) were documented and characterized. An attempt was made to determine where in the cell pathology occurred (e.g. what organelles are affected) to provide clues to search for agents that could cause such cell pathology (like toxins or toxicants).

3. GENOTYPING (from Klein and Voss 2023)

3.1. Genomic DNA Extraction and 2bRAD Library Preparation

Genomic DNA was extracted using a modified dispersion buffer extraction following Sturm et al., 2020. Extracted DNA was purified using the Zymo DNA Clean and Concentrate Kit following manufacturer's protocols and purified DNA was then quality checked on a NanoDrop 2000 (Thermofisher) and quantified on a Qubit 4.0 fluorometer (Thermofisher). DNA concentrations were then normalized to 25 ng µl-1 as a template for SNP genotyping using the 2bRAD RAD-seq method. 2bRAD libraries were prepared following Wang et al. 2012 (https://github.com/z0on/2bRAD_denovo) with the summarized modifications. Digestion of 100 ng DNA was completed using the type IIB restriction enzyme *BcgI*. Unique in-line index adapters were ligated onto digested DNA fragments and subsequent dual indices were added to pooled ligations via PCR. Digestion,

ligation, and PCR amplification were performed in triplicate on three samples as a method for identifying naturally occurring clones (Manzello et al. 2019). Pooled, uniquely indexed libraries were sequenced on a single lane of the Illumina NovaSeq using a S1 SR-100 flowcell. Sequence data were demultiplexed into 8 pools by the sequencing facility based on their unique indices, further demultiplexed using their in-line index, then quality-filtered and trimmed using custom Perl scripts (https://github.com/z0on/2bRAD_denovo).

3.2. Coral Host Genotyping

High-quality reads that aligned uniquely to the *O. faveolata* genome were used for downstream population genetic analyses. The program ANGSD was used to identify SNP loci from sequencing reads, generate genotype likelihoods, and create an identity-by-state (IBS) genetic distance matrix (Korneliussen, Albrechtsen, and Nielsen 2014). Using this genetic distance IBS matrix, a cluster dendrogram was created to identify patterns of genetic similarity. A minimum genetic distance threshold for clonal groups was defined by the lowest level of genetic similarity among a set of library-prepared technical replicates, any sample clusters that fell below this threshold were identified as natural genetic clones. One member of each clonal group was kept for subsequent analyses based on the highest number of reads and coverage. A new genetic distance IBS matrix was created after the clones and *O. franksi* were removed and used to conduct a Principal Coordinates Analysis (PcoA). An Analysis of Molecular Variance (AMOVA, 99 permutations) was conducted using the program *poppr* v2.9.2, and *adegenet* v2.1.4 on the BCF file produced by ANGSD, using both SCTLD affectedness and region as factors (Jombart et al. 2021; Kamvar et al. 2021).

Pairwise fixation index (F_{ST}) values between each SCTLD resistance group as well as between sampling sites were calculated using the package STAMPP v1.6.3, and heatmaps of these values were generated (Warnes et al. 2017; Pembleton 2021). Population structure was assessed using NGSadmix for $K = 1-8$ (the number of populations sampled plus 3 to identify potentially cryptic clusters; Skotte et al. 2013). The programs Clumpak and StuctureSelector were then used to assess K likelihoods. Clumpak uses the Evanno method, and Structure Selector uses the Puechmaille method (Kopelman et al. 2015; Puechmaille 2016; Li and Liu 2018). The program BayeScan was used to identify any outlier SNPs (50,000 burn-in, 5,000 iterations; Foll and Gaggiotti 2008).

3.3. Algal Symbiont Typing

Along with DNA from the coral host, DNA from the algal symbionts is also co-extracted and prepared into 2bRAD libraries. To isolate coral host sequences from algal sequences, high-quality 2bRAD reads were first mapped to a concatenated Symbiodiniaceae metagenome with the software package *Bowtie 2* (Langmead et al. 2009). These reads were then aligned to the *O. faveolata* genome (Prada et al. 2016). Sequence reads that mapped to both the Symbiodiniaceae metagenome and the *O. faveolata* genome were discarded from subsequent analyses. Relative alignment rates to each of the four symbiont genomic references (*Symbiodinium microadriacticum*, *Breviolum minutum*, *Cladocopium goreaui*, *Durusdinium trenchii)* were used as a proxy for the relative abundance of the four algal symbiont genera associated with each colony. A permutational multivariate analysis of variance (PERMANOVA) was run to determine significance in beta diversity across

differing disease susceptibility status as well as across sites. Abundances of each symbiont genera were square root transformed for this PERMANOVA to minimize influence of the most abundant symbiont group. A Welch's Two-Sided t-test was run to identify significance in differing abundance of the four symbiont genera among disease susceptibility status.

4. **MICROBIOME** (from Klein and Voss 2023)

4.1. **Microbial DNA Extraction and 16S rRNA Amplicon Library Preparation**

In April 2021, samples from outside this experiment were used to test two protocols for extracting microbial DNA from *O. faveolata*. The first protocol was a modified version of the Qiagen DNeasy PowerBiofilm Extraction Kit. The second was an extraction protocol using a dispersion buffer that was also used for the coral genotyping analysis (https://lexiebsturm.github.io/mcavDispersionBufferExtraction). Both extraction methods yielded usable quality and quantities of DNA however, we decided to move forward with using the dispersion buffer extraction method as it gave the best PCR amplification.
Primer sets that target the V4 and the V3-V4 region of the 16S molecule were also tested. Results using V4 primer pairs (Apprill et al., 2015), showed non-specific primer annealing to presumed host DNA. In an attempt to correct this, the V4 primers were paired with peptide nucleic acid (PNA) clamps (Lundberg et al., 2013), however host contamination was still present after amplification. Additionally, primers targeting the V3-V4 region were optimized. These primers have shown much less host contamination. therefore, we decided to move forward using the V3-V4 primer pair as tests showed it gave better amplification for the targeted region.

Microbial DNA was successfully extracted from all 90 colonies for all three timepoints using the optimized dispersion buffer extraction method. There were issues obtaining good quality and quantity of DNA from Timepoint 3 samples. Samples were eventually soaked in DNA-RNA shield overnight and then DNA was re-extracted. Extracted DNA was cleaned and then quantified using Qubit fluorometer. Aliquots (5ul) of clean DNA for each of the samples from both timepoints were prepared and sent out to Dr. Julie Meyer for her complementary analyses.

Samples were library prepped to amplify the V3-V4 region of the 16S rRNA molecule. Extracted and cleaned DNA were them library prepared for amplification targeting the *16S* rRNA V3/V4 region. This region was selected as it is universally utilized across microbiological studies, including the Earth Microbiome Project, and therefore will allow for comparison and matching against existing sequence databases (Bukin et al., 2019; Herlemann et al., 2011; Weber et al., 2017). This initial amplification PCR included 30 µL total volume reactions of each sample, including 20 ng of template DNA, 1.25 U of GoTaq Flexi DNA polymerase (Promega Corporation, Madison, WI, USA), 5X Colorless GoTaq Flexi buffer, 25 mM $MgCl^2$, 2.5 µM of each deoxynucleoside triphosphate (dNTP), and 2.5µM of each barcoded primer (Illumina 2013; Weber et al. 2017). PCR cycle lengths and temperatures followed those recommended for this polymerase with slight modifications to account for primer lengths (Weber et al. 2017). The primers selected for testing amplification for the V3/V4 region are

343FL: 5’ TATGGTAATTGTCTCCTACGGRRSGCAGCAG 3’
806RL: 5’ AGTCAGTCAGCCGGACTACNVGGGTWT CTAAT 3’ (Bukin et al., 2019).

Nextera adapters were added to these primer sequences in accordance with the sequencing facility. All first round PCR amplification product were sent to University of Rhode Island’s Bioinformatics Sequencing Core. The sequencing facility then conducted first round OCR cleanup and individual barcoding. Fully prepared samples were then sequenced on and Illumina MiSeq (600 cycle). Timepoint 1&2 samples were sequenced on the same run. Timepoint 3 samples were sequenced independently.

4.2. Characterization of Amplicon Sequence Variants (ASVs)

Adapters and primers were removed from raw sequence reads using cutadapt v 3.5.1 and further processing of amplicon libraries were completed in R 4.2.1. All sequence processing was completed following custom scripts from RRC collaborator Julie Meyer (https://github.com/meyermicrobiolab/Stony-Coral-Tissue-Loss-Disease-SCTLD-Project) (Meyer et al. 2019). Quality filtering, error estimation, merging of reads, dereplication of reads, removal of chimeras, and selection of amplicon sequence variants (ASVs) were conducted using DADA2 v. 1.26.0. Modifications to the filtering parameters were needed as sequencing yelled ~300bp paired end reads. Parameters are as follows;

truncLen=c(240,230), maxN=0, maxEE=c(2,2), truncQ=2, rm.phix=TRUE, compress=TRUE, multithread=FALSE).

DADA2 was also used to assign taxonomy to all ASVs. ASV and Taxonomy tables were imported into phyloseq v. 1.42.0 along with sample metadata to conduct microbial community analyses. Sequences that identified as chloroplasts or mitochondria were removed from dataset. ASVs with a sample mean count of less than 2000 reads were also removed from further analyses.

5. *VIBRIO CORALLIILYTICUS* ddPCR

This task quantified the presence of *Vibrio coralliilyticus* to examine the connection between *V. coralliilyticus* and intercolony differences in disease susceptibility using droplet digital PCR (ddPCR). We have successfully developed a useful gene target for the quantification of the coral pathogen *V. coralliilyticus*, which does not appear to be the primary pathogen in stony coral tissue loss disease, yet appears to play a role in the severity of disease lesions (Ushijima et al., 2020). We have shown highly consistent results between the quantification of the *V. coralliilyticus* metalloprotease gene through ddPCR and the detection of the toxic protein encoded by this gene with the *Vibriosis VcpA RapidTest*, indicating that this ddPCR target is an appropriate marker to track the coral pathogen. Extracted DNA samples were received from the Voss lab for quantification of the *Vibrio coralliilyticus* toxin gene *vcpA* by droplet digital PCR (ddPCR). The ddPCR was performed in triplicate for each sample and showed that the *vcpA* gene was present in very low levels across all 90 samples.

6. MICROBIAL METAGENOMES

Before sequencing metagenomic libraries to examine the functional potential of bacterial communities associated with *Orbicella faveolata* colonies of varying resistance to SCTLD,

we optimized metagenomic DNA extractions. Beginning with archived *Montastraea cavernosa* biomass remaining from a previous project, we modified a protocol developed by Dr. Chris Kellogg (USGS) for the physical separation of bacterial cells from cells belonging to the animal host and algal symbionts prior to DNA extractions. Our previous experience on an EPA-funded project to sequence SCLTD coral metagenomes (Meyer et al., in prep) and published SCTLD coral metagenomes (Rosales et al., 2022, Frontiers in Marine Science) has shown that this is an essential pre-processing step to amplify the bacterial signal from the coral holobiont.

We compared two extraction methods: a new kit that is designed to preferentially extract bacterial DNA over host DNA (Qiagen QIAmp Microbiome kit) and the kit preceded by the physical separation step on samples of *M. cavernosa* biomass from a previous project and *O. faveolata* samples collected by the Voss lab before sample period 1. Four metagenomic libraries (two methods x two species) were prepared and sequenced at UF's Interdisciplinary Center for Biotechnology Research with Illumina MiSeq. This miniature sequencing run allowed us to compare the relative proportions of bacterial versus eukaryotic reads for each DNA extraction method. The comparison revealed that the Qiagen QIAmp Microbiome kit produced libraries with higher proportions of bacterial reads (8% in *M. cavernosa* and 6% in *O. faveolata*) than the physical separation + Qiagen QIAmp Microbiome kit method (7% in *M. cavernosa* and 4% in *O. faveolata*). This was likely due to the loss of biomass and its constituent DNA during the physical separation step. Therefore, the 90 samples collected for the current study were extracted with the kit only.

Metagenomic libraries were successfully sequenced for 89 out of 90 samples collected during sample period 1 (May/June 2021). One high resistance sample (N-49) from Sand Key had an insufficient quantity of DNA for sequencing. An average of 123 million reads were obtained for each library (~2 Tb of data total) (Table 1). The original sequencing reads are publicly available in NCBI's Sequence Read Archive under BioProject PRJNA925892.

Table 1. Accession numbers and sequencing reads for each of 89 metagenomic libraries.

accession	sample	coral	location	resistance	resistance2	# of raw sequencing reads
AMN32816840	617	Ofav	Looe Key	intermediate	SCTLD affected	158,549,767
SAMN32816917	663	Ofav	Looe Key	intermediate	SCTLD affected	112,039,591
SAMN32816880	675	Ofav	Looe Key	low	SCTLD affected	154,747,672
SAMN32816918	679	Ofav	Looe Key	low	SCTLD affected	111,054,705
SAMN32816921	689	Ofav	Looe Key	low	SCTLD affected	132,065,719
SAMN32816844	693	Ofav	Looe Key	low	SCTLD affected	292,110,709
SAMN32816883	695	Ofav	Looe Key	low	SCTLD affected	154,727,589
SAMN32816856	699	Ofav	Looe Key	intermediate	SCTLD affected	103,262,730
SAMN32816836	713	Ofav	Looe Key	intermediate	SCTLD affected	122,288,433
SAMN32816915	719	Ofav	Looe Key	low	SCTLD affected	90,255,249
SAMN32816867	741	Ofav	Looe Key	low	SCTLD affected	150,926,561

SAMN32816913	753	Ofav	Looe Key	low	SCTLD affected	91,074,674
SAMN32816914	765	Ofav	Looe Key	intermediate	SCTLD affected	95,521,778
SAMN32816912	1004	Ofra	Sand Key	intermediate	SCTLD affected	76,675,166
SAMN32816853	1220	Ofav	Looe Key	intermediate	SCTLD affected	112,037,913
SAMN32816839	1280	Ofav	Sand Key	low	SCTLD affected	152,560,292
SAMN32816908	1332	Ofav	Sand Key	low	SCTLD affected	114,489,549
SAMN32816893	1340	Ofav	Sand Key	intermediate	SCTLD affected	116,865,259
SAMN32816866	1452	Ofav	Sand Key	low	SCTLD affected	110,821,092
SAMN32816851	1455	Ofra	Sand Key	intermediate	SCTLD affected	93,950,194
SAMN32816837	1463	Ofav	Sand Key	low	SCTLD affected	140,977,911
SAMN32816863	1470	Ofra	Sand Key	intermediate	SCTLD affected	144,520,473
SAMN32816870	1552	Ofav	Middle ECA	low	SCTLD affected	112,150,304
SAMN32816852	1557	Ofav	Middle ECA	low	SCTLD affected	134,873,437
SAMN32816895	1655	Ofav	North ECA	high	SCTLD affected	148,557,887
SAMN32816897	1656	Ofav	North ECA	high	SCTLD affected	102,793,358
SAMN32816841	1688	Ofav	South ECA	intermediate	SCTLD affected	115,750,176
SAMN32816857	1703	Ofav	North ECA	intermediate	SCTLD affected	90,815,904
SAMN32816892	1724	Ofav	Middle ECA	intermediate	SCTLD affected	150,045,657
SAMN32816849	1741	Ofav	North ECA	low	SCTLD affected	116,030,454
SAMN32816877	1742	Ofav	North ECA	high	SCTLD affected	109,537,236
SAMN32816887	1743	Ofav	North ECA	high	SCTLD affected	84,655,530
SAMN32816843	1745	Ofav	North ECA	high	SCTLD affected	107,591,803
SAMN32816884	1748	Ofav	North ECA	intermediate	SCTLD affected	101,593,829
SAMN32816846	1749	Ofav	North ECA	intermediate	SCTLD affected	104,049,754
SAMN32816911	1752	Ofav	North ECA	low	SCTLD affected	97,336,136
SAMN32816859	1753	Ofav	North ECA	low	SCTLD affected	166,046,180
SAMN32816872	1777	Ofav	South ECA	low	SCTLD affected	116,635,118
SAMN32816904	1778	Ofav	North ECA	intermediate	SCTLD affected	130,286,399
SAMN32816898	1796	Ofav	Middle ECA	low	SCTLD affected	114,093,626
SAMN32816878	1801	Ofav	South ECA	low	SCTLD affected	101,782,174
SAMN32816862	1810	Ofav	South ECA	low	SCTLD affected	105,294,294
SAMN32816907	1813	Ofav	Middle ECA	low	SCTLD affected	143,718,484
SAMN32816910	1814	Ofav	South ECA	intermediate	SCTLD affected	97,393,920
SAMN32816905	1819	Ofav	South ECA	high	SCTLD affected	190,127,243
SAMN32816855	1822	Ofav	Middle ECA	low	SCTLD affected	79,690,431
SAMN32816850	1825	Ofav	Middle ECA	intermediate	SCTLD affected	110,070,359
SAMN32816916	1922	Ofav	South ECA	intermediate	SCTLD affected	248,214,943
SAMN32816833	1923	Ofav	Middle ECA	low	SCTLD affected	111,205,786
SAMN32816906	1924	Ofav	Middle ECA	low	SCTLD affected	98,243,914

SAMN32816861	2026	Ofav	South ECA	high	SCTLD unaffected	142,371,320
SAMN32816842	2027	Ofav	South ECA	high	SCTLD unaffected	116,433,790
SAMN32816919	2032	Ofav	North ECA	high	SCTLD unaffected	151,471,471
SAMN32816909	2085	Ofav	South ECA	low	SCTLD affected	118,548,915
SAMN32816888	2105	Ofav	North ECA	low	SCTLD affected	109,523,057
SAMN32816865	2115	Ofav	North ECA	intermediate	SCTLD affected	110,821,092
SAMN32816879	2126	Ofav	Middle ECA	intermediate	SCTLD affected	114,285,027
SAMN32816885	2127	Ofav	Middle ECA	high	SCTLD unaffected	137,130,625
SAMN32816920	2129	Ofav	Middle ECA	intermediate	SCTLD unaffected	77,862,278
SAMN32816868	2311	Ofav	South ECA	high	SCTLD affected	120,307,128
SAMN32816876	2314	Ofav	South ECA	high	SCTLD unaffected	85,588,123
SAMN32816882	2405	Ofav	Middle ECA	high	SCTLD unaffected	127,026,904
SAMN32816891	2558	Ofav	Middle ECA	intermediate	SCTLD affected	129,670,693
SAMN32816873	2579	Ofav	South ECA	high	SCTLD unaffected	113,711,322
SAMN32816889	2818	Ofav	Middle ECA	intermediate	SCTLD affected	80,183,676
SAMN32816864	2907	Ofav	Middle ECA	intermediate	SCTLD affected	72,483,737
SAMN32816871	2964	Ofav	South ECA	high	SCTLD unaffected	127,625,704
SAMN32816899	3342	Ofav	Sand Key	intermediate	SCTLD affected	85,651,513
SAMN32816900	3343	Ofav	Sand Key	low	SCTLD affected	95,585,351
SAMN32816875	3420	Ofav	Sand Key	intermediate	SCTLD affected	79,588,185
SAMN32816869	3421	Ofav	Looe Key	intermediate	SCTLD affected	99,609,363
SAMN32816902	3446	Ofav	Looe Key	intermediate	SCTLD affected	149,878,572
SAMN32816845	4360	Ofav	Sand Key	low	SCTLD affected	160,865,148
SAMN32816848	4503	Ofav	Sand Key	intermediate	SCTLD affected	155,231,994
SAMN32816896	4616	Ofav	Sand Key	low	SCTLD affected	88,497,059
SAMN32816874	N46	Ofav	Sand Key	high	SCTLD unaffected	196,175,921
SAMN32816903	N48	Ofav	Looe Key	high	SCTLD unaffected	157,988,131
SAMN32816890	N50	Ofav	Looe Key	high	SCTLD affected	112,155,792
SAMN32816854	N52	Ofav	Looe Key	high	SCTLD unaffected	139,408,154
SAMN32816860	N53	Ofav	Looe Key	high	SCTLD unaffected	162,528,512
SAMN32816886	N54	Ofav	Looe Key	high	SCTLD unaffected	151,575,532
SAMN32816838	N56	Ofav	Looe Key	high	SCTLD unaffected	144,438,740
SAMN32816835	N58	Ofav	Looe Key	high	SCTLD affected	151,949,195
SAMN32816881	N59	Ofav	Looe Key	high	SCTLD affected	98,445,163
SAMN32816858	N60	Ofav	Sand Key	high	SCTLD unaffected	151,698,033
SAMN32816847	N67	Ofav	Sand Key	high	SCTLD unaffected	102,820,598
SAMN32816894	N70	Ofav	Sand Key	high	SCTLD unaffected	121,357,933
SAMN32816834	N72	Ofav	Sand Key	high	SCTLD unaffected	109,972,715
SAMN32816901	N73	Ofav	Sand Key	high	SCTLD unaffected	136,536,647

After sequencing, libraries go through a series of bioinformatics steps that include: 1) quality-filtering of the reads, 2) mapping of the reads to the publicly available *O. faveolata* genome (GCA_001896105.1) and removing the *O. faveolata* reads from the libraries, 3) mapping of the non-*O. faveolata* reads to the publicly available *Breviolum* genome (GCA_000507305.1) and removing the *Breviolum* reads from the libraries, and 4) assembly of the reads remaining after removal of *O. faveolata* and *Breviolum* reads. For this dataset (~ 2 Tb of data), the first step takes about 1 hour per library, the second step takes about 4 hours per library, the third step takes about 15 hours per library, and the fourth step takes about 2.5 days per library. These steps and additional assessments to examine the data quality at each step result in a minimum computational time of roughly 4 days per library. Some processes may be run concurrently to reduce the total computational time, but memory-intensive steps like the assembly will likely need to be run consecutively, requiring months to complete.

The 89 libraries were randomly divided into four equal groups and the first three steps described above have been completed for the first quarter of samples (22 total). After removal of *O. faveolata* and *Breviolum* reads, the phylogenetic composition of the remaining reads was assessed and showed that 4-6% of reads were bacterial, consistent with our mini sequencing run results (Table 2). This translates to roughly 3 million 150-bp bacterial reads per library or approximately 10X coverage of 10 bacterial genomes per library. The remaining unclassified and eukaryotic reads are likely part of the *O. faveolata* and *Breviolum* genomes that were not effectively removed. While our methods enriched the bacterial content of the metagenomic libraries, this clearly did not eliminate all or even most eukaryotic reads in the sequenced libraries. Therefore, the dataset produced can also be useful for additional applications and analyses, including the improvement of *O. faveolata* and *Breviolum* genome assemblies or comparisons of genetic differences across eukaryotic hosts.

Table 2. The proportion of sequencing reads classified as eukaryotic, bacterial, archaeal, or viral from the first quarter of samples after removal of reads mapped to *O. faveolata* and *Breviolum.*

Sample	Location	Resistance	Resistance2	Unclassified	Eukarya	Bacteria	Archaea	Viruses
617	Looe Key	some	SCTLD affected	67.81	26.51	4.63	0.16	0.19
693	Looe Key	low	SCTLD affected	68.34	26.19	4.45	0.16	0.18
713	Looe Key	some	SCTLD affected	63.13	29.98	4.79	0.15	0.17
1220	Looe Key	some	SCTLD affected	74.28	20.38	4.56	0.14	0.17
1280	Sand Key	low	SCTLD affected	66.91	27.36	4.62	0.15	0.18
1455	Sand Key	some	SCTLD affected	72.13	21.57	4.83	0.13	0.16
1463	Sand Key	low	SCTLD affected	66.88	27.77	4.3	0.15	0.18
1557	Middle ECA	low	SCTLD affected	66.66	27.92	4.3	0.15	0.17
1688	South ECA	some	SCTLD affected	59.54	32.09	5.25	0.13	0.16
1741	North ECA	low	SCTLD affected	58.35	32.81	5.44	0.13	0.17

1745	North ECA	high	SCTLD affected	56.44	33.77	6.06	0.13	0.16
1749	North ECA	some	SCTLD affected	55.38	34.79	5.76	0.13	0.16
1825	Middle ECA	some	SCTLD affected	68.42	26.03	4.51	0.16	0.18
1923	Middle ECA	low	SCTLD affected	67.16	27.27	4.42	0.15	0.18
2027	South ECA	high	SCTLD unaffected	68.35	25.96	4.66	0.14	0.21
4360	Sand Key	low	SCTLD affected	67.98	26.54	4.46	0.16	0.18
4503	Sand Key	some	SCTLD affected	67.01	27.58	4.33	0.15	0.18
N52	Looe Key	high	SCTLD unaffected	68.08	26.45	4.43	0.16	0.19
N56	Looe Key	high	SCTLD unaffected	67.31	26.94	4.66	0.16	0.19
N58	Looe Key	high	SCTLD affected	67.93	26.68	4.36	0.15	0.18
N67	Sand Key	high	SCTLD unaffected	66.29	28.11	4.43	0.15	0.18
N72	Sand Key	high	SCTLD unaffected	60.04	31.97	5.2	0.13	0.16

At the Disease Advisory Committee meeting on 3/22/23, NOAA researchers Michael Studivan and Ben Young presented their results for a greatly improved genome assembly for *O. faveolata.* We will therefore use this improved genome assembly for mapping and removing *O. faveolata* reads before metagenomic assembly of bacteria-enriched reads. The final metagenomic assemblies will be deposited in the IMG database.

7. PROTEOMICS (from Saunders et al 2023)

7.1. Sample Acquisition & Processing

All reagents were of highest grade (99% purity) or mass spectrometry (MS) grade commercially available. Collection permits and tissue biopsies were provided to NOAA as part of companion project by Nova Southeastern University, led by Dr. Brian Walker. Tissue biopsies were flash frozen in liquid nitrogen vapor shipper and transported to the Charleston SC, NOAA NOS Hollings Marine Laboratory. Coral biopsy samples were collected from two regions off the Florida coast: northern Broward County, FL (ECA) and southern Florida Keys (FL Keys), comprised of Sand and Looe Keys. Fifteen replicates from each of three infection-rate groups were collected (Resistant, Medium, Susceptible) from each region, for a total of 90 biopsies for each sampling period. Each colony was sampled three times during a one-year period and proteomic analyses were performed on samples collected from two of the three sampling periods (first and last, avoiding spawning).

Samples were submerged in lysis buffer (5% SDS in 50mM triethylammonium bicarbonate; Roche cOmplete™ EDTA-free protease inhibitor cocktail tablet, 1 per 50 mL lysis buffer) and tip sonicated on ice for 10 seconds at a time, 5 times. Samples were then centrifuged 2000 rcf for 5 minutes. The supernatant was decanted to a new vial, centrifuged 10,000 rcf for 10 minutes, then the supernatant was again decanted to a new vial. Protein concentrations were determined with a Pierce™ BCA Protein Assay Kit.

Protein (100 µg) was diluted with 5% SDS to a final volume of 80 µL. Disulfide bonds were reduced with dithiothreitol at 60 °C for 10 minutes. The samples were cooled at room temperature for 10 minutes prior to alkylation with calcium acetamide and incubated in the

dark for 30 minutes. Alkylation was quenched by adding 10 µl of 12% phosphoric acid. The proteins were digested with Protofi's S-traps per Protofi's protocols (Protifi, Fairport, NY), using a 1:20 trypsin:substrate ratio and incubating for 2 hours at 47 °C. The resulting peptide solution was evaporated to dryness and reconstituted with 100 µl 0.1% formic acid in water. The peptide concentration was determined with Pierce™ Quantitative Fluorometric Peptide Assay kit.

7.2. Liquid Chromatography / tandem Mass Spectrometry (LC-MS/MS) analysis

Samples were sent to the University of Arkansas Medical Sciences' proteomic core for nano-LC-MS/MS for analysis on a Thermo Orbitrap™ Eclipse. Peptides were separated by reverse phase XSelect CSH C18 using an UltiMate 3000 RSLCnano system (Thermo). The instrument method used data-dependent acquisition with higher energy collisional fragmentation. Instrument performance and data quality were performed by the University of Arkansas Medical Center's Proteomic Core.

7.3. Protein Identification

Peptide and protein identification were directed through a single MaxQuant run following conversion of raw spectral files. The annotated proteome of *Orbicella faveolata* RefSeq database (release 100: GCF_002042975.1_ofav_dov_v1) was used to search raw files. While the initial dataset was not used for further analyses, the initial observations about types of proteins involved in SCTLD were helpful to use as comparison. Data was imported into several Scaffold files and then the data was exported into mzldent files to be uploaded to the Protein Identification Database (PRIDE). The raw data files from the first data set can be found on (PRIDE) (ID: PXD030923) http://www.ebi.ac.uk/pride/archive/projects/PXD030923.

Only proteins that were identified in all samples from Periods 1 & 3 were used for analysis and the raw spectral data files were uploaded to PRIDE (PRIDE ID: PXD038195). As a quality control for data analyses, a weighted gene co-expression network analysis (Weighted correlation network analysis, 2023) was conducted on the log-transformed raw peptide data of samples separately from Periods 1 and 3 to remove any sample outliers that might skew the data. In Period 1, there were two samples (Sand_Resistant_21-N49 and Sand_Medium_21_1470) removed as outliers, while in Period 3 only one sample (Looe_Medium_22_713) was identified as an outlier and removed from further analyses. When evaluating the raw data of these samples afterwards, these samples had either extensive missing peptide values or very low overall mass spectral signal intensities relative to the other samples. Low signal intensity can indicate that the isolated protein sample was of poor quality and thus justification for being considered an outlier.

7.4. Identifying Differential Abundances of Proteins

Initially, samples were analyzed by clustering all the regions together and only evaluating "susceptible" versus "resistant" coral samples. However, the regions were distinct enough in treatment patterns that it made sense to evaluate them separately to determine whether there were differences in response to SCTLD and/or antibiotic treatment. ECA in particular had fewer antibiotic treatments when compared to Sand or Looe Key.

Both sampling regions (ECA and FL Keys) had differing protein changes between susceptibility groups and collection periods. These changes could be attributed to location of the samples and all differences related to that (e.g., weather, temperature, salinity, pH, etc). Although Sand and Looe Keys initially were grouped together as "FL Keys", the treatment data varied enough such that those locations also were evaluated individually.

This separation of the FL Keys into groups can help explain the intra-/inter-regional differences in disease progression even among colonies that are relatively close to each other. Furthermore, rather than only searching for proteins that were similarly changing in their abundance levels between all three regions, we wanted to evaluate differences in abundance levels between all three regions.

7.5. Functional Analysis

The identified proteins and their relative quantifications were then used to identify molecular factors and potential mechanisms of susceptibility and resistance to SCTLD. GO and KEGG databases were searched to gain more information on other proteins potentially involved.

7.6. QA/QC: included in analytical methods

Samples were provided to the project from the Walker companion project which contains other QA/QC protocols. QA/QC was performed on LC-MS/MS data by University of Arkansas.

8. TRANSCRIPTOMICS

8.1. RNA extraction and library preparation

The tissue samples collected from the 90 colonies of *Orbicella faveolata* at the three different sample periods resulted in 270 samples that were snap-frozen and stored at -80°C for RNAseq analysis. We extracted RNA from all the samples using ZymoBIOMICS Magbeads DNA/RNA kit (cat.# R2136). A fraction of the samples were quality checked with TapeStation high-sensitivity tapes. We use Qubit 3 high-sensitivity kit (cat. # Q32852) to determine the RNA concentration of all samples. RNA concentrations ranged from 1 to 36 ng/µl (Table1). We build cDNA libraries with the QuantSeq 3'mRNA-Seq Library Prep kit (cat.# 015, FWR) following the protocol for RNA with low quality/quantity with unique dual identifiers. This protocol builds cDNA libraries with an expected length of 200bp per read. All libraries were quality checked with qPCR prior to amplification to determine the number of cycles for amplification. The number of cycles per library varied from 13 to 28 cycles. The 270 libraries were sent to Lexogen (Vienna, Austria) for quality check and sequencing in one lane of NOVAseq S2 flow cell for a predicted 8 million reads per sample.

8.2. Sequencing quality check and RNAseq analysis

All the sequencing data was analyzed in Pegasus, the high-performance computer cluster at the University of Miami. All the scripts used in this step of the analysis are publicly available at the GitHub repository Cnidimmunity-Lab/SCTLD_RRC in the folder called "hpc". All quality steps for the following analysis were done with FastQC (version 0.12.1) and summarized with Multiqc (version 1.14). Raw sequencing data were first quality checked to inspect for adapter contamination and the overall quality of the reads. Due to

adapter contamination and sequencing artifacts present in the reads we performed a trimming step with TrimGalore (version 0.6.10) using the settings recommended for sequencing data specific to the NOVAseq platform (see Github repository for details). After a second round of quality check analysis, another trimming was performed with the same software to clean the polyA tails still present in our reads. The 3rd quality check still showed some adapter contamination that did not represent an issue for advancing to the mapping step. Sequences were then aligned to the available genome from *Orbicella faveolata* (Accession #: PRJNA381078, Prada et al., 2016) using STAR (version 2.7.10b, Dobin et al., 2013). The parameters used to run this software are also detailed in the scripts available in the repository Cnidimmunity-Lab/SCTLD_RRC. Counts of reads per gene were obtained using an internal option from the same software.

8.3. Mapping and read counts quality check

From this point forward, the analysis for the read counts and gene expression analysis was done in R open-source software (version 4.2.2). All the scripts used to analyze this data can be found in the GitHub repository Cnidimmunity-Lab/SCTLD_RRC. We used the MultiQC report from the alignment to filter all the samples that had a minimum of 4 million uniquely mapped reads to the genome. We then filtered genes with low expression to reduce the noise that these genes might bring to the analysis. This quality threshold left us with 144 samples each with 19253 genes to run differential gene expression analysis. Amongst those samples, we had 79 colonies with the vast majority corresponding to sample periods 2 and 3.

8.4. Gene expression analysis

We used DEseq2 (version 1.38.3, Love et al., 2014) to model the data and obtain genes differentially expressed between the different categories used to characterize the phenotypic response to SCTLD exposure.

9. SYMBIODINIACEAE

Following the collection of samples taken from the unified samples and shared across RRC, a single core was shared between researchers. A small biopsy, ~2mm, was taken from each core and used for Symbiodiniaceae analyses and the remaining sample was transferred to Dr. Nikki Traylor-Knowles Lab.

Each sample was placed in a pre-labeled 1.5mL Eppendorf tube with 500uL 1% SDS in DNA Buffer solution. A 100uL aliquot of each sample was then extracted following established organic extraction protocols (Baker and Cunning et al. 2016). The resulting DNA was then analyzed using an actin-based real-time PCR (qPCR) assay for algal symbiont identification (to the genus level) and quantification of *Symbiodinium*, *Breviolum*, *Cladocopium*, and *Durusdinium*.

10. CHEMICAL DEFENSES

10.1. Sample handling

All samples were flash frozen in liquid nitrogen on the boat immediately after collection. They remained frozen and stored in a -80 freezer at NSU until transported or shipped on dry ice to the Smithsonian Marine Station. Once they arrived at the Smithsonian Marine Station, they were freeze dried for 24 hours until the coral samples were fully dry to

facilitate more efficient extractions. All glassware and vials were prewashed with HPLC grade methanol before extraction to remove any contaminating organic compounds that might interfere with metabolomic analysis. All solvents used for extraction were HPLC grade. One technician in Dr. Paul's laboratory, Mr. Jay Houk, conducted all the extractions and partitions of the extracts throughout this project to ensure consistency in methodology. All freeze-dried coral samples were extracted in 2:2:1 ethyl acetate: methanol: water three times to ensure extraction efficiency and then dried by rotary evaporator. A ~5 mg subset of each extract was transferred to solvent resistant Eppendorf tubes and sent to the Garg laboratory at Georgia Tech for metabolomic analysis.The remaining extracts were used for antimicrobial assays and bioassay-guided fractionation at the Smithsonian Marine Station.

Extractions were completed for all samples from all three collection periods (n=270), and all the necessary solvent controls (n=32) were prepared. This was considerable effort that took most of the technician's time for a 3-month time period right after the Fall 2021 samples were collected and for another month after the spring 2022 samples were collected.

A ~5 mg aliquot of all 270 samples was weighed into solvent resistant Eppendorf tubes. Sample sizes ranged from 4.5-5.7 mg. Appropriate solvent controls (n=32) were also included. Samples were shipped and received by Neha Garg's laboratory on Jan. 21, 2022 and May 6, 2022. The extraction method and Excel file with all extraction data and amounts sent were sent previously as deliverables.

In consultation with chemist Dr. Sarath Gunasekera in our laboratory at SMS, we developed a method of partitioning the remaining extracts from all 270 samples so that we could remove the salts and test them for antimicrobial activity against a putative coral pathogen, *Vibrio coralliilyticus*. To use a relevant strain of *V. coralliilyticus*, we used OfT6-21, which had been previously isolated from *Orbicella faveolata* that was infected with SCTLD. Prior to processing any coral extracts, solvents by themselves were run through our partitioning scheme (n=3) and sent to the Garg laboratory for verification of methods. A minor contaminant was detected in the butanol (n-BuOH) layer, and the partitioning scheme was modified to prevent any solvent from contacting the vial lid, which was thought to be the source of the contaminant.

For partitioning the coral extracts, the dried extract was dissolved in 3 ml of ethyl acetate with sonication to dissolve the extract. Once dissolved, 3 ml of HPLC-grade water was added and sonicated (5 seconds) to mix the organic and aqueous layers. The vials were allowed to stand for up to 2 hours to allow the two layers to separate. Once clarified (1.5-2 hours), a glass pipette was used to transfer the water and ethyl acetate layers into separate pre-washed vials. The ethyl acetate partition was dried in vacuo at 35 °C in a Savant speed-vac, and any trace amounts of water remaining in the partition were frozen and lyophilized to dryness (30-60 minutes). Next, 3 ml of butanol was added to the water layer and sonicated to mix (5 seconds). Once clarified (2-3 hours), the water layer was returned to the original vial and frozen. The butanol layer was dried in vacuo at 45 °C in a Savant speed-vac, and any trace amounts of water remaining in the partition were frozen and lyophilized to dryness (30-60 minutes). All samples have now been partitioned, resulting in 270 EtOAc partitions and 270 butanol partitions, and are being stored frozen.

10.2. **Protocol for disk diffusion assays for Reef Resilience Consortium coral extracts**

Initial coral extracts were partitioned, and the ethyl acetate (EtOAc) and butanol (BuOH) partitions of each were tested for antimicrobial activity against the known coral pathogen *Vibrio coralliilyticus* OfT6-21. These methods used disk diffusion assays, often called Kirby-Bauer disk diffusion assays, that are often used for tested human pathogens and other bacteria.

Glycerol stocks of the pathogenic challenge strain OfT6-21were revived onto seawater agar (SWA) (4 g tryptone, 2 g yeast /L seawater) and grown overnight at 28 °C. The morning of each assay, 4 ml of seawater broth was inoculated with three colony forming units and grown in a shaking incubator at 28 °C and 200 rpm. For testing, the culture was adjusted to OD600 0.50 +/- 0.05 (ThermoScientific Genesys 180) and 200 µl of inoculum was added to each 150 mm SWA plate. The inoculum was dispersed with sterile beads and left to dry for 15 minutes prior to administering treatment disks.

While we have previously assayed probiotic bacterial extracts at 125 µg/disk, these coral extracts produced zones of inhibition (ZOIs) that were too large to interpret at this concentration. A subsample of extracts was assayed at a range of concentrations from 10-25 µg/disk and 15 µg/disk was found to produce measurable results. To ensure accuracy, each treatment was resuspended and transferred to a freshly weighed vial. The BuOH partitions were completely dissolved in methanol, and 1:1 EtOAc:MeOH was required to completely solubilize the EtOAc partitions. Each aliquot was transferred via glass pipet to a prewashed 7 ml scintillation vial (MeOH 3x) and dried in vacuo at 35 °C (ThermoScientific Savant SPR121P).

Concentrate was resuspended to 0.75 mg/ml and 20 µl (15 µg) was administered to each 6.35 mm paper disk* and allowed to dry under a sterile laminar flow hood for 20 minutes (ThermoScientific remel blank paper disks Cat. # R55054). Solvent controls with EtOAc and MeOH were also prepared, and 62.5 µg of Nalidixic acid was prepared as a positive control. Disks were applied treatment side down to the plate. The assay was incubated for 24 hours at 28 °C prior to scoring. The radius of each zone of inhibition was measured with calipers from the edge of disk to the edge of ZOI. Diameters across the entire zone, including the paper disk, can also be a metric reported based on the Kirby-Bauer method.

**The BuOH soluble treatment disks were prepared via P20 pipette with a polypropylene tip, while the EtOAc soluble were added via 25 µl glass syringe (Hamilton 84855) that was washed (6x) between samples. Because the Nalidixic acid was dissolved in mQ water at (3.125 mg/ ml), these disks were prepared first to allow for a longer dry time.*

11. METABOLOMICS

Dr. Neha Garg received the set of organic extracts of sample periods 1 and 2 (SP1, SP2) from Dr. Valerie Paul in February 2022, and acquired liquid chromatography tandem mass spectrometry (LC-MS/MS) metabolomics data in the positive and negative mode. The final set of organic extracts from sample period 3 (SP3) was received and data was acquired in the positive mode and negative mode in May 2022. The LC-MS/MS spectra acquired in

positive mode from SP1-3 were submitted to the repository Mass spectrometry Interactive Virtual Environment (MassIVE) and can be accessed at https://massive.ucsd.edu/ with the identifier MSV00008881. The LC-MS/MS data acquired in negative mode from SP1-3 can be accessed on MassIVE with the identifier MSV000089980. The LC-MS/MS data acquired in positive mode was preprocessed using MZmine2 to perform mass detection, chromatogram building, chromatogram deconvolution, isotopic grouping, retention time alignment, duplicate removal, and missing peak filling. The processed data was submitted to the Global Natural Products Social Molecular Networking (GNPS) platform for feature-based molecular networking analysis. The job can be accessed at https://gnps.ucsd.edu/ProteoSAFe/status.jsp?task=aac15156dba8406f8f34b2356b7a9acd. The uploaded MS/MS spectra were searched against GNPS spectral libraries. Cytoscape was used to visualize the molecular network. Multivariate analyses were performed using MetaboAnalyst 5.0. The in silico tool MolDiscovery (v.1.0.0) was used to aid metabolite annotations and SIRIUS with CSI:FingerID and CANOPUS was used to predict chemical compound classes.

12. LIPIDOMICS

This task analyzed the organic extracts generated and further fractionated by the laboratory of Valerie Paul on samples previously collected for this project using the institute's Thermo Fisher Scientific Orbitrap ID-X Tribrid mass spectrometer coupled to an ultra-high-performance liquid chromatography to obtain a comprehensive lipidome of coral species. The remaining extracts were stored at -20°C for any future manipulations.

13. FECUNDITY

A total of 91 coral tissue samples of *Orbicella faveolata* embedded in paraffin wax blocks were received in November 2022 from Aine Hawthorn. Blocks were sectioned on a Leica RM2235 microtome; a total of four sections (5 µm thick) (encompassing longitudinal and transverse views) were cut from each block, flattened on a warm water bath, and mounted on slides 9 (a total of 2 slides per block). Slides were placed on a warming plate to dry, photographed, then transferred to a warming oven.

One slide from each sample (2 sections) was cleared in xylene (3x), rehydrated through a graded series of ethanol, and stained with modified Heidenhain's azocarmine-aniline blue. Stained slides were then dehydrated through a graded series of ethanol, cleared in xylene, and a coverslip was applied using Cytoseal 60 mounting medium. Mounted slides were dried for 24 hours then viewed in an Olympus BX 43 light microscope at magnifications ranging from 4X to 60X and photographed with an Olympus DP21 digital camera.

Histological sections were assessed for the presence or absence of male and female gonads, the reproductive stage of gametes, the number of oocytes or ova per gonad and number of gonads per polyp, and oocyte size (maximum diameter). Fecundity per polyp was estimated as the product of the average number of gonads per polyp in cross-section and the average number of oocytes or ova per gonad in longitudinal section.

Fisher Exact tests were used to assess differences in the percent presence of gametes (oocytes and spermaries) between sites and with respect to SCTLD status, including

histopathology supported resistance and SCTLD status. Analysis of Variance (ANOVA) was used to assess differences in fecundity, oocyte stage, and oocyte size between sites and with respect to SCTLD status, including histopathology supported resistance and SCTLD status. All statistical tests were conducted using RStudio and JMP 16.